UCRL-16931

University of California

Ernest O. Lawrence Radiation Laboratory

FLUCTUATIONS OF ENERGY LOSS BY HEAVY CHARGED PARTICLES IN MATTER

Berkeley, California

DISCLAIMER

UCRL-16931

UNIVERSITY OF CALIFORNIA

Lawrence Radiation Laboratory
Berkeley, California

AEC Contract No. W-7405-eng-48

FLUCTUATIONS OF ENERGY LOSS BY HEAVY CHARGED PARTICLES IN MATTER

Howard David Maccabee

(Ph.D. Thesis)

July 20, 1966

FLUCTUATIONS OF ENERGY LOSS BY
HEAVY CHARGED PARTICLES IN MATTER

Contents

FLUCTUATIONS OF ENERGY LOSS BY HEAVY CHARGED PARTICLES IN MATTER

Howard David Maccabee

Lawrence Radiation Laboratory
University of California
Berkeley, California

July 20, 1966

ABSTRACT

Significant fluctuations of energy loss are expected in certain cases of the passage of fast heavy charged particles through "thin" absorbers. When the number of particle-electron collisions in the upper collision-loss interval is small, the energy-loss distribution is asymmetric and is characterized by a broad peak around the most probable energy loss (which is significantly less than the mean energy loss) and by a high-energy-loss "tail." Several theories predict the energy-loss distribution function, but previous experimental work is incomplete with respect to verification of theory over the whole significant range of the parameters involved. We have passed beams of 730- and 45-MeV protons, 910-MeV helium ions, and 370-MeV π-mesons through silicon semiconductor detectors of varying thicknesses, and measured the resulting energy-loss distributions.

Within the limits of experimental error, there is very good agreement between the measured energy-loss distributions and those predicted by the theory of Vavilov, and good agreement on the value of the most probable energy loss.

We tabulate our results and discuss their physical and biological implications.

I. INTRODUCTION

When a charged energetic particle passes through matter, it loses its energy by several competing processes. For heavy charged particles (i.e. particle mass >> electron mass) in the velocity range considered here, the predominant mode of energy loss is that involving inelastic collisions with the electrons of the material, resulting in ionization and excitation of the atoms of the material. Because the collisions are discrete and random, statistical fluctuations in the number of collisions are expected.

In first approximation, the probability of energy loss ϵ in a single electronic collision is proportional to ϵ^{-2}. Thus collisions resulting in a large energy transfer to an electron are relatively infrequent compared with small-energy-transfer collisions. Although they are relatively infrequent, the large-energy-transfer collisions account for a significant proportion of the total energy loss. In a "thin" absorber (one in which the total energy lost is small compared with the kinetic energy of the particle), the probable number of large-energy-transfer collisions may be so small that the random statistical variations in this number are relatively large, and result in significant fluctuations in the energy lost in this mode, and thus fluctuations in the total energy loss occur.

Several existing theories of this phenomenon predict the distribution of energy losses occurring when a heavy charged particle passes through a thin absorber. The purpose of this work is to investigate

the fluctuation phenomenon experimentally, to compare experimental distributions with theoretical predictions, and to summarize our results in a way that is useful to investigators in other fields. Toward this end, we first review previous theoretical and experimental work in this area and then describe our experimental methods (using semiconductor detectors and accelerated heavy charged particle beams.) We then show the measured energy-loss-frequency distributions, compare them with theoretical distributions, and discuss the limitations of our method. Finally, we tabulate our results graphically and discuss their implications for radiation physics and biology.

II. REVIEW OF PREVIOUS WORK

A. Theoretical

The theory of energy loss of heavy charged particles in matter is well developed and has been reviewed by Fano,[1] Starodubtsev and Romanov,[2] Bichsel,[3] Uehling,[4] Bethe and Ashkin,[5] Evans,[6] Rossi,[7] Allison and Warshaw,[8] and others. We present here only a brief summary of the development of the expression for the average rate of energy loss, as background to our later discussion of the theory of fluctuations of energy loss.

Although several authors, including Rutherford and Thomson, had considered the problem, the classical theory of charged-particle energy loss as we know it began with Bohr in 1913,[9] and the relativistic refinements with Bohr in 1915.[10] Assuming that the electrons of the stopping material may be treated as free, Bohr derived the equivalent of this nonrelativistic expression for the average rate of energy loss:

$$\frac{dE}{dx} = -\frac{4\pi e^4 z^2 NZ}{mv^2} \int \frac{b\ db}{b^2}, \qquad (1)$$

where $e \equiv$ charge of the electron,

$z \equiv$ particle charge number,

$N \equiv$ number of atoms/cm^3 of the material,

$Z \equiv$ atomic number of the material,

$m \equiv$ electron mass,

$v \equiv$ particle velocity,

and $b \equiv$ impact parameter of particle-electron collision.

The integration is to be performed over all values of b from b = 0 to b = ∞. This integral is infinite, however, and thus we must choose limits from physical considerations of the maximum impact parameter (determined by the atomic binding of the electron) and the minimum (determined by the maximum possible energy transfer to an electron in a single collision).

We can understand the above expression in terms of the following simplified arguments (a rigorous treatment yields identical results). Consider a single collision of a heavy charged particle of charge ze and velocity v, whose track is a distance b from a stationary free electron. The momentum p transferred to the electron in the collision is the product of the Coulomb force F and the effective collision time t, which we approximate by (2b/v), the effective collision distance divided by the particle velocity. Thus

$$p \cong F \cdot t \cong \frac{ze^2}{b^2} \cdot \frac{2b}{v} = \frac{2ze^2}{bv} . \qquad (2)$$

Then the kinetic energy ϵ given to the electron is

$$\epsilon = \frac{p^2}{2m} = \frac{2z^2e^4}{mb^2v^2} . \qquad (3)$$

Now $\omega(b)\, db\, dx$, the number of electrons that the particle "sees" between b and b + db along track segment dx is given by the volume of

an annular shell, $2\pi b\ db\ dx$, times the electron density of the material NZ, where N is the atom density and Z the atomic number:

$$\omega(b)\ db\ dx = 2\pi NZ\ dx\ b\ db\ . \tag{4}$$

Thus the total energy imparted to electrons along track dx at distance b is

$$dE(b) = \frac{4\pi e^4 z^2 NZ\ dx}{mv^2}\ \frac{b\ db}{b^2}\ , \tag{5}$$

and the rate of energy loss to electrons at all impact parameters is given by the integral over all b:

$$\frac{dE}{dx} = -\frac{4\pi e^4 z^2 NZ}{mv^2}\int \frac{b\ db}{b^2}\ . \tag{1}$$

Note that the above arguments also yield the functional dependence of the probability ω of an energy loss ϵ per unit path length (often called the collision spectrum). Since each collision at distance b corresponds uniquely to an energy loss ϵ, we may write

$$\omega(\epsilon)\ d\epsilon = \omega(b)\ db\ , \tag{6}$$

$$\omega(\epsilon)\ d\epsilon = 2\pi NZb\ db\ . \tag{7}$$

But from Eq. (3),

$$b^2 = \frac{2z^2 e^4}{mv^2 \epsilon}\ , \tag{8}$$

$$\therefore \quad 2b\ db = -\frac{2z^2e^4}{mv^2}\frac{d\epsilon}{\epsilon^2}, \tag{9}$$

$$\therefore \quad \omega(\epsilon)\ d\epsilon = -\frac{2\pi e^4 z^2 NZ}{mv^2}\frac{d\epsilon}{\epsilon^2}; \tag{10}$$

thus

$$\omega(\epsilon)\ d\epsilon \propto \frac{d\epsilon}{\epsilon^2}. \tag{11}$$

In this formulation, the total energy loss in track segment dx is given by the integral of the energy loss in a single collision times its frequency:

$$dE = \int \epsilon\omega(\epsilon)\ d\epsilon\ dx, \tag{12}$$

i.e.,

$$\frac{dE}{dx} = -\frac{2\pi e^4 z^2 NZ}{mv^2}\int \frac{\epsilon\ d\epsilon}{\epsilon^2}. \tag{13}$$

The limits of integration are controlled by the physical constraints on the maximum and minimum energy loss in a single collision. Thus

$$\frac{dE}{dx} = -\frac{2\pi e^4 z^2 NZ}{mv^2}\ ln\ \frac{\epsilon_{max}}{\epsilon_{min}}. \tag{14}$$

The maximum energy loss in a single collision, ϵ_{max}, is determined by the kinematics of the electron–heavy-particle collision. Consider this problem in the center-of-mass system, with the electron of velocity -v colliding with an "infinitely" heavy stationary particle. The maximum

momentum transfer for a "head-on" encounter is +2mv, and thus the maximum particle-energy change is

$$\epsilon_{max} = \frac{p_{max}^2}{2m} = \frac{4m^2v^2}{2m} = 2mv^2 \quad \text{(nonrelativistic)}. \qquad (15)$$

Bohr derived the minimum energy loss in a collision from the consideration that the collision time must be smaller than the time of vibration of the bound electron in order that the Coulomb force from the particle shall predominate over the atomic binding forces. Bohr also introduced the relativistic correction terms $[-\ell n\,(1 - \beta^2) - \beta^2]$ to account for the relativistic increase in the maximum energy transfer and the decrease in the minimum due to Lorentz contraction of the Coulomb field of the heavy particle.

In 1930, Bethe introduced the quantum-theoretical treatment of this problem, applying the Born approximation to the collisions between the heavy particle and the atomic electrons.[11] Bethe defined I, the average excitation potential of the atomic electrons, and approximated it as the geometric mean of the maximum and minimum excitation energies:

$$I^2 \cong \epsilon_{max} \cdot \epsilon_{min}\,, \qquad (16)$$

$$\therefore\ \ell n \frac{\epsilon_{max}}{\epsilon_{min}} = \ell n \frac{\epsilon_{max}}{I^2/\epsilon_{max}} = \ell n \left(\frac{\epsilon_{max}}{I} \right)^2 = 2\,\ell n \frac{\epsilon_{max}}{I}. \qquad (17)$$

We are thus left with this expression for the average rate of energy loss:

$$\frac{dE}{dx} = - \frac{4\pi e^4 z^2 NZ}{mv^2} \left[\ln \frac{2mv^2}{I} - \ln (1 - \beta^2) - \beta^2 \right] . \qquad (18)$$

This formula (often called the Bethe-Bloch formula) is very widely used, and the conditions for its validity are these:

(a) I is determined experimentally.

(b) DeBroglie wavelength of the incident particle is large compared with the collision diameter, i.e.,

$$\frac{ze^2}{\hbar v} \ll 1 \text{ or } \beta \gg \frac{z}{137} .$$

(c) The velocity of the incident particle is large compared with the velocities of atomic electrons, i.e.,

$$E_o \gg \frac{M}{m} I_n ,$$

where I_n is the ionization energy of the nth electron.

(d) The incident charge is small, $z/Z < 1$, and there is no charge exchange.

(e) The energy loss due to elastic scattering on nuclei is negligible.

(f) Cerenkov radiation is negligible.

These conditions are generally satisfied for protons with $E_o > 1.5$ MeV and α particles with $E_o > 5$ MeV in light materials. For lower energies, the particle velocity is comparable to the velocity of the K-shell electrons, and an inner-shell correction term $(-C/Z)$ is added within the brackets. For very high energies ($\beta \to 1$), the polarization of the

medium becomes important and a density-effect term ($-\delta/2$) is added within the brackets:[1]

$$\frac{dE}{dx} = -\frac{4\pi e^4 z^2 NZ}{mv^2}\left[\ell n \frac{2mv^2}{I(1-\beta^2)} - \beta^2 - \frac{c}{Z} - \frac{\delta}{2}\right]. \qquad (19)$$

This is the standard expression for the average rate of energy loss.

Since the electron-collision process by which a charged particle loses its energy is a random process, we may expect fluctuations to occur about the mean energy loss. The theory of energy-loss fluctuations (often called energy-loss straggling) was first discussed by Flamm[12] in 1914 and Bohr[10] in 1915. The problem of the distribution of energy losses of a charged particle passing through a given thickness of material is intimately related to the problem of the distribution of ranges of particles with a given energy (range straggling), but we shall not discuss the latter problem here. We also limit ourselves, in general, to the problem of "thin" absorbers--those in which the mean energy lost is small compared to the initial kinetic energy of the particle.

Bohr treated the fluctuation problem by dividing the electron collisions into energy groups in such a way that the variation of ϵ in each group is small, while the number of collisions in the group is large. In Bohr's treatment, if the value of ϵ for the $\underline{r}$th group is ϵ_r, the mean number of collisions in the group is ω_r, the actual number of collisions for a given particle is $\omega_r(1 + s_r)$, then the total energy loss in a given thickness x is

$$\Delta = \sum_r \epsilon_r \omega_r (1 + s_r) \; ; \tag{20}$$

denoting by $\bar{\Delta}$ the average value of the energy loss, we can write

$$\Delta - \bar{\Delta} = \sum_r \epsilon_r \omega_r s_r \; . \tag{21}$$

Since ω_r is large, we assume a Gaussian distribution for f, the probability that s_r has a value between s_r and $s_r + ds_r$,

$$f(s_r)\, ds_r = (\omega_r/2\pi)^{1/2} \exp(-\tfrac{1}{2}\, \omega_r s_r^{\,2})\, ds_r \; . \tag{22}$$

Using a fundamental theorem of probability [if a implies b, then $f(a)\, da = f(b)\, db$] and denoting by $f(\Delta)\, d\Delta$ the probability that Δ has a value between Δ and $\Delta + d\Delta$, Bohr deduced that

$$f(\Delta)\, d\Delta = (2\pi\sigma^2)^{-1/2} \exp[-(\Delta - \bar{\Delta})^2/2\sigma^2]\, d\Delta \; , \tag{23}$$

where

$$\sigma^2 = \sum_r \omega_r \epsilon_r^{\,2} = x \int \epsilon^2 \omega(\epsilon)\, d\epsilon \; . \tag{24}$$

Evaluating ϵ and $\omega(\epsilon)$ as above, Bohr derived the equivalent of

$$\sigma^2 = 4\pi e^4 z^2 NZx \; , \tag{25}$$

or equivalently,

$$\frac{d}{dx} (\overline{\Delta^2} - \bar{\Delta}^2) = 4\pi e^4 z^2 NZ \; . \tag{26}$$

Bohr correctly noted that the conditions for the validity of this treatment (i.e., variation of ϵ in group small, number of collisions in group large) are equivalent to the condition that the dimensionless

parameter

$$\kappa \equiv d\omega/(d\epsilon/\epsilon) \gg 1.* \tag{27}$$

Bohr evaluated this parameter for heavy particles as

$$\kappa = \pi e^4 z^2 NZx/m^2 v^4 . \tag{28}$$

In summary, when the number of collisions in each energy interval is large (i.e., $\kappa \gg 1$), the energy-loss-probability distribution is Gaussian, with fluctuations about the mean given by expressions (23) and (25). Bohr also noted that for small κ, the most probable energy loss Δ_{mp} is smaller than the mean, and he derived an approximate expression for Δ_{mp}.

In 1929, Williams attempted to calculate accurately the complete energy-loss spectrum for any form of the collision spectrum $\omega(\epsilon)\, d\epsilon$, for small values of parameter κ.[13] He divided the electron collisions into two groups--one for which the energy loss ϵ in a collision is less than ξ, and the other for which ϵ is greater than ξ. Here ξ is defined so that a particle traversing the absorber suffers, on the average, one collision for which ϵ is greater than ξ, that is,

$$x \int_{\xi}^{\infty} \omega(\epsilon)\, d\epsilon = 1 , \tag{29}$$

or, after evaluation from (10) above,

---

*Bohr actually used the notation λ for this parameter. In this treatment we have tried to follow the notation of Landau (see Ref. 25).

$$\xi = 2\pi e^4 z^2 NZx/mv^2 \ . \qquad (30)$$

Clearly the number of collisions in the lower energy group is large, and continuous statistics may be applied. The number of collisions in the higher energy group is by definition small, however, and thus discrete Poisson statistics must be used. Williams denoted by $A(\Delta - \alpha)$ the probability that the particle loses a total energy $(\Delta - \alpha)$ due to the lower-energy collisions, and by $B(\alpha)$ the probability of energy loss (α) due to higher energy collisions. Since the collision processes are independent, we have

$$f(\Delta) = \int A(\Delta - \alpha)B(\alpha)\, d\alpha \ . \qquad (31)$$

Williams evaluated these functions numerically, plotted generalized straggling curves, showed that the shape of the straggling distribution depends on the functional form of the collision spectrum, and proved that most of the broadening of the energy-loss distribution is due to collision-energy losses in the neighborhood of ξ.

In 1937, Livingston and Bethe gave a quantum-theoretical treatment of the fluctuation problem[14] and derived the expression

$$\frac{d}{dx}\left(\overline{\Delta^2} - \bar{\Delta}^2\right) = 4\pi e^4 z^2 N \left(Z' + \sum_n k_n \frac{I_n Z_n}{mv^2} \ell n \frac{2mv^2}{I_n} \right), \qquad (32)$$

where Z' is the "effective" atomic number, Z_n the number of electrons in the nth shell, I_n their average excitation energy, and k_n a constant on the order of unity. For high energies, (32) reduces to

$$\frac{d}{dx}\left(\overline{\Delta^2} - \bar{\Delta}^2\right) = 4\pi e^4 z^2 NZ' , \tag{33}$$

which is similar to Bohr's classical expression (26).

In 1942, Niels Bohr prepared his more refined and comprehensive treatment of the penetration of atomic particles through matter, including the effect of resonance collisions and nuclear scattering on straggling, but the war delayed publication until 1948.[15]

In 1944, Lev Landau derived the rigorous equation for the energy-loss distribution function, and gave an analytic solution for the case in which $\xi \ll \epsilon_{max}$.[16] He denoted by $f(x,\Delta)$ the probability that a particle of given initial energy E_o will lose an amount of energy lying between Δ and $\Delta + d\Delta$ on traversing a layer x of matter. The distribution function f is normalized so that $\int f\, d\Delta = 1$. If $\omega(E,\epsilon)$ is the probability (per unit path length) of an energy loss ϵ for a particle of energy E, and we assume $\Delta \ll E_o$, we can write

$$\omega(E,\epsilon) \cong \omega(E_o,\epsilon) \cong \omega(\epsilon) . \tag{34}$$

The "kinetic" equation for f is obtained by equating the rate of change of the distribution function, $\partial f/\partial x$, to the "collision integral," which expresses the difference between the number of particles that acquire, due to ionization losses along dx, a given energy E, and the number of particles that leave the given energy interval:

$$\frac{\partial f}{\partial x} = \int_0^\infty \omega(\epsilon)[f(x,\Delta - \epsilon) - f(x,\Delta)]d\epsilon \ . \qquad (35)$$

We may think of this expression as a transport equation, where the first term in the brackets represents particles "scattering into" the given energy interval by collisions with energy transfer ϵ, and the second term in the brackets represents "scattering out." Since Eq. (35) does not contain explicitly the independent variables x and Δ, Landau was able to find the solution by applying the Laplace transformation with respect to the variable Δ, using p as the transform variable:

$$\varphi(x,p) \equiv \int_0^\infty f(x,\Delta)e^{-p\Delta}\, d\Delta \ . \qquad (36)$$

Then we have

$$f(x,\Delta) = (2\pi i)^{-1} \int_{-\infty+\sigma}^{+i\infty+\sigma} e^{p\Delta}\varphi(x,p)\, dp \ , \qquad (37)$$

where the integration is carried out over a straight line parallel to the imaginary axis and shifted to the right by σ. Multiplying (35) by $e^{-p\Delta}$ and integrating with respect to $d\Delta$, we obtain

$$\frac{\partial\varphi(p,x)}{\partial x} = -\varphi(p,x) \int_0^\infty \omega(\epsilon)(1 - e^{-p\epsilon})\, d\epsilon \ . \qquad (38)$$

Integrating (38) with the initial condition that at x = 0, f is a delta function and thus $\varphi(p,0) = 1$, we get

$$f(x,\Delta) = (2\pi i)^{-1} \int_{-i\infty+\sigma}^{i\infty+\sigma} \exp[p\Delta - x \int_0^\infty \omega(\epsilon)(1 - e^{-p\epsilon})\, d\epsilon]\, dp \,. \quad (39)$$

This is the general solution for the distribution function and, in principle, it may be evaluated when $\omega(\epsilon)$ is known. In order to manage this equation, Landau assumed that $p\epsilon_o \ll 1$ and $p\epsilon_{max} \gg 1$, where ϵ_o is a characteristic energy of the order of the mean electron binding energy, and used the familiar

$$\omega(e) = \frac{2\pi e^4 z^2 NZ}{mv^2} \frac{d\epsilon}{\epsilon^2} \,. \quad (10)$$

After manipulation and the introduction of the quantity

$$u/p = \xi = 2\pi e^4 z^2 NZx/mv^2 \,, \quad (30)$$

he obtained

$$f(x,\Delta) = \xi^{-1}\varphi(\lambda) \,, \quad (40)$$

where

$$\varphi(\lambda) = (2\pi i)^{-1} \int_{-i\infty+\sigma}^{i\infty+\sigma} e^{u \ln u + \lambda u}\, du \quad (41)$$

and

$$\lambda \equiv \left\{\Delta - \xi\left[\ln \frac{\xi \cdot 2mv^2}{I^2(1-\beta^2)} - \beta^2 + 1 - C\right]\right\} \cdot \xi^{-1} \,, \quad (42)$$

where $C \equiv$ Euler's constant $= 0.577 \cdots$. Thus the function of two variables $f(\Delta,x)$ turns out to equal the product of ξ^{-1} and a universal function $\varphi(\lambda)$ of a nondimensional variable λ. This function has been calculated numerically and is shown in Fig. 1. It has a maximum at $\lambda = -0.05$ and thus Δ_{mp}, the most probable value of the energy loss, is given by

$$\Delta_{mp} = \xi \left[\ell n \frac{\xi \cdot 2mv^2}{I^2(1 - \beta^2)} - \beta^2 + 0.37 \right] . \qquad (43)$$

Also, the probability of an energy loss lying between Δ and $\Delta + d\Delta$ is

$$f(x,\Delta)\, d\Delta = \varphi\left(\frac{\Delta - \Delta_{mp}}{\xi} \right) d\left(\frac{\Delta - \Delta_{mp}}{\xi} \right) . \qquad (44)$$

We now examine the conditions for validity of this treatment. As $u \equiv \xi p$, the assumptions reduce in the region of interest ($u \approx 1$) to

$$\xi/\epsilon_o \gg 1 ; \qquad \xi/\epsilon_{max} \ll 1 . \qquad (45)$$

The first condition implies that the observed energy losses must be large enough compared with the electron binding energy, i.e., many collisions in the lowest collision-loss interval. The second implies that the observed energy losses must be small compared with the maximum energy loss in a single collision, i.e., very few collisions in the highest collision-loss interval. In fact, the second condition, upon substitution, yields

$$\frac{\xi}{\epsilon_{max}} = \frac{2\pi e^4 z^2 NZx/mv^2}{2mv^2} = \frac{\pi e^4 z^2 NZx}{m^2 v^4} = \kappa \ll 1 . \qquad (46)$$

Note that this condition is the exact opposite of the condition of validity (27) of Bohr's treatment. Thus, when the number of collisions in the highest collision-loss interval is small, (i.e., $\kappa \ll 1$), the distribution of total energy losses is highly asymmetric, with a broad

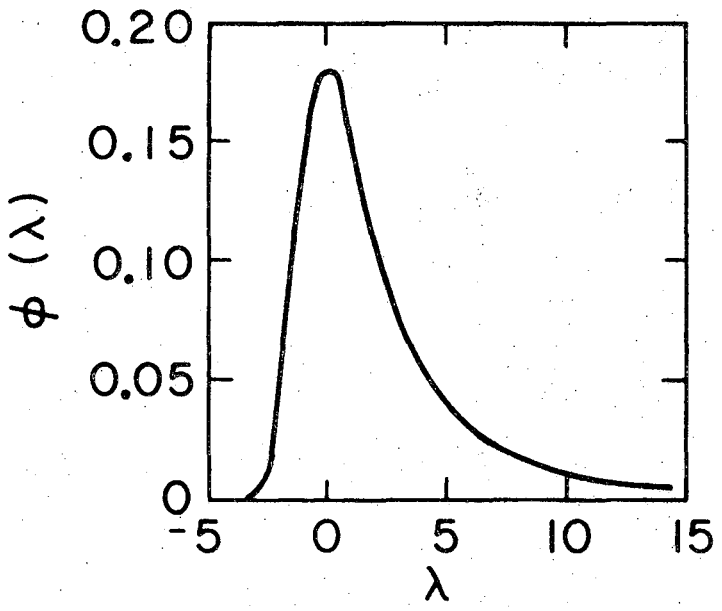

MUB 11789

Fig. 1. Plot of Landau function φ (λ) versus λ.

peak (FWHM $\approx$ 30%) around the most probable energy loss (which is significantly smaller than the mean energy loss) and a long "tail" corresponding to higher energy losses. This fluctuation phenomenon is often called the "Landau effect." Perhaps the best way to explain the shape of this curve is by returning to Williams' two-group dichotomy. The peak, centered on Δ_{mp}, represents a "Gaussian" due to the numerous collisions where $\epsilon < \xi$, and the long tail is the result of "folding in" a "Poisson" distribution corresponding to the average of one collision for which $\epsilon > \xi$.

In 1948, Symon treated the intermediate cases between the Landau distribution and the Gaussian.[17] Symon derived the general relations between the moments of the collision spectrum and the semi-invariants and moments of the energy-loss distribution, and used a modified Edgeworth expansion to calculate a single-parameter family of curves of varying skewness which provide a smooth transition between the extreme cases. This result follows from the introduction of a set of weighted parameters which characterize approximately the energy-loss distribution function $f(x,\Delta)$; these parameters are the weighted skewness, the weighted rms fluctuation, and a parameter relating Δ_{mp} to $\bar{\Delta}$, and are respectively related to Symon's third, second, and first "generalized" moments of the collision spectrum $\omega(\epsilon)$. He presented instructions for using his parameters and the family of distribution curves, and also treated the problem of "thick" absorbers (i.e., $0.1E_o < \Delta < 0.9E_o$).

In 1950, Blunck and Leisegang considered quantitatively the problem of distant resonance collisions with the atomic electrons, where

the amount of energy transferred is of the order of the binding energies of the various atomic shells.[18] These collisions are often called "glancing collisions." By taking into account $\overline{\epsilon^2_{res}}$, the second moment of the resonance collision spectrum, they showed that significant broadening of the energy-loss distribution occurs when their parameter b^2 is greater than three:

$$b^2 = 2x\overline{\epsilon^2_{res}}/\xi^2 \cong \bar{\Delta}Z^{4/3}\cdot 20\text{ev}/\xi^2 .$$

The second quantity is an estimate of b^2 by Blunck and Westphal, to be used when $\overline{\epsilon^2_{res}}$ is difficult to evaluate.[19] When $b^2 \ll 3$, broadening of the straggling curve due to resonance collisions is negligible.

It is instructive to note here the importance of the moments of the collision spectrum in the theory of energy-loss fluctuations. If we define as the nth moment of the collision spectrum,

$$\overline{\epsilon^n} \equiv \int_{\epsilon_{min}}^{\epsilon_{max}} \epsilon^n \omega(\epsilon)\, d\epsilon , \tag{48}$$

then we can express, in terms of the moments, the quantities

$$\begin{aligned} \bar{\Delta} &= \overline{\epsilon^1}x , \\ \sigma^2 &= \overline{\epsilon^2}x , \\ \xi &\cong \overline{\epsilon^0}\cdot\epsilon_{min}x , \\ \kappa &\cong \overline{\epsilon^0}\cdot(\epsilon_{min}/\epsilon_{max})x . \end{aligned} \tag{49}$$

Symon showed that the skewness of the distribution curve is related to $\overline{\epsilon^3}$; Symon[17] and Blunck and Leisegang[18] showed that the distribution

function $f(x,\Delta)$ could be expanded in terms of the moments. In particular, Blunck showed that Landau's expression (39) can be written

$$f(x,\Delta) = (2\pi i)^{-1} \int_{-i\infty+\sigma}^{i\infty+\sigma} e^{p\Delta - xg(p)}\, dp \,, \tag{50}$$

where

$$g(p) = \int_0^\infty \omega(\epsilon)(1 - e^{-p\epsilon})\, d\epsilon = -\sum_{n=1}^\infty \overline{\epsilon^n}(-p)^n/n! \,, \tag{51}$$

and that Landau's solution was equivalent to neglecting all moments of the resonance collision spectrum with $n > 1$:

$$\overline{\epsilon^n} = \overline{\epsilon_{res}^n} + \overline{\epsilon_{free}^n} \,. \tag{52}$$

Lewis, in 1951, solved the "Boltzmann" equation for the energy-loss distribution function in a different way, and considered the application to range straggling.[20]

In 1953, Fano presented a general analysis of (a) the energy spectrum resulting from the degradation of ionizing radiations, and (b) range-energy straggling.[21] He discussed the connections between the theoretical approaches of several previous authors, and pointed out two approximations in the Landau treatment, i.e., the use of an approximate collision spectrum and the extension of the upper limit of integration to $\epsilon = \infty$, thereby introducing a spurious possibility of energy losses $\epsilon > \epsilon_{max}$.

In 1954, Moyal considered the problem of the distribution of energy losses by ionization and its relation to the number of ion pairs produced.[22] He showed that, in terms of the reduced energy variable $\lambda \cong (\Delta - \Delta_{mp})/\xi$, a good asymptotic (for large numbers of collisions)

approximation for Landau's solution is

$$\varphi(\lambda)\, d\lambda = (2\pi)^{-1/2} \exp[-\tfrac{1}{2}(\lambda + e^{-\lambda})]\, d\lambda \,. \qquad (53)$$

Moyal also showed that the numbers of ion pairs produced can be represented by the same "universal" distribution, and thus accounted for the experimental fact that ion-pair numbers are proportional to primary energy loss. By postulating a Breit-Wigner cross section for the quantum resonance collisions, he concluded that resonance effects should not broaden the straggling curve, in contradiction to the conclusions of Blunck et al. The source of this discrepancy probably lies in the questionable assumption of a Breit-Wigner shape (i.e., $\sigma(\epsilon)\, d\epsilon \propto d\epsilon/[(\epsilon - I)^2 + \Gamma^2]$) for the particle-electron resonance cross section.

In 1955, Hines attempted a more accurate solution of the proton-energy-loss transport equation, by applying the Mellin transform instead of the Laplace.[23] His solution for the distribution function is of the form

$$f(x,E) = (2\pi i)^{-1} \int_{-i\infty+\sigma}^{i\infty+\sigma} \exp[-s \ln E + (s-1) \ln (E_o - x\beta + a_1(s) + a_2(s)x^2]\, ds \,, \qquad (54)$$

where $E \equiv E_o - \Delta$, and is much narrower than the Landau distribution for low-energy protons.

Herring and Merzbacher, in 1957, gave an alternative derivation for Landau's general distribution function (39), based on an infinite sum of weighted Poisson distributions, and also discussed the distribution of the numbers of ion pairs.[24]

In 1957, P. V. Vavilov published his rigorous solution of the problem of fluctuations of ionization loss by heavy particles in "thin" absorbers.[25] Using ϵ_{max} as the upper limit of integration in Landau's expression (39), and the relativistic values

$$x\omega(\epsilon) = \frac{\xi}{\epsilon^2}\left(1 - \beta^2 \frac{\epsilon}{\epsilon_{max}}\right), \tag{55}$$

$$\epsilon_{max} = 2mv^2/(1 - \beta^2) , \tag{56}$$

and defining

$$\kappa \equiv \xi/\epsilon_{max} , \tag{57}$$

$$\lambda_1 \equiv \frac{\Delta - \bar{\Delta}}{\epsilon_{max}} - \kappa(1 + \beta^2 - c) , \tag{58}$$

Vavilov obtained

$$f(x,\Delta) = (\pi\xi)^{-1}\kappa\exp[\kappa(1 + \beta^2 c)] \int_0^\infty \exp(\kappa f_1)\cos(y\lambda_1 + \kappa f_2)\, dy , \tag{59}$$

where

$$\begin{aligned} f_1 &\equiv \beta^2[\ell n\, y - Ci(y)] - \cos y - y\,Si(y) , \\ f_2 &\equiv y[\ell n\, y - Ci(y)] + \sin y + \beta^2 Si(y) , \\ Si(y) &\equiv \int_0^y \frac{\sin u}{u}\, du \quad \text{(sine integral)} , \\ Ci(y) &\equiv \int_{-\infty}^y \frac{\cos u}{u}\, du \quad \text{(cosine integral)} . \end{aligned} \tag{60}$$

When $\kappa = 0$, this function reduces to the Landau distribution (40), and when $\kappa \gg 1$, the function becomes a Gaussian. For intermediate values of κ, numerical integration yields a family of curves with parameters κ and β^2, which effect a smooth transition between the Landau spectrum and the Gaussian. Thus Vavilov showed analytically that the parameter κ is most significant in the study of fluctuations of ionization energy loss.

The problem of binding-effect corrections to the energy-loss distribution function was considered by Rosenzweig in 1959.[26] By applying perturbations to Symon's development, he showed that in the cases in which binding effect is important (e.g., protons $\lesssim$ 5 MeV), the width of the distribution is increased, and the most probable energy loss lies further from the mean energy loss.

In 1961, Börsch-Supan evaluated numerically Landau's expression (41) for $\varphi(\lambda)$, and tabulated his results for a wide range of λ.[27] It is interesting to note the discrepancies between his values and Landau's (e.g., Börsch-Supan finds the maximum of $\varphi(\lambda)$ at $\lambda = -0.225$, whereas Landau's value is $\lambda = -0.05$.)

Ritson developed several simple approximate rules for evaluating the fluctuation phenomena, by substituting for constants and assuming that $Z/A \approx 1/2$ for most materials.[28] For example, when

$$\begin{aligned} &\beta^4/(1 - \beta^2) \ll 0.077 s z^2 \quad \text{(Gaussian distribution valid)}, \\ &\beta^4/(1 - \beta^2) \gg 0.077 s z^2 \quad \text{(Landau distribution valid)}, \end{aligned} \tag{61}$$

where $s \equiv \rho x$ = "pathlength" in g/cm^2.

In 1962, Lindhard and Nielsen estimated the effect of nuclear collisions on energy-loss fluctuations;[29] they found that it results in an FWHM* contribution of about 6 keV for 6-MeV α particles, and becomes more important for higher charge numbers and lower velocities.

Fano, in 1963, published a thorough review of the penetration of protons, α particles, and mesons.[1] In it he discussed the connections between the different theories of energy-loss fluctuations, and showed in particular how the Blunck-Leisegang correction can be applied to the rigorous Vavilov distribution. If we denote by $f_V(\Delta,x)$ the Vavilov distribution, the corrected distribution is given by

$$f(\Delta,x) = (\xi b\sqrt{\pi})^{-1} \int_{-\infty}^{\infty} f_V(\Delta - u,x)\exp[-(u^2/\xi^2 b^2)]\, du \ . \qquad (62)$$

Berger discussed, in 1963, the Monte Carlo calculation of the penetration and diffusion of fast charged particles.[30] It is clear that much of the fluctuation phenomenon is due to the few collisions in the highest collision-loss interval, and it thus appears that a mixed computational technique could be well adapted to the problem considered here, i.e., analytical calculation for the lower collision-loss intervals where collisions are very numerous, and Monte Carlo for the higher intervals.

In 1964, Morsell used Monte Carlo techniques with three different assumed discrete collision spectra in order to predict the energy-loss distribution of 992-keV protons in thin carbon films.[31] Skofronick et al. used similar methods in their study of γ-ray yield curves from

---

*FWHM $\equiv$ full width at half maximum = 2.356 standard deviations for a Gaussian distribution.

semithick aluminum targets.[32]

Breuer used a simple relation for the width of the Landau distribution, i.e.,

$$\text{FWHM}_{\text{Landau}} = 3.98\xi \ , \tag{63}$$

and Blunck's broadening corrections to calculate the ionization correction for electron scattering cross sections in 1964.[33]

The numerical quadrature of Vavilov's rigorous (but difficult) expression (59) was performed by Seltzer and Berger in 1964.[34] They provided a systematic and comprehensive tabulation of the Vavilov distribution in terms of the parameters κ and β^2, and furnished tables relating κ and β^2 to the absorber thickness and particle energy.

Finally, in 1966, Golovin et al. gave a slightly different formula for the correction to the Vavilov distribution due to atomic electron binding.[35] Their corrected expression is

$$f(x,\Delta) = (\pi\epsilon_{max})^{-1}\exp[\kappa(1 + \beta^2 c)] \int_0^\infty \exp[\kappa(f_1 - Dy^2/\epsilon_{max})]\cos(y\lambda + \kappa f_2)\, dy \ , \tag{64}$$

where

$$D \equiv \frac{4}{3} \sum_n I_n (Z_n/Z) \ln (2mv^2/I_n) \cong \xi b^2/2 \ . \tag{65}$$

This correction should lead to essentially similar results as the Blunck-Leisegang correction.

A Note on Electrons

Much of the theory we have discussed may be carried over directly for charged particles that are not heavy, such as electrons. The

exceptions are due to the physical properties of electron-electron collisions: in a collision with an identical particle, quantum-mechanical exchange effects can occur, and the electron can lose all of its energy in a single collision, i.e., $\epsilon_{max} = E$. There is an increased probability for large-angle scattering, which tends to vitiate our concept that the path length is equal to absorber thickness. Also, radiation losses must be considered for the more energetic electrons.

Summary of Theory and Evaluation of Constants

If $\kappa \gg 1$, the energy-loss distribution is Gaussian [Eq. (23)] with the most probable energy loss Δ_{mp} equal to the mean energy loss $\bar{\Delta}$, and variance σ^2.

If $\kappa \lesssim 0.01$, the Landau distribution (40) is valid, with Δ_{mp} considerably less than $\bar{\Delta}$, and FWHM = 3.98ξ.

If $0.01 \lesssim \kappa \lesssim 1$, the Vavilov solution (59) must be used for these intermediate cases.

If we let $s \equiv \rho x$ = thickness of absorber in g/cm^2, then

$$\kappa = 0.150 \frac{sZz^2}{A} \left(\frac{1 - \beta^2}{\beta^4} \right), \tag{66}$$

$$\xi = 0.1536 sZz^2/A\beta^2 \quad \text{(in MeV)}, \tag{67}$$

$$\bar{\Delta} = 2\xi \left[\ell n \frac{2mv^2}{I(1 - \beta^2)} - \beta^2 - \frac{C}{Z} - \frac{\delta}{2} \right], \tag{68}$$

$$\sigma^2_{Bohr} \cong 0.157 sZz^2/A \quad \text{(in MeV}^2\text{)}, \tag{69}$$

$$\Delta_{mp}(\text{Landau}) = \xi \left[\ell n \frac{2mv^2 \xi}{I^2(1 - \beta^2)} - \beta^2 + 0.37 \right] . \qquad (70)$$

If the Blunck parameter $b^2 \cong \bar{\Delta}Z^{4/3} \cdot 20\text{eV}/\xi^2 > 3$, this treatment must be corrected for resonance broadening, and if $\beta^2 \to 1$, Δ_{mp} must be corrected for density effect.

B. Experimental

There has been a large amount of experimental work done on the penetration of protons, α particles, and mesons in matter, and many experimenters have touched on the problem of fluctuations of energy loss in "thin" layers. As background to our experimental work, we present here an eclectic review of the previous work on fluctuations, without any claim to comprehensiveness.

Before the widespread availability of fast heavy charged particles from accelerators and the discovery of cosmic rays, natural α particles were the only available source of heavy particles for studies of straggling. Because natural α particles are relatively slow, their energy-loss distributions are Gaussian and relatively narrow in most practical cases. Thus the earliest work on non-Gaussian fluctuations was done with β particles and cathode rays (electrons). We therefore include here some of the experimental work on electrons.

White and Millington found, in 1928, that the velocity loss distribution of natural betas shows a systematic divergence from the Bohr theory.[36] Other early work was done by Briggs, Lewis, and Wynn-Williams,

Bennett, Furry, and Paul and Reich.[37] Chen and Warshaw found agreement with the Landau-Blunck theory of the most probable energy loss for Cs^{137} conversion electrons in thin foils.[38] Birkhoff used Ba^{137} conversion electrons to find straggling widths greater than the theoretical.[39] Rothwell used minimum-ionizing electrons to find agreement with Landau on Δ_{mp}, but an increased width on the low-energy-loss side of the peak.[40] Goldwasser, Mills, and Hanson found good agreement with the Landau distribution for 9.6- and 15.7-MeV electrons in light elements.[41] Kalil and Birkhoff found agreement with Blunck-Leisegang for 624-keV electrons in heavy elements,[42] and Hungerford and Brikhoff found agreement in light elements.[43] Kageyama found agreement with Landau's Δ_{mp} for 1.4-MeV electrons.[44] In 1962, Rauth and Hutchinson measured the distribution in energy of the primary energy-loss events of 5- to 20-keV electrons in very thin foils.[45]

The cosmic-ray spectrum is a plentiful, if inhomogeneous, supply of fast heavy charged particles. We list here some of the experiments which dealt with the energy-loss fluctuations of cosmic ray and accelerator mesons. Bowen and Roser in 1951 found good agreement with the Landau distribution for minimum-ionizing cosmic-ray muons,[46] as did Hudson and Hofstadter.[47] Cranshaw reviewed the application of energy-loss theory to fast-particle experiments, and found agreement with Blunck-Landau for mesons.[48] Parry et al. found agreement with Landau for cosmic-ray mesons in argon,[49] and Bowen used both cosmic-ray muons and cyclotron-produced mesons to show agreement with Landau's Δ_{mp}.[50] Palmatier et al., however, found a broader distribution than the Landau

prediction,[51] as did van Putten and Vander Velde for accelerator pions at 1.5 and 2.55 BeV/c.[52]

The advent of particle accelerators made possible intense beams of high-energy protons and α particles which are ideal for studies of energy straggling. Indeed, a knowledge of energy-loss fluctuations is necessary for the interpretation of many accelerator experiments. Madsen and Venkateswarlu found good agreement with the Bohr theory for low-energy protons in 1948,[53] but Madsen in 1953 found deviations, perhaps due to foil inhomogeneity.[54] Nielsen found moderate agreement with Lindhard and Scharff's modification of Bohr's theory for protons and deuterons of 1.5 to 4.5 MeV.[55] Porter and Hopkins used 5.3-MeV alphas to find deviations from a Gaussian in the form of a pronounced "tail."[56] Reynolds et al.[57] found a broader-than-Landau distribution for 426-keV protons, which Hines' theory explained.[23] Igo, Clark, and Eisberg and Igo and Eisberg found moderate agreement with Landau for 31-MeV protons.[57] Chilton et al. found straggling of 400- to 1050-keV protons to be of the same order of magnitude as the predictions of the Livingston-Bethe-Bohr theory.[58] Gooding and Eisberg found good agreement with the Landau-Symon theory for 37-MeV protons in 1957,[59] and Demichelis found agreement with Livingston-Bethe for 5.3-MeV alphas in 1959.[60] Koch, Messier, and Valin found agreement with Landau on Δ_{mp} of protons and pions of 615 to 1478 MeV/c,[61] and Miller et al. found very good agreement with the Landau distribution curve for protons and pions of 3 to 4 BeV/c.[62] Labeyrie noted the Landau effect for cosmic high-energy particles in 1961.[63]

The work of van Putten and Vander Velde,[52] Koch et al., Miller et al. and Labeyrie is of special interest because they showed the usefulness of semiconductor detectors for measurements of energy loss of high-energy charged particles. In particular, Miller et al. suggested in 1961 that thick semiconductor detectors with uniform depletion layers offer the best means of accurate evaluation of the theories of energy-loss fluctuation.

Rosenzweig and Rossi did a detailed study of statistical fluctuations in the energy loss of 5.8-MeV α particles passing through a proportional counter of variable effective thickness.[64] They found general agreement with the Symon theory for κ values from 0.11 to 3.56, provided that corrections were applied for the effects of electron binding and δ-ray* escape from the detector; their measurements, however, are limited by the statistics and inherent resolution of their counter system. Morsell measured energy-loss distributions of 992-keV protons in thin carbon films, and found good fits with distributions computed by Monte Carlo techniques.[31] Galaktionov, Yech, and Lyubimov found agreement with the Landau distribution for protons and pions of 600 MeV/c in spark chambers.[65] Lander et al. measured the shift in the Landau peak due to silicon recoils from 730-MeV protons in their study of coherent production in semiconductor detectors, but observed a 20% broadening of the FWHM.[66] Grew found agreement with Symon on the most probable energy loss of 50- to 160-MeV protons in semiconductor detectors, but noted broadening of the distribution due to collimator

---

*A δ ray is an energetic recoil electron from an ionizing collision with energy $\gtrsim$ 1 keV.

scattering.[67] Finally, Rotondi and Geiger in 1966 observed good agreement with Livingston-Bethe for Po^{210} α particles in air.[68]

Summary of Experimental Work

There is good experimental evidence for the validity of the Bohr-Livingston-Bethe theory for natural α particles and low-energy protons, for which $\kappa \gg 1$. Similarly, there is strong evidence for the validity of the Landau-Blunck-Leisegang theory for electrons and high-energy protons and mesons, for which $\kappa \lesssim 0.01$. There is only a small amount of unambiguous data, however, in the intermediate region of $0.01 \lesssim \kappa \lesssim 1$, where Symon's interpolation and Vavilov's exact expression are held to be valid. The purpose of our experiments is to supply the needed data for all the low and intermediate range of the significant parameter κ.

III. EXPERIMENTAL METHOD

Our experimental method basically consists of passing a beam of fast heavy charged particles through a silicon semiconductor detector and measuring the energy losses in the detector. Semiconductor detectors are used because of their superior resolution for this purpose, the relative uniformity and thickness of their sensitive layers, the linearity of their response, and their high stopping power; heavy-charged-particle beams from accelerators are convenient because they can be precisely controlled and suffer comparatively little scattering in the detectors. In a given experiment, the detector is mounted in a plane normal to the beam axis and bias voltage is applied. The charge pulses formed due to ionization and excitation in the detector are then amplified, and sorted (individually) in a multichannel pulse-height analyzer (abbreviated PHA). Information from the PHA is then printed out in the form of counts per channel versus channel number. This information may then be processed to yield a plot of relative probability versus energy loss in the detector, with the assumption that the pulse height is directly proportional to the energy loss in the detector.

We first describe briefly the characteristics of the particle beams used, then in more detail, the detectors, associated electronics, and calibration techniques.

A. High-Energy Beams of Heavy Charged Particles

There are certain inherent advantages in using accelerator beams of heavy charged particles for the study of energy-loss fluctuations,

in contrast to the problems in the use of natural α and β particles, cosmic-ray mesons, and electron beams. Accelerator beams are generally precisely controlled in intensity, homogeneity, and beam "optics," and can be made very close to mono-energetic. High-energy beams can have enough range of penetration so that absorbers upwards of 0.1 g/cm^2 can be regarded as "thin." Heavy-particle beams experience relatively little scattering in their electronic collisions in the material, by contrast with the tortuous path of electrons, whose path length is often not identical with the thickness of absorber.

Cosmic rays are neither homogeneous, mono-energetic, nor uniform in intensity or alignment. Natural alphas and betas have small ranges of penetration such that making foils which are "thin" in energy loss becomes difficult, and foil inhomogeneity is a recurring problem.

We have used beams of 730-MeV protons, 910-MeV α particles (He^{++} ions), and 370-MeV negative pions from the 184-inch synchrocyclotron at the Lawrence Radiation Laboratory, Berkeley, and 45.3 MeV protons from the Berkeley 88-inch isochronous (sector-focussed) cyclotron. We have thus bracketed a range of β^2 from 0.09 to 0.92. The external 730-MeV proton beam has an energy spread of 14 MeV and a flux of up to 2×10^{10} particles/cm^2-sec over approximately 25 cm^2, while the alpha beam has a slightly smaller flux.[69] In practice, the peak current in a 184-inch proton beam pulse is 120 μA (64 pulses per second, each of 500 μsec duration), which is far too large for our detection system, owing to problems with accidental coincidences, pulse superposition, charge collection, etc., so that the synchrocyclotron is operated during

our experiments in the "stretched-beam" or "long-spill" mode, at the lowest practical intensity. The pion beams in the meson "cave" of the 184-inch cyclotron have an energy spread of about 10%, and a flux on the order of 1000 particles/cm^2-sec over approximately 100 cm^2. The proton beam of the 88-inch cyclotron is continuously variable in energy from 15 to 55 MeV. The beam which was used in Cave #2 had an energy of 45.3 ± 0.1 MeV and was obtained by scattering the original high-intensity beam (range: 2.458 g/cm^2 Al) at a lab angle of 11.2° from a gold target of 200 μg/cm^2.

B. Semiconductor Detectors

In many experiments on the penetration of energetic particles in matter, a standard method is used: a beam of known energy and intensity is passed through an absorber of known thickness, and a particle detector and/or a magnetic spectrometer is used to measure the energy spectrum of the emergent particles. The energy-loss distribution is obtained by subtraction of the spectrum of remaining energies from the initial energy. Our experiments are a variation of this method--we combine the functions of absorber and detector in a single device. That is, we use a planar semiconductor detector of known thickness as our absorber, and measure the charge pulses formed at the detector contacts due to the ionization and excitation of the semiconductor material by the charged particles. Since the charge pulse is in general a linear function of the ionization and excitation energy deposited in the detector,[70] we have a direct method of measurement of the energy-loss spectrum of the

particles. (Lander has reported an interesting variation on the same theme--the idea of combining the functions of target and semiconductor detector in studies of coherent scattering.[66])

This idea is not new--gas detectors and solid scintillators have been used in the same capacity, but there are several inherent advantages in the use of semiconductor detectors. The density of the solid semiconductor is on the order of a thousand times that of a gas, yielding that many more energy-loss collisions per unit path length. The average energy required to create a charge pair in silicon is 3.66 eV[71] (approximately a tenth of the value for gas) yielding ten times as many charge pairs and thus improving statistics and resolution. Semiconductor detectors exhibit no saturation effects as in scintillators, and no wall effect as in gas counters. Semiconductors have a great enough charge carrier mobility* in relation to their size so that they have a short pulse duration, allowing high count rates, fast coincidence logic, etc.

Until recently, however, semiconductor detectors were limited in sensitive thickness to fractions of a millimeter. The development of the "lithium-drifting" process[72] by Pell and others has solved this problem, permitting fully compensated depletion layers upwards of 5 mm in thickness. In addition, lithium-drifted "p-i-n" detectors are generally more uniform in depletion-layer thickness than the thinner "p-n" detectors. These advances in technology have made possible

---

*E.g., silicon electron mobility-- 1350 cm^2/volt sec. at 300°K,[71]
silicon hole mobility-- 480 cm^2/colt sec. at 300°K.

reliable detectors with good enough resolution to measure energy-loss distributions accurately, and with sufficient thickness to explore the intermediate range of the parameter κ for high-energy particles.

Before proceeding further, we will try to explain simply the construction and operation of semiconductor detectors, especially the lithium-drifted silicon detectors which we have mainly used. Perhaps the simplest analogy is that of a solid-state ionization chamber, i.e., passage of a charged particle results in ionization in the solid, with attraction of opposite charges toward the particle track, and repulsion of the like charges; e.g., electrons are attracted to a proton track, and positive ions are repelled. This initial charge separation is amplified by an externally applied electric field which sweeps out the charges to collecting electrodes of opposite polarity. The essence of this process is thus the use of a material in which:

(a) the spontaneous generation of charge carriers (due to thermal agitation, etc.) is small compared with the charge formed by ionization,

(b) the number of charge-trapping impurities is small,

(c) resistivity is such that an electric field can be maintained which is sufficient to sweep out all the charge carriers before recombination occurs,

(d) carrier lifetime and mobility are sufficient for efficient charge collection,

(e) the mean energy per hole-electron pair is low enough for good energy resolution.

The two materials known to approach these requirements are single-

crystal silicon and germanium.* These atoms have four valence electrons bonded equally with four nearest-neighbor atoms. At very low temperatures, all valence electrons are bound and the materials act as insulators; at higher temperatures, some of the covalent bonds are broken by thermal excitation and electron-hole pairs are produced, i.e., electrons "jump the forbidden band-gap" (1.12 eV at 300°K in Si)[71] from the valence band to the conduction band. Semiconductor material with no electrically active impurities is called intrinsic, and conduction is dominated by thermally excited charge pairs. In most practical cases, however, impurities are present, and conduction is dominated by charge carriers introduced by the impurities--this is called extrinsic material.

When an element of valence 5 (e.g., phosphorus) is deliberately substituted for silicon atoms at crystal lattice sites, only four electrons are needed to complete the covalent bond structure and the fifth is easily excited into the conduction band. These impurities are called donors, and the material is called n-type, since conduction is dominated by negative charge carriers. Similarly, replacement of silicon atoms by valence-3 atoms (e.g., boron) produces mobile "holes;" these impurities are called acceptors and the material is called p-type.

A third case of interest is that of foreign atoms, placed in the interstices of the crystal lattice, which can act as either donors or acceptors, e.g., lithium (valence 1), which acts as an interstitial

---

*For convenience, we discuss only silicon in much of the following treatment.

donor in silicon and germanium. This case is particularly interesting because under certain conditions the positively charged lithium atoms can migrate close to acceptor atoms and pair with (i.e., compensate) the negatively charged acceptors. This "lithium-drifting" process can thus result in the creation of artificial "intrinsic" material of high resistivity (often referred to as i-type).

A detailed discussion of solid-state physics and semiconductor junction theory is clearly beyond the scope of this work. Suffice it to say that when there are discontinuities between two or three regions (e.g., p-n, p-i-n junctions), all free charge carriers can be depleted from a sizable layer under reverse bias conditions, that is, when a positive voltage is applied to the n-type side of the junction. Under these conditions, a strong electric field can be maintained, with low noise. More expert treatments of this subject have been given by Goulding,[71] Dearnaley,[73] and others.

In the making of a lithium-drifted detector,[74] the donor lithium is first evaporated onto the surface of bulk p-type silicon, then the temperature is raised to about 400°C and lithium diffuses into the silicon. A reverse bias of about 500 V is then applied to the resulting p-n junction, and the positive lithium ions slowly migrate into the p region, where they tend to accurately and completely compensate the acceptor atoms. At 130°C, it takes about 60 hours to drift an intrinsic region 3 mm thick. Evaporation of gold contacts on the n and p surfaces completes the process. A cutaway diagram of a lithium-drifted silicon detector is given in Fig. 2, and a photograph of a finished

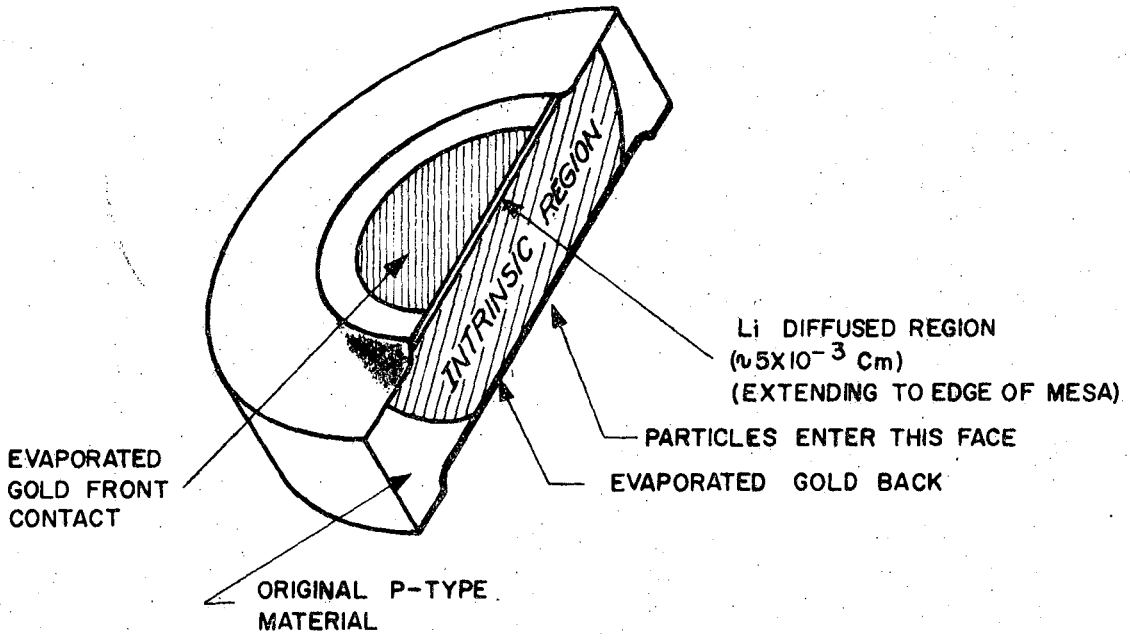

FIG 2.
CUTAWAY VIEW OF LITHIUM-DRIFTED SILICON DETECTOR

MUB-6981

detector is given in Fig. 3.

We thus have a detector with a macroscopic layer of intrinsic material which is depleted of free charge carriers under reverse bias conditions. Normally the positive voltage applied to the n-type surface is given by the formula

$$V_{min} = 100T + 50 \text{ (V)} , \qquad (71)$$

where T ≡ device thickness in mm. This voltage is generally sufficient for a pulse-collection time on the order of 100 nanoseconds. Under these conditions, the depletion layer is sensitive to the formation of any new charge pairs, as by the passage of an ionizing particle. As one might guess, the detector is also sensitive to ionization or excitation produced by photons, and thus the detectors are usually mounted and operated in a lighttight box.

Normally, the leakage current (or dark current) due to thermal noise at room temperature is a few microamperes. When the best possible resolution is required, this value can be reduced to the nanoampere region by cooling the detectors down to dry-ice evaporation temperature ($-78.5^{\circ}C$) or to liquid-nitrogen boiling temperature ($77^{\circ}K$). This is generally done by conduction, e.g., mounting the detector on a base of heat-conducting metal which is continuous with a wire or rod leading to a reservoir of coolant. A simplified drawing of a cooled detector holder in shown in Fig. 4. The temperature is then monitored by a thermocouple gauge connected to a thermocouple soldered on the detector base, and can be controlled precisely by a simple electrical resistance

ZN-5365

Fig. 3. Photograph of finished lithium-drifted silicon detector.

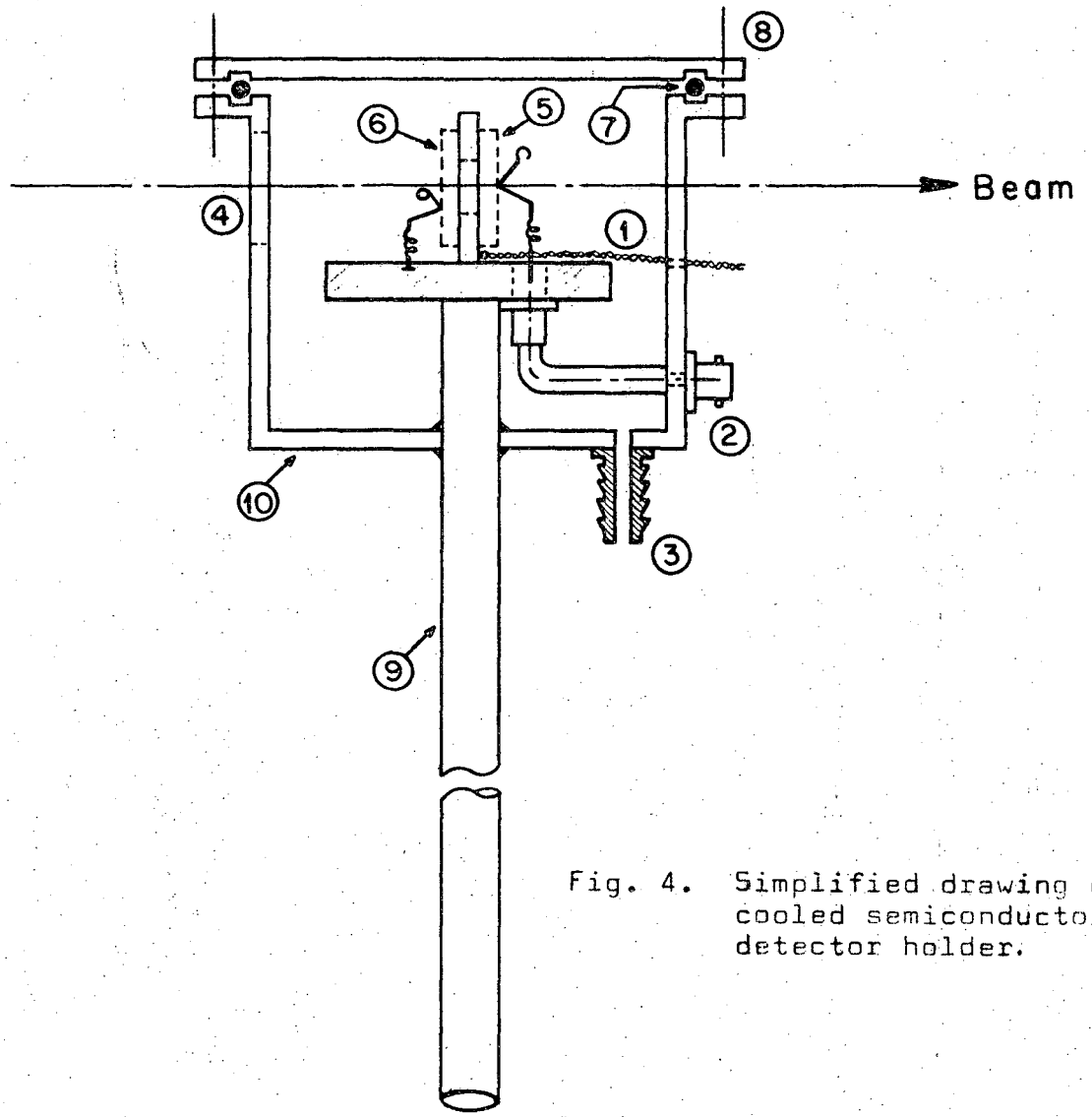

Fig. 4. Simplified drawing of cooled semiconductor detector holder.

1. Thermocouple Wires
2. BNC Cable Connection
3. Vacuum Port
4. Vacuum-Radiation Window - 2 mil Mylar
5. Si Detector held by spring voltage clip
6. Calibration Source held by spring clip
7. Vacuum Ring
8. Quick-seal fastening
9. Heat-conducting Al Base
10. Vacuum tight casing - 1/8" Lucite painted black

MUB 11902

"heat leak." (Due to its narrower band gap of 0.67 eV at room temperature, germanium has a much higher thermal leakage current, and Ge detectors must always be stored and operated at liquid-nitrogen temperature; this inconvenience is mainly responsible for the choice of silicon for most detectors, except when the higher Z of Ge is desirable for X- and γ-ray detection, or when their slightly better resolution is needed.)

When a charged particle passes through a semiconductor detector, the kinetic energy loss of the particle is accompanied by kinetic energy gain of the electrons of the material. These energetic secondaries immediately produce more lower-energy electrons, etc., and the energy degrades into three main categories:

(a) energy used to raise a lattice electron from the valence band to the conduction band and produce a lattice hole,

(b) energy lost by lattice interactions, most of which appears in optical vibration modes, i.e., production of optical phonons,

(c) thermal energy lost to the lattice by the large number of very-low-energy electrons produced at the end of the cascade.

It is clear that if all the ionization energy were translated into hole-electron pairs, the energy per hole-electron pair would just be the band-gap energy (e.g., 1.12 eV for Si); since the average energy per pair is actually 3.66 eV for Si, it is evident that most of the ionization energy ends up in the vibrational and thermal modes. This phenomenon has been discussed by Van Roosbroeck[75] and is expressed in the form of the yield,

$$\text{yield} = \frac{\text{band-gap energy}}{\text{average energy per hole-electron pair}} \cong 30\% \text{ for Si.} \quad (72)$$

At any rate, the number of electrons and holes created is equal to the energy loss of the particle, Δ, divided by the average energy per hole-electron pair. The electrons are swept by the electric field toward the positive electrode, and vice versa, and thus the information on the particle energy loss appears in the form of the magnitude of the charge pulse collected at the detector contacts. It is now necessary to use an electronic system to process this information into usable form.

The collection time for a charge carrier crossing the whole depletion layer is given by

$$T_{coll} = \frac{x^2}{\mu \cdot V}, \quad (73)$$

where x = depletion layer thickness, μ = carrier mobility, and V = bias voltage [e.g., for $x = 2$ mm, $\mu = 1350$ cm^2/V-sec (electron in silicon), and $V = 250$ V, $T_{coll} = 120$ nanoseconds]. Most of the charges do not have to cross the whole depletion layer, and thus the pulse-rise time is a fraction of T_{coll}.

It is clear that in order to avoid pulse buildup in the detector and associated electronics, the number of particles incident on the thicker detectors must be kept below approximately 10^7 per second. Even more stringent limitations are placed by the necessity to avoid radiation damage to the detectors. For example, Mann and Yntema have shown that an integrated proton flux of $10^8/\text{cm}^2$ can result in signifi-

cant deterioration in the response of lithium-drifted silicon detectors.[76] In order to avoid these problems, we have generally limited the incident beam currents so that detectors were not exposed to more than 10^7 particles.

We have used lithium-drifted silicon detectors of sensitive thicknesses between roughly 0.5 and 5 mm. When thinner detectors were needed for work with lower-energy particles, we used silicon diffused p-n junction detectors with depletion layers between roughly 0.04 and 0.25 mm. Since the density of the silicon used is 2.33 g/cm^3, we have been able to cover more than two orders of magnitude in "path length," from 0.0085 g/cm^2 to 1.094 g/cm^2. Since the values of β^2 available have bracketed nearly an order of magnitude, we have thus been able to explore nearly three orders of magnitude in κ, from $\kappa = 0.0029$ to $\kappa = 2.23$.

C. Electronics

In order to take advantage of the good resolution, low noise, and fast pulse characteristics of the semiconductor detectors, an amplification system with similar characteristics is necessary. We have used preamplifiers and linear amplifier systems designed by Goulding and Landis especially for such applications.[77]

In order to minimize capacitance, cable lengths from detector to preamplifier are kept as short as possible (always less than 1 foot), while the cable length between preamplifier (in the irradiation cave) and amplifier (in the counting room) may run as much as 100 feet.

Preamplifiers used are of the charge-sensitive type, mainly because their gain does not depend on the detector capacitance, i.e., voltage output is directly proportional to charge input. When optimum resolution was of paramount importance, we used the UCRL type 11X2951 P-1 preamplifiers, with an EC-1000 vacuum tube in the first stage. This unit is rated at 5 keV resolution (FWHM) for a detector capacity of 20 pF (picofarads), and a normal output gain of 1.25 μV per ion pair, or 356 mV per MeV lost in the detector, and a risetime of less than 20 nsec. When high detector capacitance (i.e., very thin depletion layer) made optimum resolution impossible or large pulse size made it unnecessary, the UCRL type 11X3391-P3 miniaturized preamplifiers were used, with a type 2N3458 field-effect transistor in the first stage. Figure 5 shows the cooled detector holder, EC1000 preamplifiers, and associated equipment mounted in front of the cyclotron beam port.

The linear amplifier system used was the UCRL type 11X198 OP-1 (all solid state) containing a linear pulse amplifier with gain adjustable from 1 to 1350; a rise time of 75 nanoseconds; integral, differential, and delay-line pulse shaping; a single-channel analyzer; biased amplifier; and fast and slow coincidence logic. We find that (empirically) choosing the best time constants for the pulse shaping is of critical importance in optimizing the signal-to-noise ratio. An additional function of the pulse shaping is to convert the round-top exponential tail pulse from the preamplifier into a flat-top trapezoidal pulse which is acceptable to later logic steps.

In the course of preliminary experimentation, we found a significant

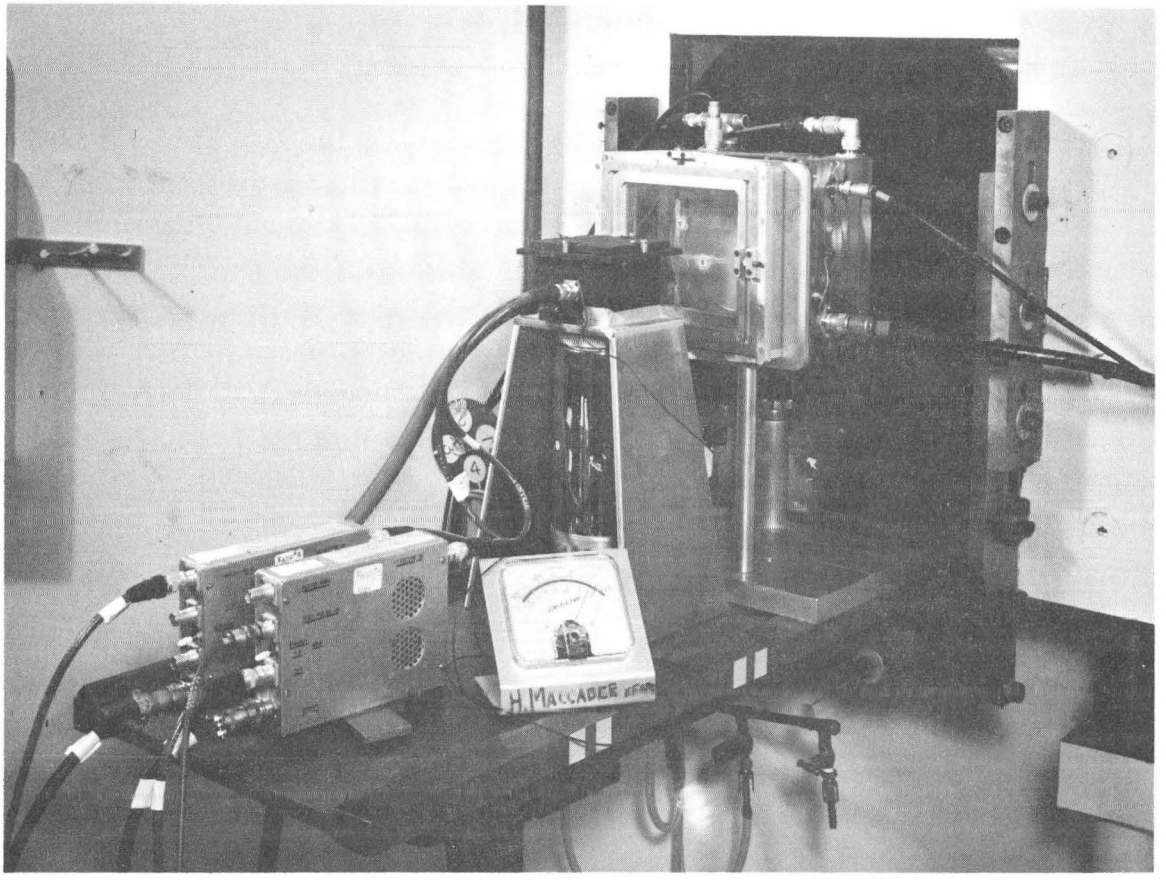

ZN-5728

Fig. 5. Photograph of cooled detector holder (black box), stand, liquid nitrogen Dewar flask, thermocouple gauge, preamplifiers, alignment cross hairs, and ionization chambers for beam monitoring, shown mounted in front of beam port in medical cave of 184-inch synchrocyclotron.

proportion of detected pulses to be anomalously small, due to particles that pass through the circumference of the sensitive "intrinsic" area (see Fig. 2). In order to avoid this difficulty, we instituted the use of an auxiliary detector with smaller sensitive area (~5 mm diam), aligned directly behind the main (analyzing) detector. The pulses from particles passing through the auxiliary detector are similarly amplified, shaped, and sized, and used as trigger pulses for a coincidence gate on the main pulses. Pulses from the main detector are accepted only if they are in coincidence with pulses from the auxiliary detector, i.e., only if they result from particles which have passed through both detectors. This system assures that the events analyzed are from the center area of the main detector; the system serves in lieu of collimators, which are impractical for beams with ranges of the order of a meter of aluminum. A block diagram of the experimental system used is shown in Fig. 6.

The pulses from the main detector that pass the coincidence gate are then sorted as to pulse size by a 400-channel pulse-height analyzer.* This analyzer accepts only flat-topped pulses of less than 10 V, so amplifier shaping and gain must be adjusted accordingly. The output of the PHA is fed to a digital printer† which prints out the data on a paper tape in the form of counts per channel versus channel number. Alternatively, the PHA output may be fed to an "X-Y plotter," which

---

*Technical Measurements Corp. Model 404-6.

†Technical Measurements Corp. Model 500.

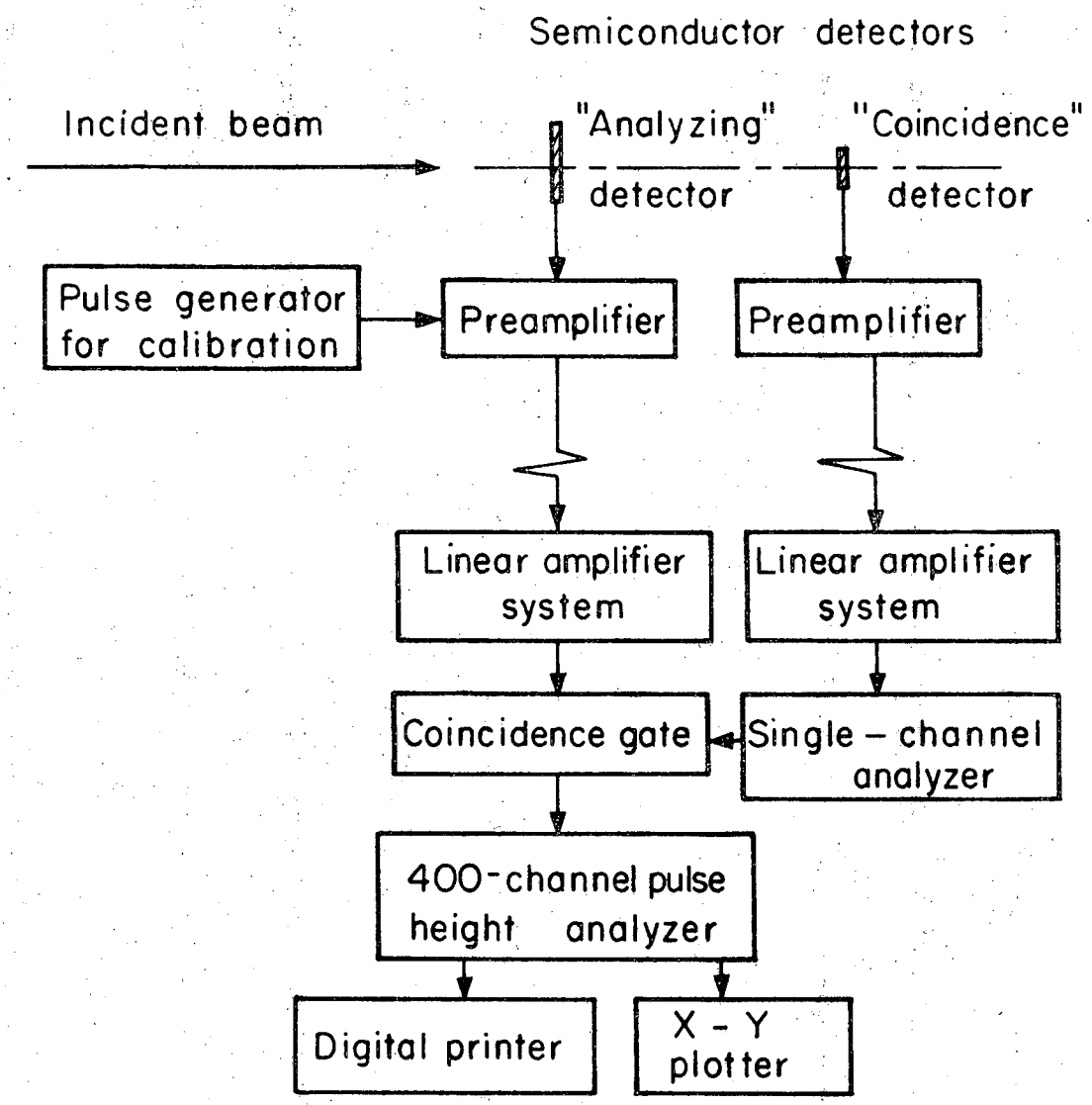

Fig. 6. BLOCK DIAGRAM OF EXPERIMENTAL SYSTEM.

MUB-9083

plots points corresponding to the number of counts in each channel, and is used to help visualize the shape of the pulse-height spectrum.

Bias voltages for the detectors and the preamplifier input tubes are furnished by standard types of regulated dc power supplies, while line voltage fluctuations are minimized by a standard ac voltage regulator. Pulse shapes and sizes throughout the system are monitored with a standard dual-trace oscilloscope, which is especially useful for simultaneously comparing pulses from both the main (analyzing) detector and the auxiliary (coincidence) detector. Figure 7 shows the amplifier and pulse-height-analysis systems rack mounted with the associated electronics.

D. Calibration

A tabulation of counts per channel versus channel number is useful only if channel number can be related to energy loss in the detector, and a frequency distribution of energy losses is useful only if related to the thickness of the detector (absorber). These two tasks are included under the title of calibration.

The calibration of channel number to energy loss is done by a standard method of spectrometry. The detector is exposed to radiation from a standard source with a known energy spectrum, the resulting pulse-height spectrum is printed out, and the channel numbers of peaks in the output spectrum are correlated with the energies of known peaks in the input spectrum. Linear interpolation or extrapolation then yields the energies corresponding to all other channel numbers. The

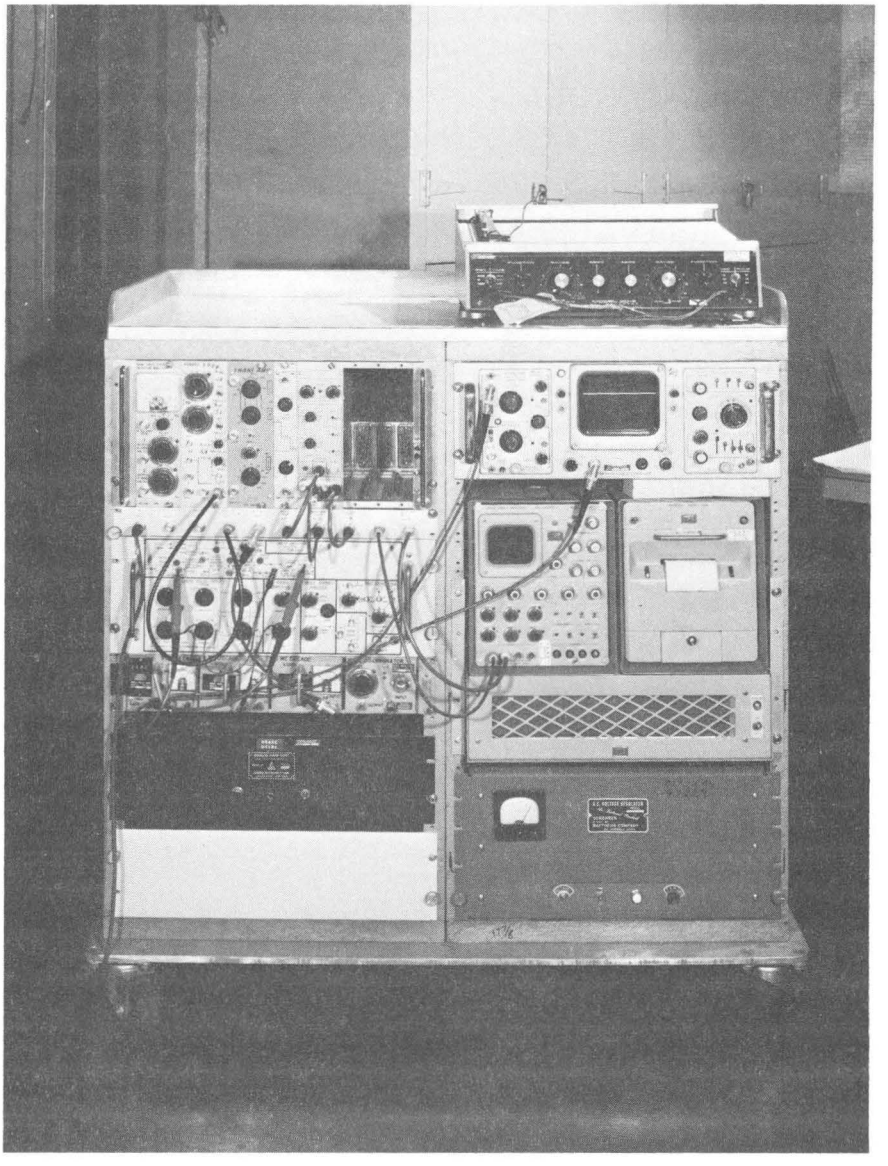

ZN-5729

Fig. 7. Photograph of rack-mounted electronic system, including (clockwise) x-y plotter, oscilloscope, pulse-height analyzer and digital printer, ac voltage regulator, dc power supply, beam-monitoring scalers, linear amplifier system, detector bias supply, and pulse generator.

linearity of the system may be checked easily, e.g., by looking at the system output when peaks corresponding to different energies of a known linear pulse generator are fed in.

Because amplifier gains are often changed during experiments, a slight modification of this calibration method is used in practice. The known energy-loss peaks are used to calibrate the dial of a linear pulse generator, and then the calibrated pulse generator is used to generate peaks in the output spectrum which bracket the peaks due to the experimental data. Interpolation yields the energies corresponding to the data peaks, etc., and since the calibration pulses are fed into the system along with the data pulses (i.e., before amplification), changes in gain do not affect the calibration. The sources we used for calibration were $_{83}Bi^{207}$, $_{95}Am^{241}$, and--when a low-energy peak was vital--$_{27}Co^{57}$. Bismuth-207 emits internal conversion electrons of 0.481, 0.553, 0.972, and 1.044 MeV, which are stopped by detectors with thickness greater than 1.9 mm. Americium-241 emits an α particle of 5.477 MeV, which has a range of only 0.027 mm of silicon, and is thus useful for checking the thickness of the detector entrance window. Cobalt-57 emits a γ ray of 122 keV and another less intense γ of 136 keV; separating the two photo peaks, which are only 14 keV apart, is a useful test of the detector and system resolution, although silicon is a rather inefficient material for stopping γ rays, due to its low atomic number. $_{83}Bi^{212}$ (6.05- and 6.09-MeV α) and $_{84}Po^{212}$ (8.7-MeV α) were also used in the 45-MeV proton-run calibration. Calibrations are performed in vacuum (a few microns of Hg) to avoid air scattering and

stopping, with the source mounted inside the detector holder about 2 cm from the entrance face of the detector.

Measurement of the sensitive thickness of the detector is slightly more difficult. A rough estimate (±4%) is obtained by subtracting the dead-layer thickness (known from past experience) from the easily measured over-all thickness. This estimate can be made more accurate (±2%) by actually measuring the dead layer, i.e., noting the residual energy deposited by an α particle of known energy after passing through the dead layer. A more accurate determination for the thicker detectors is made by exposing them to a spectrum of α particles with ranges of the order of the detector thickness, e.g., 30- to 100-MeV alphas. The maximum energy lost in the detector (i.e., the cutoff of the measured spectrum) corresponds to an α particle whose range is exactly equal to the sensitive thickness; particles with less range deposit less energy, and particles that pass through the detector deposit less because the ends of their tracks are not in the sensitive region. The accuracy of this method, developed by Raju,[78] is within ±2%.

Another method used for thickness calibration is the exposure to 910-MeV alphas with a well-known energy-loss spectrum (e.g., Gaussian); if the relation between the most probable energy loss and the absorber thickness is known, the measured Δ_{mp} is also a measure of the sensitive thickness of the detector. The accuracy of this method is also within ±2%, and this method may be used for cross-checking.

The normal experimental routine used follows this rough pattern. In the weeks before a scheduled cyclotron "run," we check the detectors

as to previous radiation damage, dead-layer thickness, and leakage (noise) current, and attempt a best estimate of depletion-layer thickness for each detector chosen. We then check the electronic system for linearity and resolution, using the pulse generator, and also attempt to determine the pulse-shaper time constants for optimum signal-to-noise ratio. The coincidence system and single-channel analyzer are also adjusted for acceptance and rejection of the proper pulses. The day before the run, the pulse generator is calibrated in energy as accurately as possible, by use of the radioactive sources; and all electronics are left on overnight in order to avoid the problem of warm-up drift the next day.

At the time of the run, the first step after "getting the beam" is to adjust the beam intensity to a level not injurious to the detectors, by monitoring with a scintillator or ionization chamber, and then the beam is turned off. The analyzing detector of choice is then placed in the detector holder, which is aligned with the beam and evacuated, and cooling to the desired temperature begins. Electrical connections are completed, and the detector bias voltage is applied. The beam is then turned on again and the pulse spectrum and pulse shapes in the system are checked. If all is in order, data are accumulated in the pulse-height analyzer until there are at least 5000 to 10 000 counts in the channels of greatest interest (10 000 counts yield a standard deviation of 100, or 1%.) The beam is then turned off and the cycle is repeated for the next detector chosen, while the data are being printed out, plotted, and labeled.

Immediately after the run, the pulser calibration may be checked again briefly. The data are then analyzed and compared with theory. The data reported in this work are the result of experiments covering approximately 2 years, and represent about 70 hours of cyclotron time.

IV. RESULTS

A. Comparison with Theory

After each experiment, the data in the form of counts per channel versus channel number are processed with the calibration information to yield a plot of counts per energy-loss interval versus energy loss.

For comparison, the Vavilov theoretical distribution is numerically evaluated by a computer code which uses the pertinent initial parameters of the experiment as input information. This code, which was developed by Seltzer and Berger and modified by Heckman and Brady,[79] takes the particle mass, velocity, and charge, and the "path length" s, the mean excitation potential I, and A/Z of the absorber, and computes ϵ_{max}, ξ, κ, and $\bar{\Delta}$, as well as a table of probability versus deviation $D \equiv (\Delta - \bar{\Delta})/\bar{\Delta}$. By use of simple calculations and a normalization such that the maximum probability corresponds to the maximum number of counts per channel, this table is converted to theoretical counts versus energy loss, and plotted on the same axes as the experimental data. For silicon-absorber data, we used A/Z = 2.0064, s = $(2.33\ g/cm^3)(x)$, where x is our best value of the depleted thickness, and I_{Si} = 176 eV. This value for the mean excitation potential is gotten by multiplying $(Z_{Si}/Z_{Al})I_{Al}$, where I_{Al} = 163 eV, the accepted value for aluminum.[80] The best method of obtaining I_{Si} would be an empirical determination from stopping power or range measurements; Bichsel has reported a value of I_{Si} = 170 eV,[81] but since the energy-loss formula depends only logarithmically on I, the difference is insignificant for our

purposes.

Figures 8 through 26 show the experimentally measured energy-loss distributions as compared with the theoretical predictions of Vavilov. For clarity, the ordinate has been expressed in terms of relative probability instead of counts. Vertical error bars are shown on the experimental points, corresponding to $\sigma \approx N^{1/2}$, where N = the number of counts in the energy interval. Although horizontal error bars are not shown, it should be understood that the accuracy of the experimental energy losses is probably no better than ±1%, owing to uncertainties in the channel-number–to–energy calibration, etc., and that the accuracy of the theoretical energy losses is probably no better than ±1% owing to uncertainties in the depletion thickness, I_{Si}, etc. For convenience, the calculated values of Δ_{mp} (the most probable energy loss), $\bar{\Delta}$ (the mean energy loss), and the Vavilov parameter κ are shown on each figure. The figures are arranged in order of decreasing κ.

Figure 8 shows the energy-loss distribution of 45.3-MeV protons in 0.265-g/cm^2 silicon, $\kappa = 2.23$. Note the slight asymmetry of the curve and that Δ_{mp} is slightly less than $\bar{\Delta}$. In general, there is very good agreement between theory and experiment on the value of Δ_{mp} and the shape of the curve, with a mild deviation on the low-energy side. We will discuss the deviations in this and the following distributions in a later section.

Figure 9 shows the energy-loss distribution of 910-MeV α particles (He^{++} ions) in 1.094-g/cm^2 Si, $\kappa = 1.69$. Note the clear beginnings of a high-energy-loss "tail." Figure 10 shows the distribution for 895-MeV

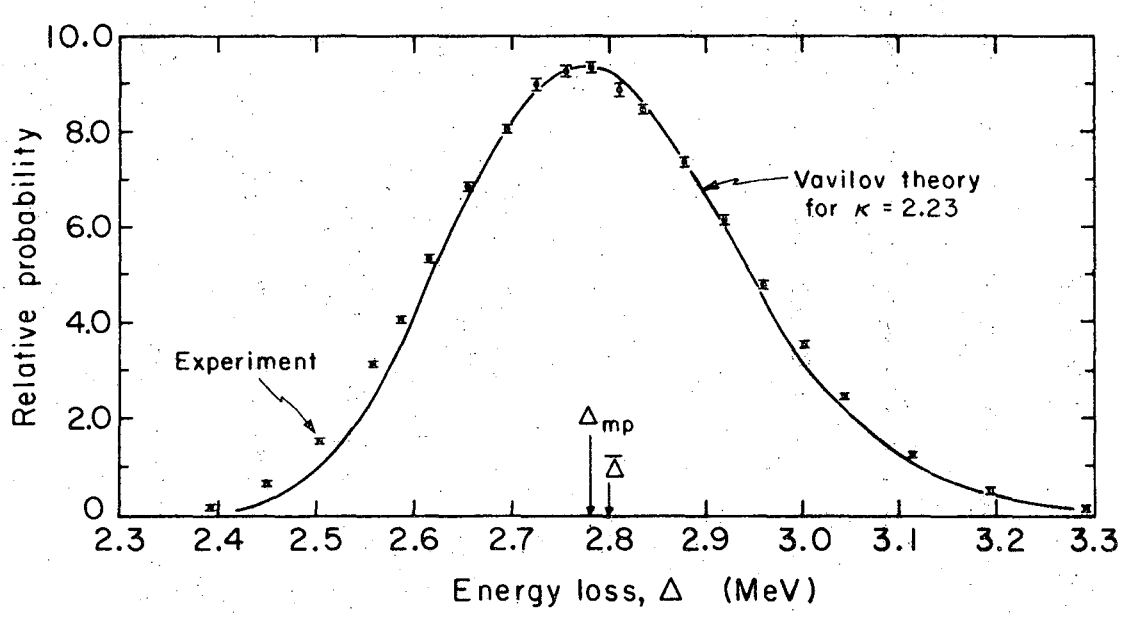

MUB 11530

Fig. 8. Energy loss distribution of 45.3-MeV protons in 0.265-g/cm^2 Si, κ = 2.23.

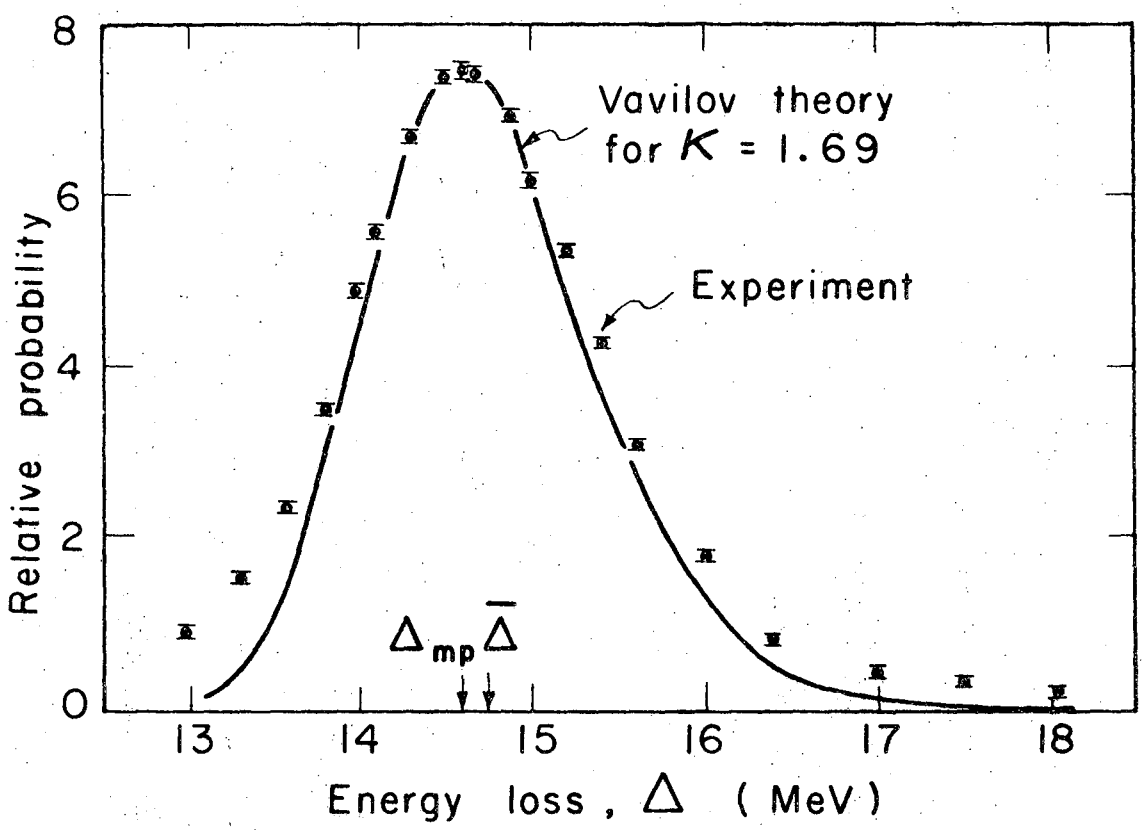

MUB 11430

Fig. 9. Energy loss distribution of 910-MeV alpha particles (He^{++} ions) in 1.094-g/cm^2 silicon, K = 1.69.

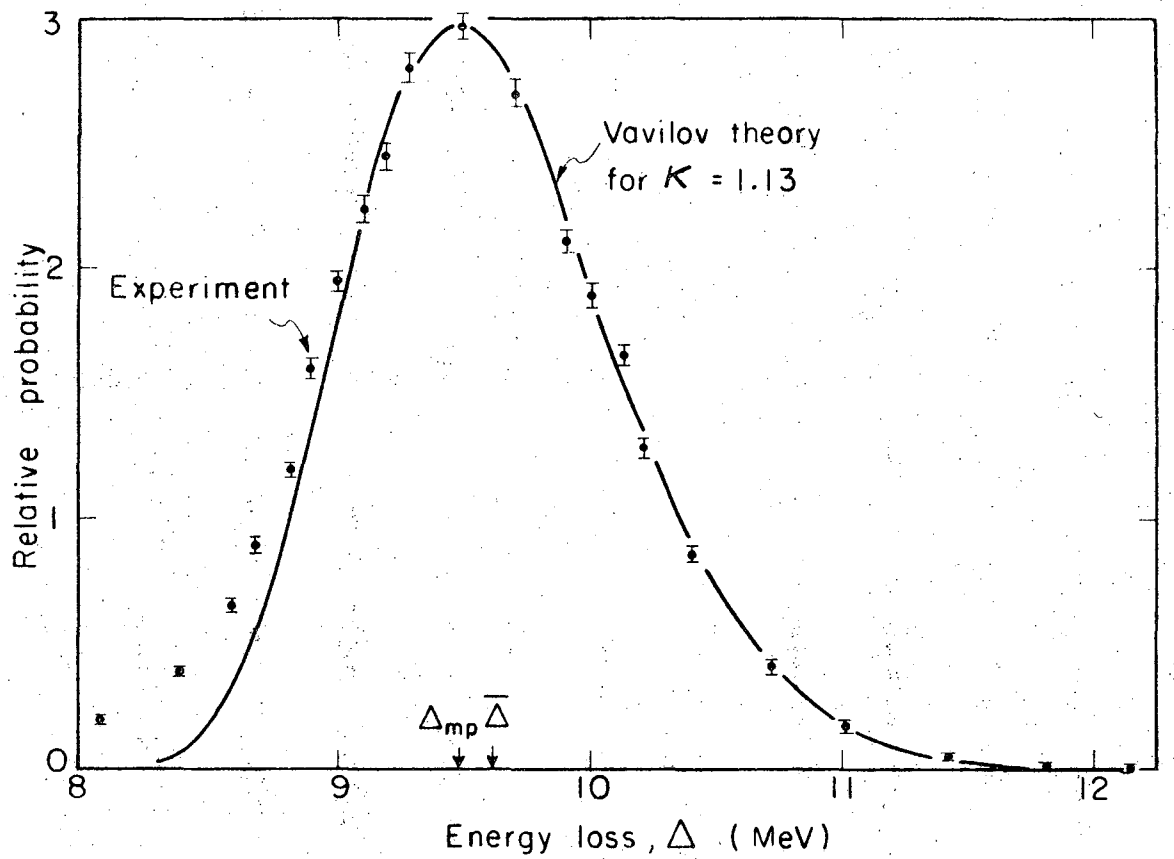

Fig. 10. Energy loss distribution of 895-MeV alphas in 0.707-g/cm^2 Si, κ = 1.13.

alphas in 0.707-g/cm^2 Si, κ = 1.13. Figure 11 shows the energy-loss distribution of 45.3-MeV protons in 0.127-g/cm^2 Si, κ = 1.07. There is excellent agreement between theory and experiment, with a very small deviation on the low-energy side.

Figure 12 shows the distribution for 895-MeV alphas in 0.560-g/cm^2 Si, κ = 0.892. The energy-loss distribution of 910-MeV alphas in 0.413-g/cm^2 Si is shown in Fig. 13, κ = 0.638. It appears that agreement would have improved if 0.411-g/cm^2 had been used as the thickness value; this adjustment, however, is well within the limits of experimental error. Figure 14 shows the distribution for 45.3-MeV protons in 0.070-g/cm^2 silicon, κ = 0.590. Note, in general, the very good agreement between the theoretical and experimental distributions for these higher intermediate cases (Figs. 8 through 14), where κ is of the order of unity. Note also the increase in the asymmetry with decreasing κ, the increasing tendency toward a high-energy-loss tail, and the decrease of Δ_{mp} relative to $\bar{\Delta}$.

Figure 15 shows the energy-loss distribution of 45.3-MeV protons in 0.383-g/cm^2 Si, κ = 0.323. Figure 16 shows the distribution for 910-MeV alphas in 0.206-g/cm^2 Si, κ = 0.318; agreement might be improved if 0.205-g/cm^2 were used as the thickness in the theoretical calculation; this adjustment is also within the limits of error. The distribution for 910-MeV alphas in 0.107-g/cm^2 silicon is shown in Fig. 17, κ = 0.165, and Fig. 18 shows the comparable distribution for κ = 0.160, 45.3-MeV protons in 0.019-g/cm^2 Si.

Figure 19 shows the energy loss distribution of 895-MeV α particles

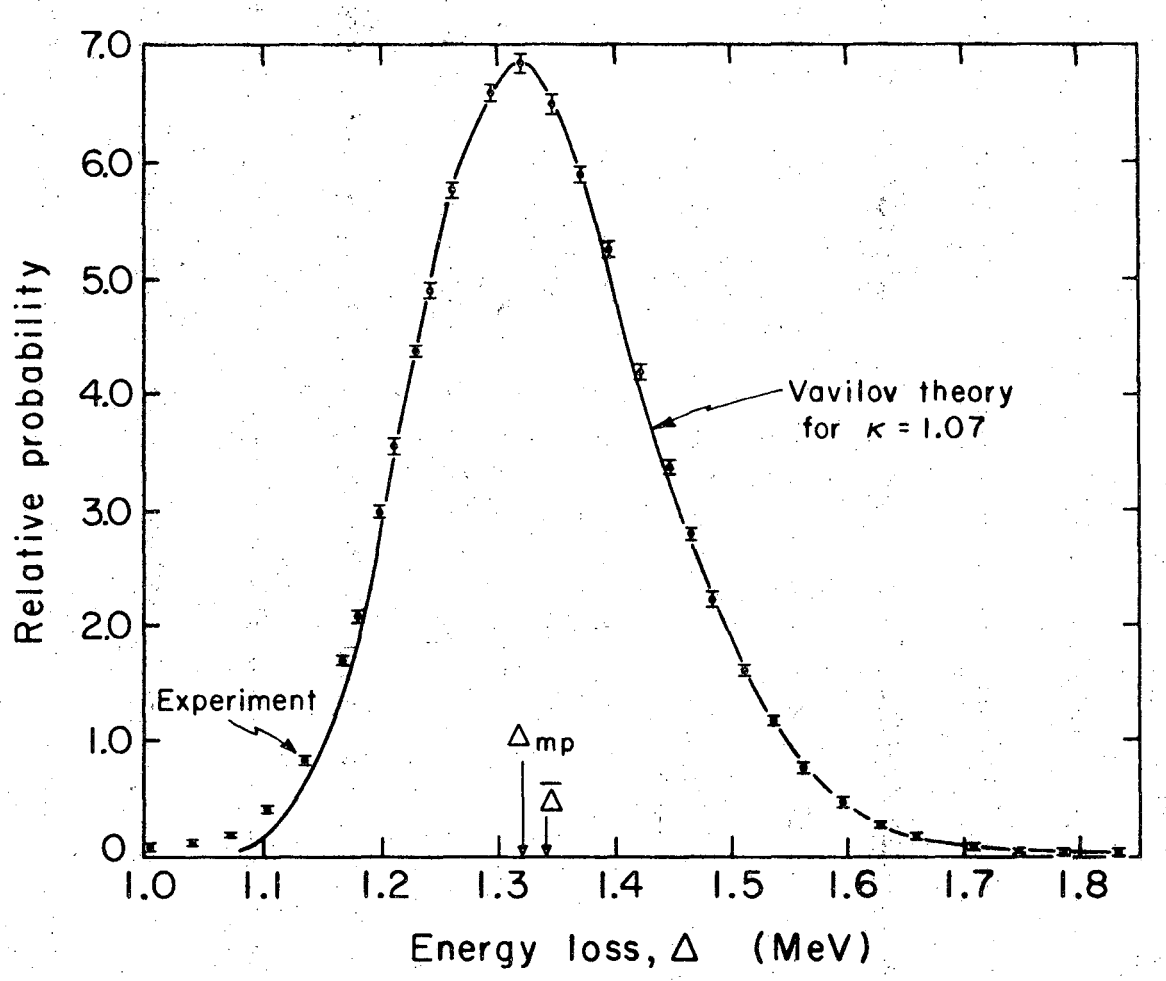

Fig. 11. Energy loss distribution of 45.3-MeV protons in 0.127-g/cm^2 Si, $\kappa = 1.07$.

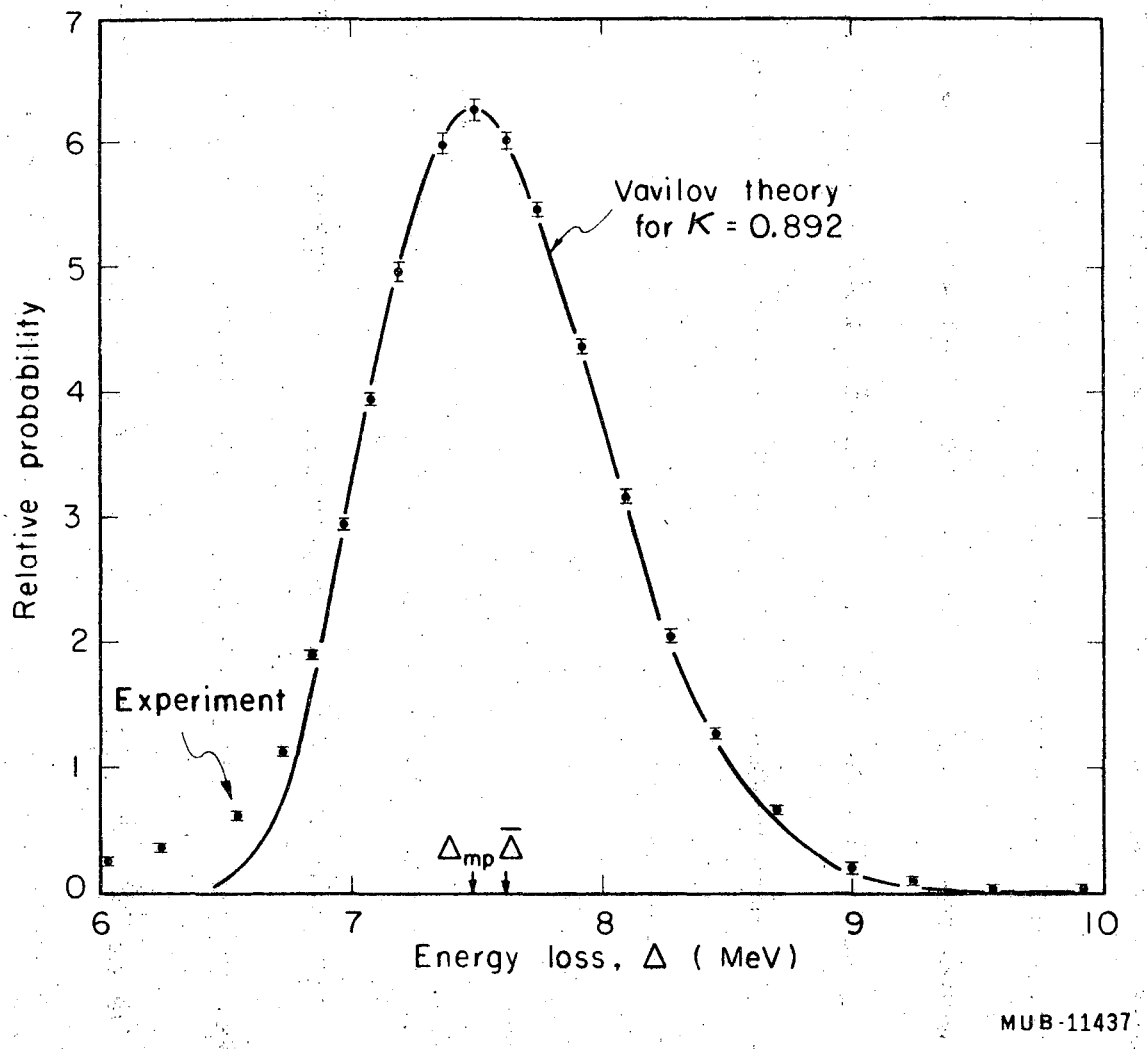

Fig. 12. Energy loss distribution of 985-MeV alphas in 0.560-g/cm^2 Si, κ = 0.892.

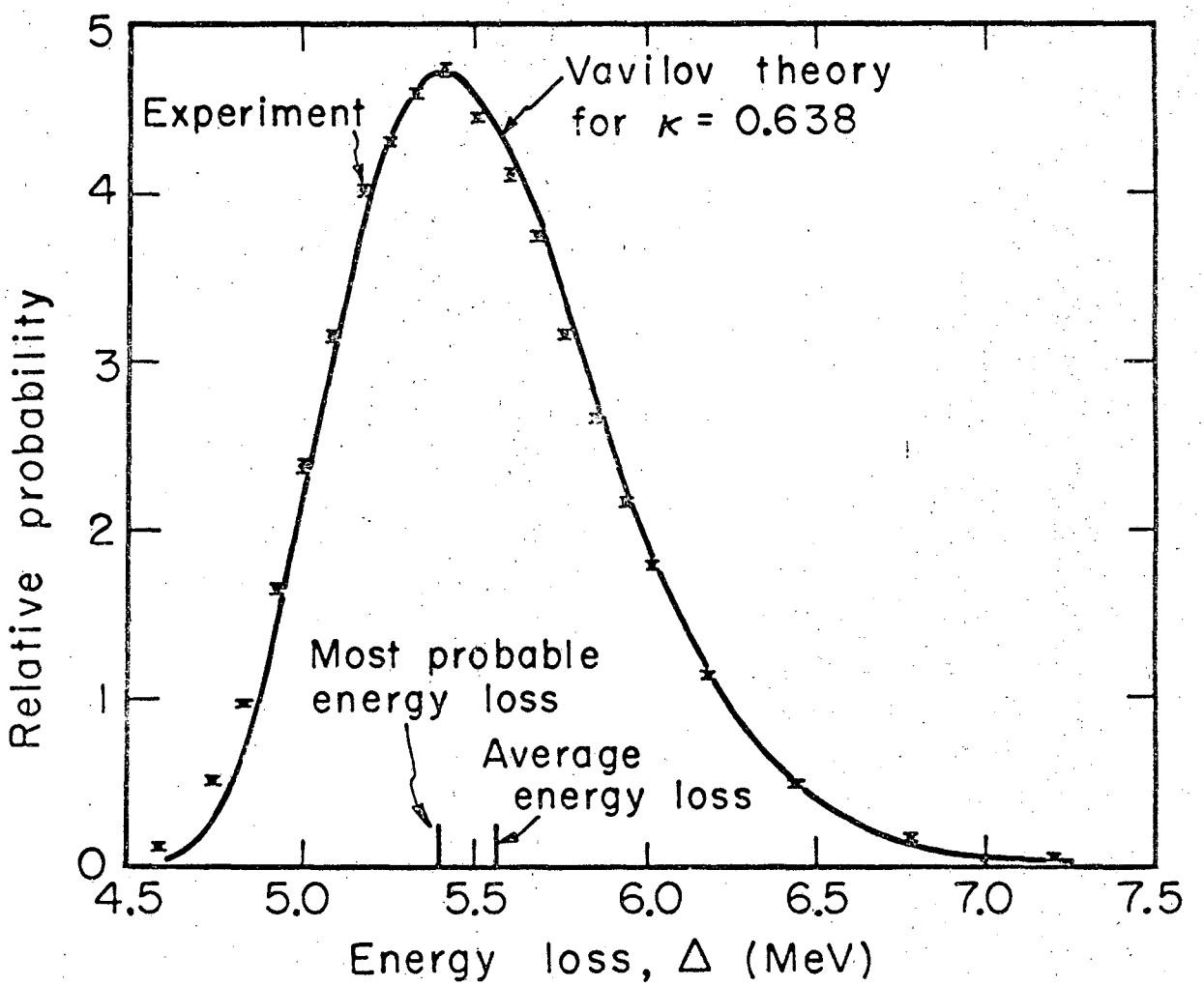

MUB-9084

Fig. 13.

Energy loss distribution of 910-MeV alphas in 0.413-g/cm^2 Si, $\kappa = 0.638$.

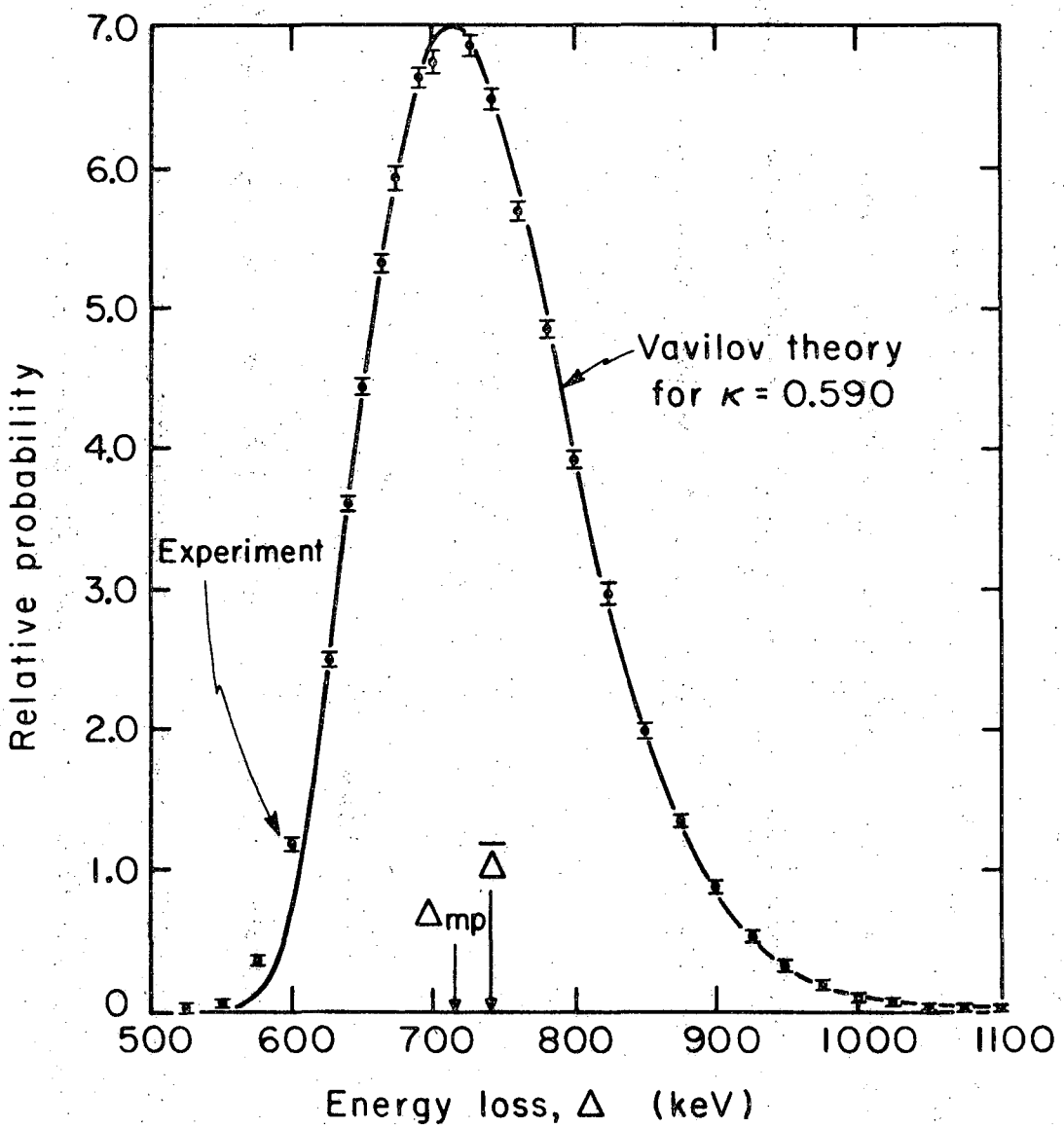

Fig. 14. Energy loss distribution of 45.3-MeV protons in 0.070-g/cm^2 Si, $\kappa = 0.590$.

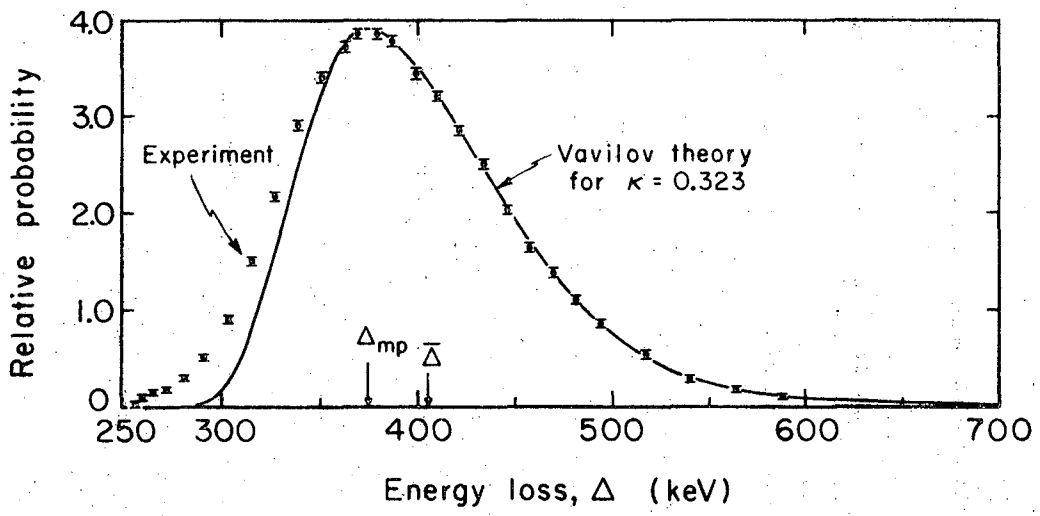

Fig. 15. Energy loss distribution of 45.3-MeV protons in 0.0383 g/cm^2 Si, κ = 0.323.

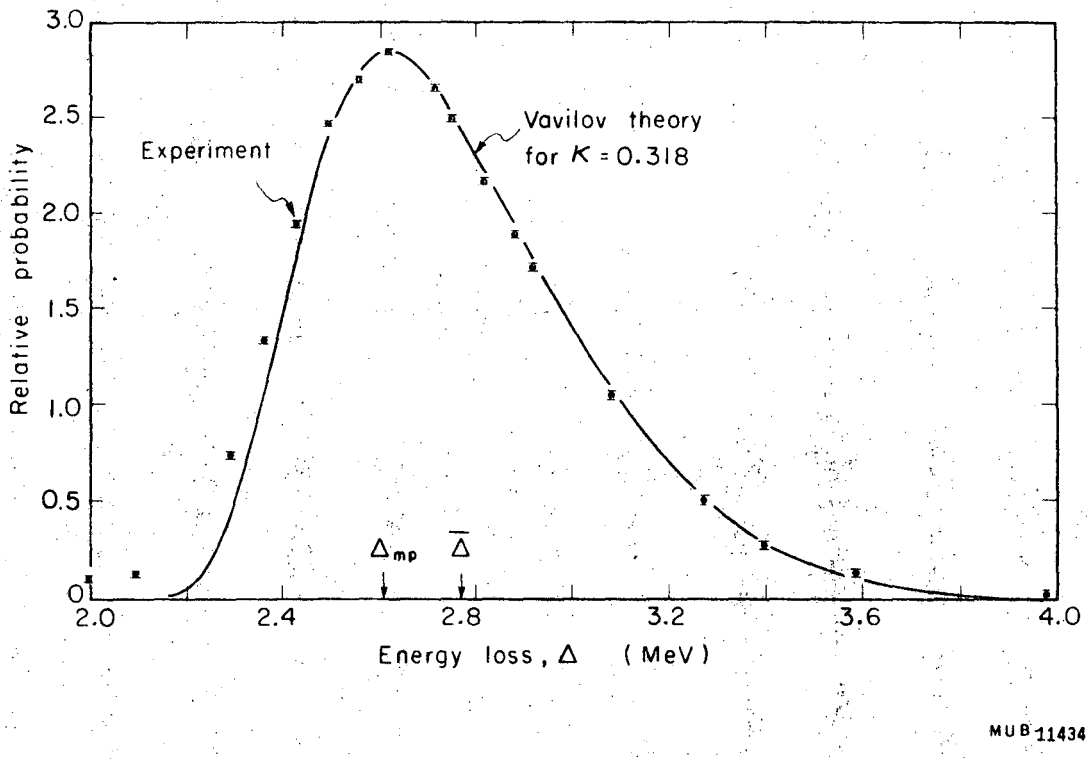

Fig. 16. Energy loss distribution of 910-MeV alphas in 0.206-g/cm^2 Si, $\kappa = 0.318$.

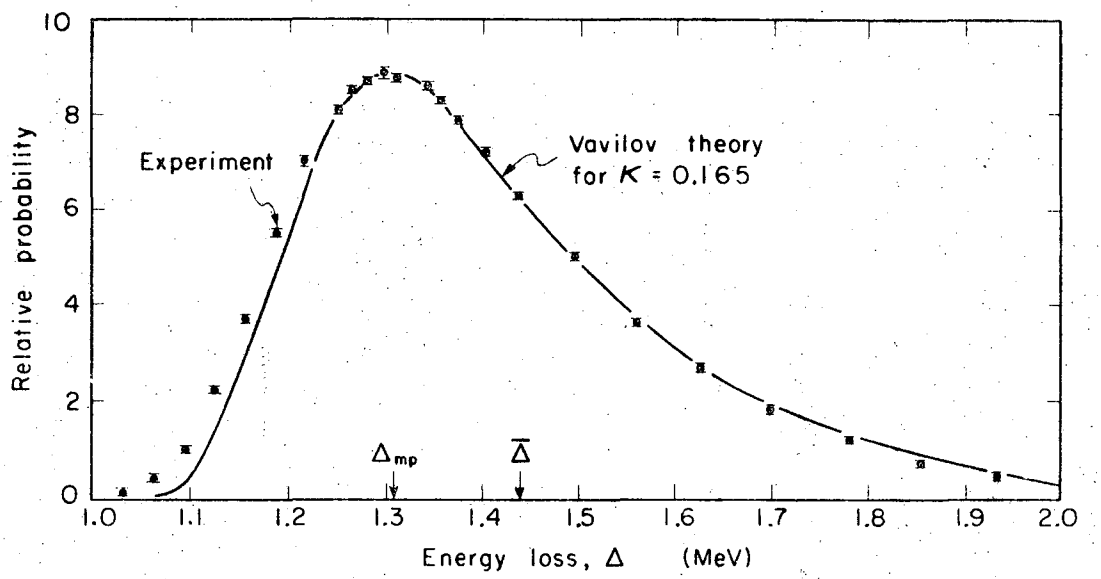

MUB 11436

Fig. 17. Energy loss distribution of 910-MeV alphas in 0.107-g/cm^2 Si, κ = 0.165.

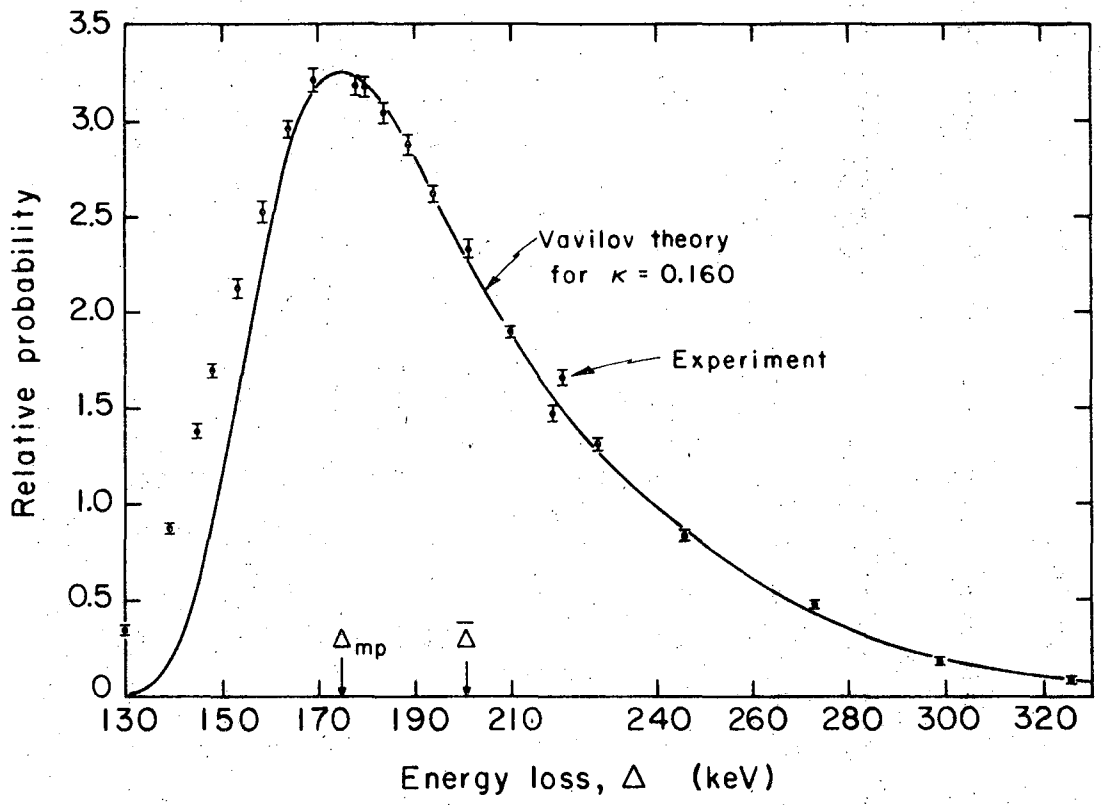

Fig. 18. Energy loss distribution of 45.3-MeV protons in 0.019-g/cm^2 Si, $\kappa = 0.160$.

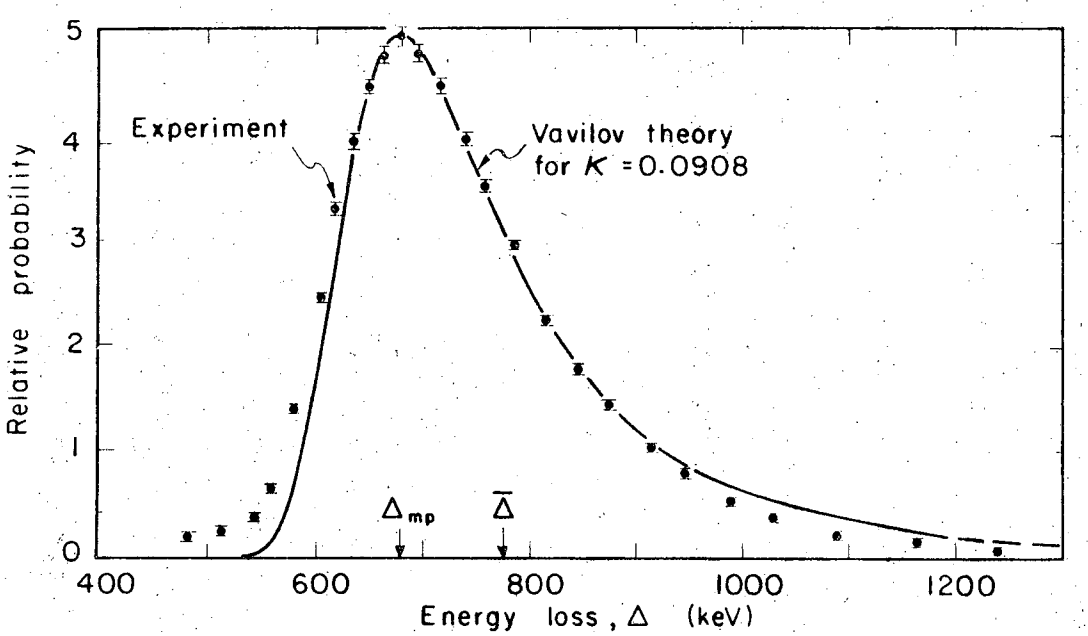

Fig. 19. Energy loss distribution of 895-MeV alphas in 0.057-g/cm^2 Si, κ = 0.0908.

in 0.057-g/cm^2 Si, $\kappa = 0.0908$. Figure 20 shows the distribution for 45.3-MeV protons in 0.0085-g/cm^2 silicon, $\kappa = 0.0716$. This corresponds to an ultrathin depletion layer, of thickness 1.4 mils. Note the broadening of the experimental distribution. This broadening is due to the finite resolution of the detection system, which becomes worse for detectors with high capacitance, such as this one. We discuss this broadening in the next section on resolution.

Figure 21 shows the energy-loss distribution of 730-MeV protons in 0.66-g/cm^2 Si, $\kappa = 0.0338$; the distribution for 730-MeV protons in 0.413-g/cm^2 Si, $\kappa = 0.021$, is shown in Fig. 22. Note the pronounced asymmetry of the distributions in these cases (Figs. 15 through 22) of lower intermediate values of κ ($0.01 < \kappa < 1$), the growth of the high-energy-loss tail, and the marked shrinkage of Δ_{mp} relative to $\bar{\Delta}$. Agreement between theory and experiment is, in general, very good for these cases, with a continuing small deviation on the low-energy-loss side.

The energy-loss distribution of 730-MeV protons in 0.231-g/cm^2 silicon, $\kappa = 0.0118$, is shown in Fig. 23. Figure 24 shows the distribution for 730-MeV protons in 0.108-g/cm^2 Si, $\kappa = 0.0055$. The energy-loss distribution of 370-MeV π^- mesons in 0.45-g/cm^2 Si is shown in Fig. 25, with $\kappa = 0.0031$. Note that in this case the depletion layer thickness is sufficient to keep the capacitance down and prevent resolution broadening, but the low-energy deviation is still present, increasing the width at half maximum by around 30 keV. Figure 26 shows the energy-loss distribution of 730-MeV protons in 0.057-g/cm^2 silicon,

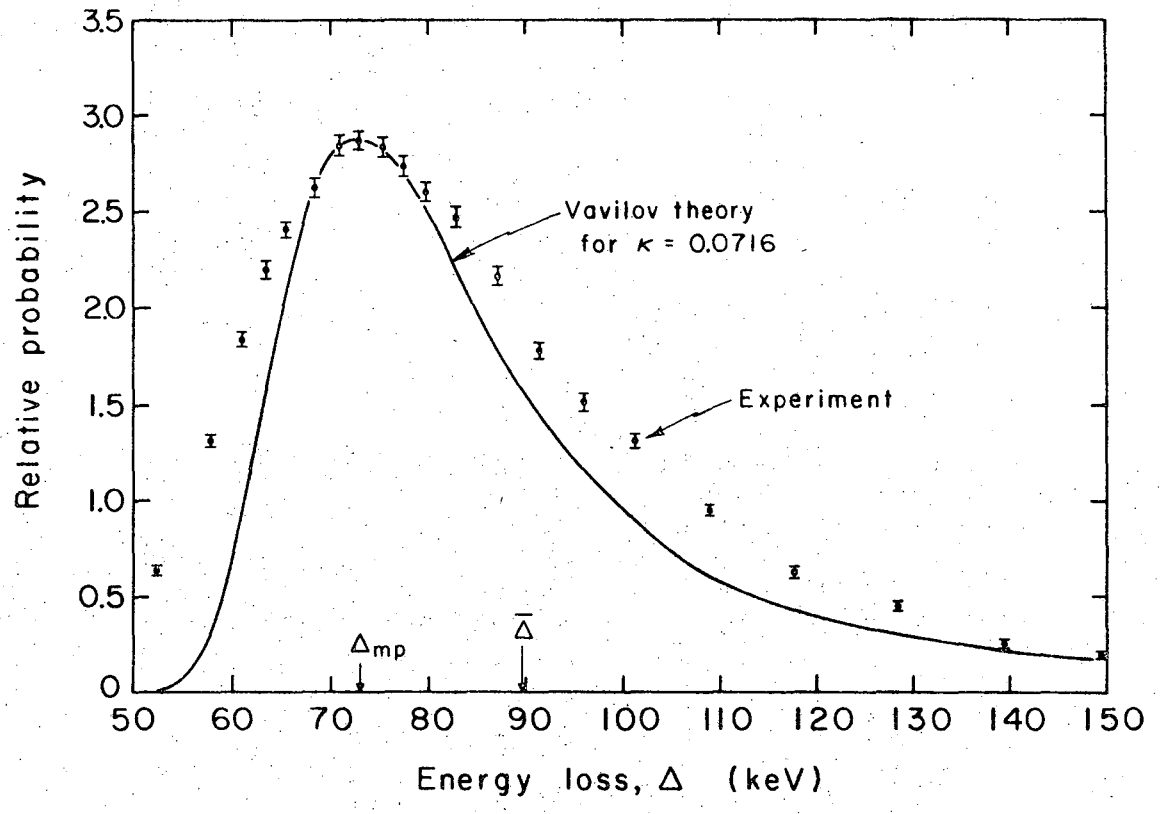

Fig. 20. Energy loss distribution of 45.3-MeV protons in 0.0085-g/cm^2 Si, κ = 0.0716.

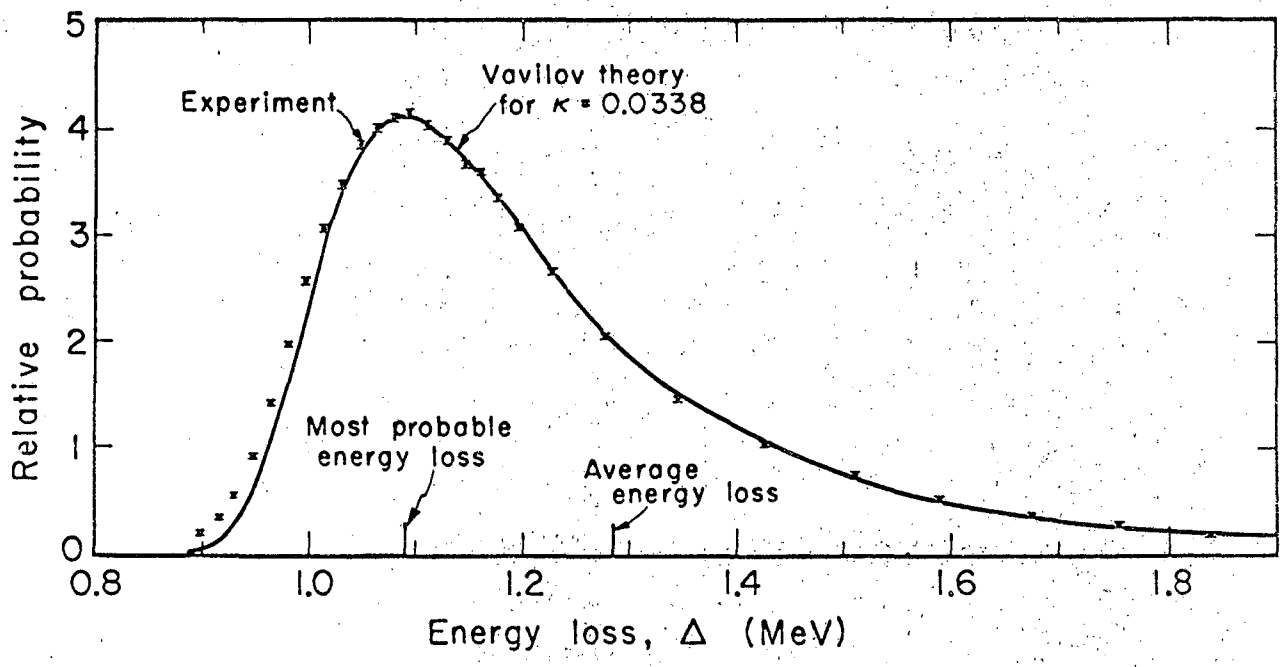

Fig. 21.

Energy loss distribution of 730-MeV protons in 0.66-g/cm^2 Si, $\kappa = 0.0338$.

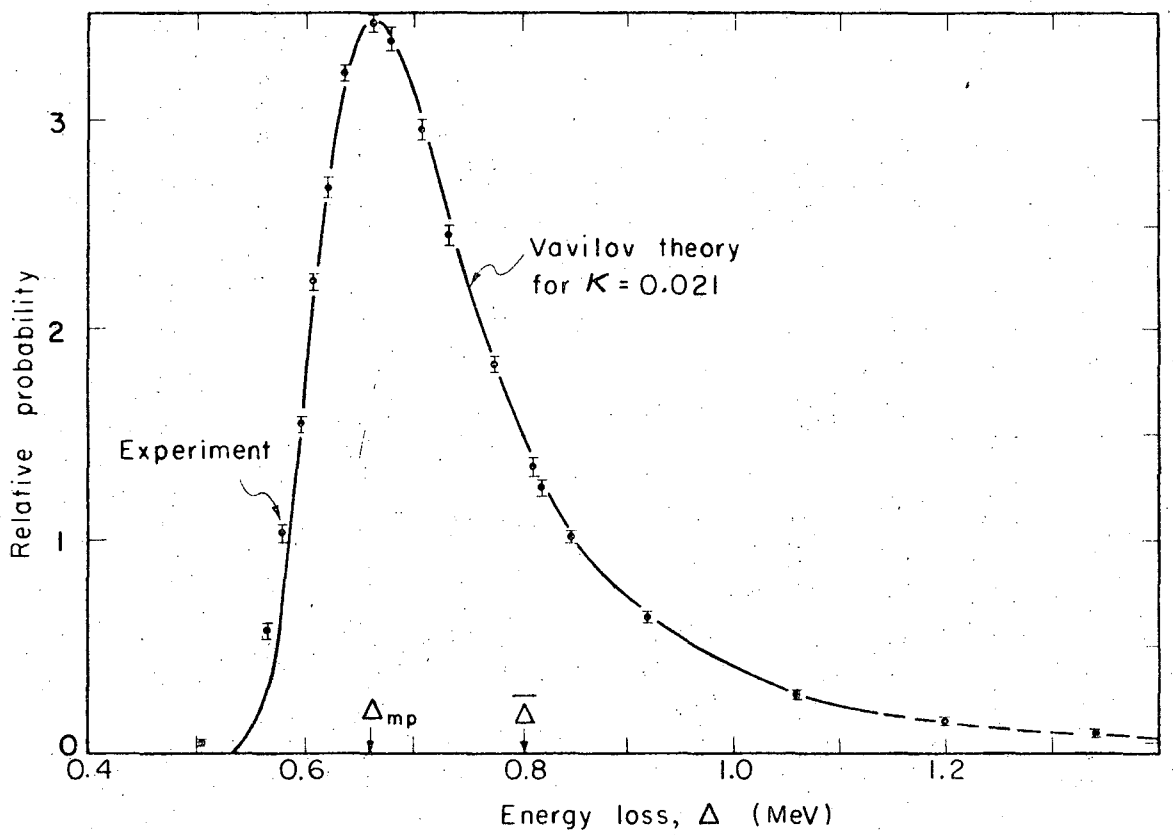

Fig. 22. Energy loss distribution of 730-MeV protons in 0.413-g/cm^2 Si, K = 0.021.

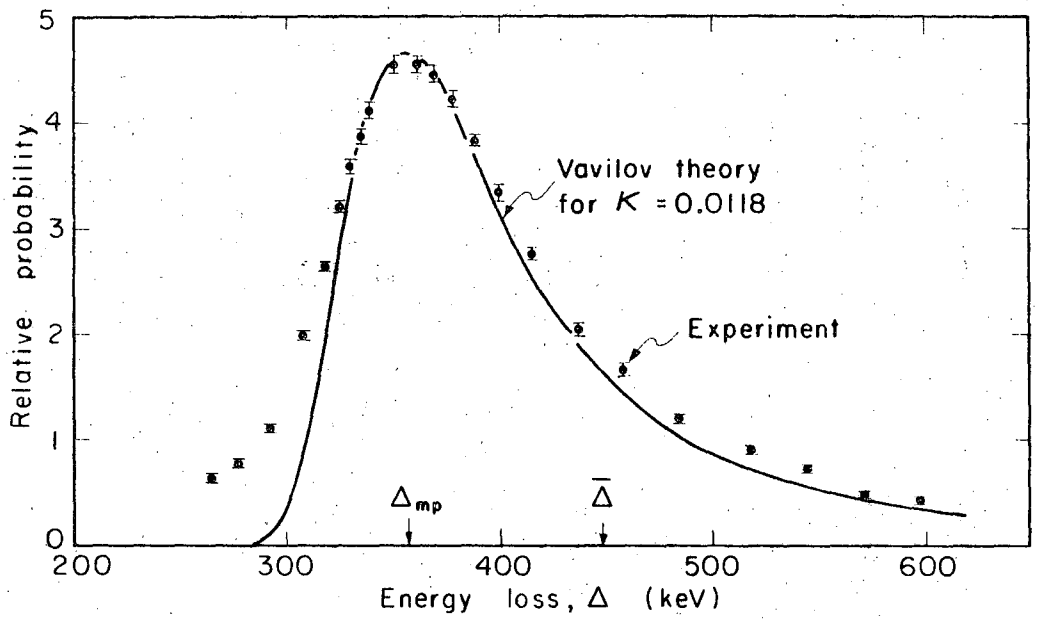

Fig. 23. Energy loss distribution of 730-MeV protons in 0.231-g/cm^2 Si, K = 0.0118.

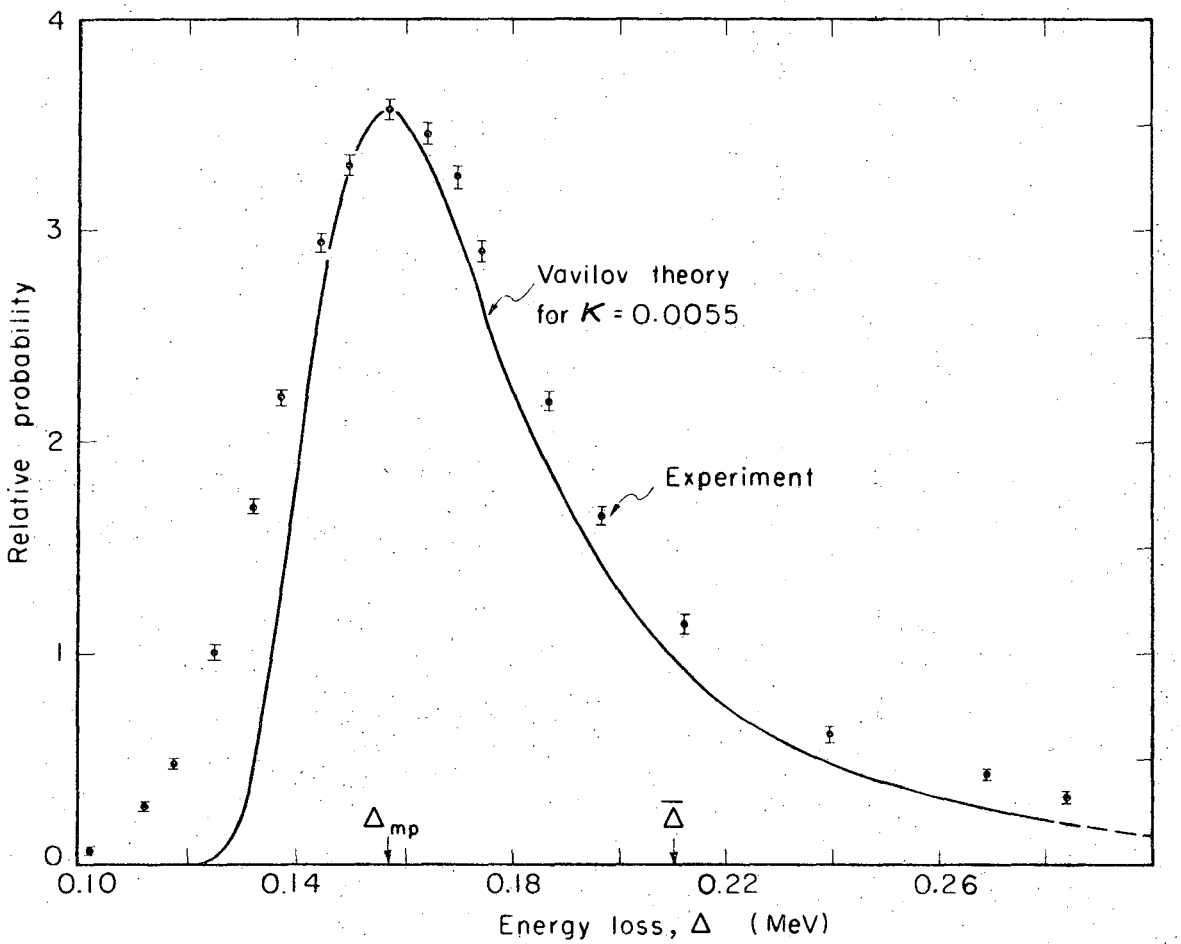

Fig. 24. Energy loss distribution of 730-MeV protons in 0.108-g/cm^2 Si, $\kappa = 0.0055$.

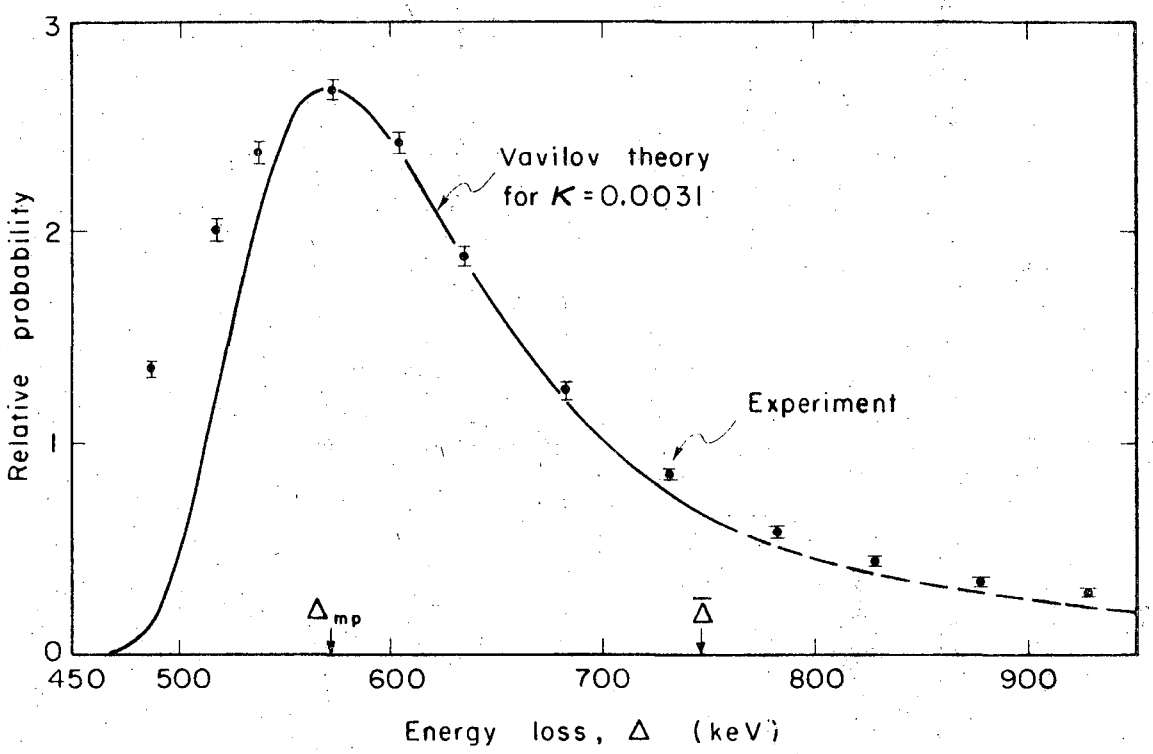

MUB 11435

Fig. 25. Energy loss distribution of 370-MeV negative pi mesons in 0.45-g/cm^2 Si, κ = 0.0031.

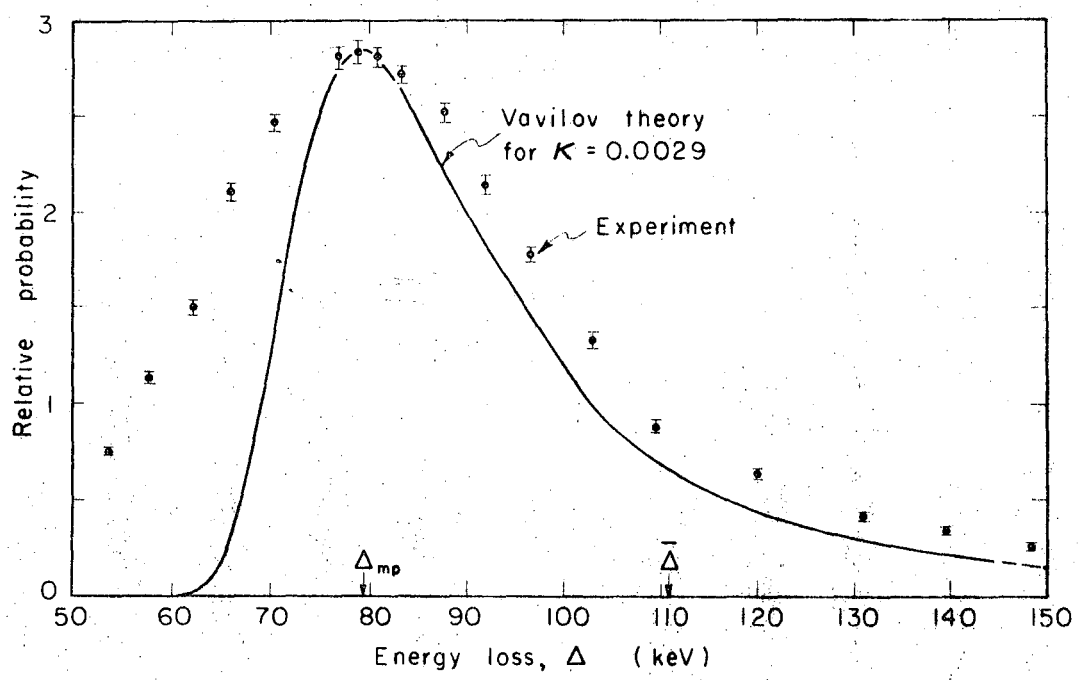

MUB 11429

Fig. 26. Energy loss distribution of 730-MeV protons in 0.057-g/cm^2 Si, κ = 0.0029.

$\varphi(\lambda)$ versus λ for $\beta^2 = 0.5$

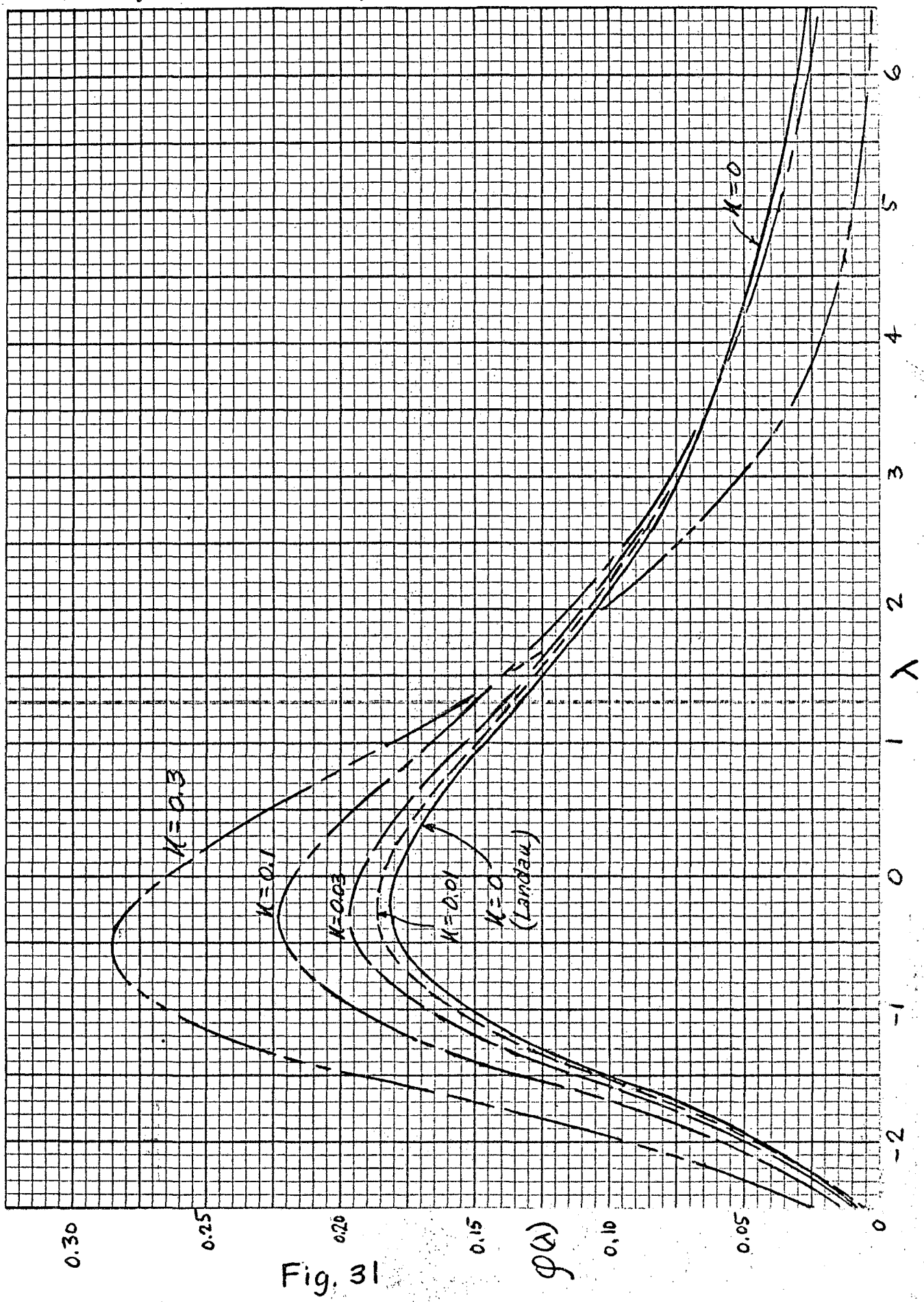

Fig. 31

$\kappa = 0.0029$. In these cases of very small κ (Figs. 23 through 26, $\kappa \lesssim 0.01$), the Vavilov theory reduces to the Landau distribution, with a very long high-energy-loss tail; the theoretical $\Delta_{mp} \approx 0.75\ \bar{\Delta}$, while the theoretical FWHM $\approx 0.3\ \Delta_{mp}$. The experimental distributions, however, are broadened by resolution effects, and are not directly useful for the detailed verification of the theory. There is good agreement, however, on the value of the most probable energy loss, and moderately good agreement as to the shape of the distributions. It should be noted here that the Landau distribution is already well justified in the literature. (See Section II.B.)

In summary, the agreement between the experimental and Vavilov theoretical distributions for intermediate values of κ ($0.01 \lesssim \kappa \lesssim 1$) is very good to excellent. The finite resolution of our experimental system, due to increased capacitance in the thinnest detectors, prevents the exact verification of the Landau distribution for $\kappa \lesssim 0.01$, although there is good agreement on Δ_{mp} and on the shape of the curve.

B. Resolution of System

The measuring ability of any experimental system is limited by its inherent resolution. Even with a δ-function input, fluctuations within the system result in a finite nonzero spread in the output signal. Indeed, the Landau fluctuation may itself be regarded as a resolution limitation on the measurement of the energy loss of fast charged particles in matter. The resolution of our system for measuring the fluctuations of energy loss is in turn limited by two main effects:

statistical fluctuations in the number of hole-electron pairs due to a fixed energy loss in the detector, and electrical noise in the system.

Normally, one could evaluate the root-mean-square fluctuation $\langle n \rangle$ in the number of pairs produced by

$$\langle n \rangle = \left[\frac{\text{energy absorbed in the detector}}{\text{average energy per hole-electron pair}} \right]^{1/2}. \qquad (74)$$

For the worst case of interest here, this formula would yield

$$\langle n \rangle = (80 \text{ keV}/3.66 \text{ eV})^{1/2} = (21\,800)^{1/2} = 147 \text{ pairs}.$$

This corresponds to a fluctuation of only 147/21 800 = 0.68%, or 0.55 keV, and is clearly negligible. In actuality, the fluctuation is even smaller than this, owing to the fact that the hole-electron pair production process is not statistically independent of the thermal and vibrational energy-loss modes in the semiconductor. This phenomenon is expressed by the formula $\overline{n_o^2} = F\langle n \rangle^2$, where n_o is the observed rms fluctuation and F is the Fano factor, which is less than unity and has been evaluated by Van Roosbroeck as approximately 0.25 in silicon.[75]

The resolution limitation introduced by electrical noise is much more serious in our case. In particular, there is noise due to detector leakage current (primarily due to thermal excitation), and there are shot noise and "flicker-effect" noise (due to plate-current fluctuations), both of which increase directly as the total input capacitance (see Ref. 71, Eqs. 3.14, 3.15). The total input capacitance is made up of the detector capacity C_D and the amplifier input capacity, which we neglect in the following treatment. The detector capacity may be

evaluated by

$$C_D = 1.1(kA/4\pi x) \text{ picofarads}, \qquad (74)$$

where k is the dielectric constant of silicon, 12,

A is the depletion layer area in cm^2,

x is the depletion layer thickness in cm.

For example, our detector of 0.057-g/cm^2 depletion thickness has a capacity of 60 pF, and our detector of 0.0085-g/cm^2 thickness has a capacity of ~ 200 pF. To get an estimate of the effect of these capacitances on resolution, we can simulate the detector with an equivalent capacitor, inject monoenergetic pulses, and measure the output spectrum. The result of this measurement, with the EC-1000 preamplifier and equal RC clipping and integrating time constants of 0.5 μsec, is 13 keV (FWHM) for 60 pF and 27 keV (FWHM) for 200 pF. Note that these values impose a lower limit for the system resolution, and the resolution with an actual detector and "real" pulses is bound to be worse, even if the detector is cooled to minimize leakage current. In an actual experiment, the system resolution is measured by attaching the detector of interest (cooled if desired) and injecting essentially monoenergetic particles from a radioactive source--e.g., Bi^{207}-- or pulses from the pulse generator.

The effect of system resolution on our measurements of the energy-loss distribution can be calculated by folding in the resolution spectrum f_{res} with the "actual" energy-loss spectrum f_{act}; this yields the measured spectrum f_{meas}:

$$f_{meas}(\Delta) = \int_{all\ u} f_{act}(\Delta - u) f_{res}(u)\, du \ . \qquad (76)$$

Obviously, unfolding a measured distribution to obtain the "actual" distribution is rendered quite difficult by the fact that f_{res} and f_{meas} are not simple continuous analytic functions, but sets of discrete measured points. For practical purposes, we assume that f_{res} may be represented by a Gaussian (a good approximation) and that the peak in f_{act} may be represented by a Gaussian (a fair approximation), and use the well-known relation that the folding in of two Gaussians yields a Gaussian with width equal to the square root of the sum of the squares of the component widths. Specifically,

$$FWHM^2_{meas} = FWHM^2_{act} + FWHM^2_{res} \ . \qquad (77)$$

We now apply this calculation method to the more serious cases of resolution broadening noted in Section IV.A. These cases occur when the resolution width approaches the theoretical FWHM. Table I shows the results of a comparison between $FWHM_{act}$, the actual value as calculated from the above formula, and the theoretical value of the full width at half maximum, $FWHM_{the}$.

Table I. Comparison of experimental and theoretical distribution widths.

Figure number	FWHM (in keV)			
	Measured	Resolution	Actual	Theoretical
18	70	24	65.6	63.4
20	39.5	27	28.8	28.8
23	110	25	107	103
24	59.6	35	48.2	48.4
26	40.5	30	27.2	26.7

In summary, the resolution of the experimental system, due mainly to electrical noise, has a broadening effect on the measured energy-loss distribution when the resolution width is comparable to the theoretical FWHM. Simple corrections for this effect yield good agreement between the theoretical and experimental distribution widths.

C. Sources of Error

We now attempt to analyze the sources of error in our experimental method and evaluate their contribution to the results. It is also necessary to consider the validity of our assumptions and the applicability of the uncorrected Vavilov theory to the physical problem investigated. We pay special attention to the possibility of accounting for the small but consistent deviations from theory found on the low-energy-loss end of the measured distributions.

Consider first the effect of nuclear collisions on the energy-loss distributions. We can get an estimate of this effect by considering the

probability for a nuclear collision in the traversal of the detector by one particle. The total cross section for inelastic interaction of protons of 150 to 700 MeV in silicon has been evaluated by Denisov et al. as about 0.4 barn.[82] The probability of nuclear interaction in a single proton traversal of 1-g/cm^2 Si, for example, is given by

$$N\sigma x = \frac{6 \times 10^{23}}{28g} 0.4 \times 10^{-24} \text{ cm}^2 \times \frac{1 \text{ g}}{\text{cm}^2} = 0.0086 \ .$$

Thus, in the worst case less than 1% of the particles will experience a nuclear interaction, with a negligible effect on the energy-loss spectrum of all the particles. This conclusion agrees with the calculation by Lindhard and Nielsen.[29] In fact, the violent nuclear interactions will probably not even been "seen" by the system, as large-angle scattering violates the coincidence requirements, and ultrahigh-energy losses lie on the far right end of the high-energy-loss tail, which we have not measured. The coincidence requirement and the selection of the energy-loss interval studied also serve to nullify the effect of any stray radiation in the cave.

If many of the particles pass through the detector at an angle other than normal to its plane, they will experience larger energy losses because of their greater path lengths through the detector. The effect of angular spread of the incident beam is negligible because of the collimating effect of the coincidence detector, but the problem of multiple scattering within the detector must be evaluated. The mean-square angle of deflection for a particle traversing a "thin" absorber

is given by[2]

$$\overline{\theta^2} = \frac{8\pi z^2 Z^2 e^4}{M^2 v^4} Nx \ln \frac{\theta_{max}}{\theta_{min}} . \qquad (78)$$

The evaluation of this expression in our worst case, 45-MeV protons in 0.265-g/cm^2 Si, yields a root-mean square deflection of about 1.5 deg, which would yield an average path-length increase of 0.03% (cos 1.5 deg = 0.9997). This effect is negligible.

Energy losses due to radiation are also of negligible importance. The bremsstrahlung radiation intensity is proportional to the square of the particle deceleration, i.e., proportional to z^2Z^2/M^2, but M^2 for heavy particles is so large as to render this effect negligible for our purposes. The energy loss due to Cerenkov radiation by the 730-MeV protons is of the order of 1 keV/cm and thus is negligible compared with ionization loss.[2]

Consider now the spread in energy of the incident beam; we have until now assumed it to be monoenergetic. A measure of this effect in our worst case is provided by the difference between the mean dE/dx of 730- and 715-Mev protons:

$$\frac{dE/dx|_{715}}{dE/dx|_{730}} \cong \frac{\beta^2_{730}}{\beta^2_{715}} = \frac{(0.826)^2}{(0.823)^2} = \frac{0.682}{0.677} = 1.007.$$

Thus the increase or decrease in the mean energy-loss value for a proton with the maximum deviation in initial energy is only about 0.7%. Since most particles are much closer to the modal energy, we can neglect this effect.

The problem of nonuniformity of foil thickness has been quite serious for many of the low-energy experiments on energy-loss fluctuations. The extent of the nonuniformity of the semiconductor detectors we used, however, is less than 25 microns,[83] and its effect is clearly negligible for all the lithium-drifted and most of the p-n junction detectors. It might become important for the thinnest p-n junctions, but the effect would probably be hidden in this case by the effect of noise on resolution.

As mentioned earlier, errors are introduced in the experimental measurements owing to such factors as uncertainties in the channel-number–to–energy calibration due to small system nonlinearities (e.g., in pulser output), electronic drift (e.g., in amplifier gain), and dead-layer effect. There are also errors introduced in the comparison with theory by uncertainties in depletion-layer thickness, I_{Si}, etc. The combined effect of these errors is probably less than ±2%, and would be expressed by a shift in the whole distribution to the left or right on the energy scale in a given case, not by a small consistent deviation on the low-energy-loss end.

Let us now consider effects that <u>could</u> result in the observed deviations in the low-energy-loss end. Golovin et al. have shown that in certain cases (e.g., when $\beta^2 = 0.6$, $\kappa = 0.01$, $Z \gtrsim 29$), the effect of resonance collisions with bound atomic electrons would be just such a deviation. (Ref. 35, Fig. 3) In order to evaluate this effect in our worst case, we estimate the Blunck parameter b^2 for 730-MeV protons in 0.057-g/cm^2 Si:

$$b^2 \cong \frac{\bar{\Delta}Z^{4/3} \cdot 20\text{eV}}{\xi^2} = \frac{0.11 \times 10^6\text{eV} \cdot 33 \cdot 20\text{eV}}{(0.006)(0.006)10^{12}\text{eV} \cdot \text{eV}} \cong 2 .$$

The value of the parameter is below the threshold where resonance effects become important, but not far below. In lieu of the numerical integration of Golovin's complex expression, we make the conditional statement that the deviation is probably in part due to "glancing" resonance collisions.

Another physical effect which could cause an increase in the number of very-low-energy-loss traversals is the phenomenon of "channeling." In single crystals of high purity, such as our silicon detectors, there is a certain probability that an incident particle will enter the crystal parallel to and between the crystal planes and thereby traverse the crystal on a path with very low electron density, resulting in an anomalously low energy loss. (A similar but smaller effect, called "blocking," occurs when traversal of high-electron-density regions results in anomalously high energy loss.) Dearnaley,[84] Erginsoy, Wegner, and Gibson,[85] and others have studied this effect and have shown that, for example, when 40-MeV α particles with an effective angular definition of ± 0.05 deg traverse a 100-micron single-crystal silicon detector parallel to the [110] direction, a significant fraction loses only about half the normal energy. There is reason to believe that channeling effects are relatively unimportant in our case, however. First, the angular definition of our beam in the worst case (45.3-MeV p^+) is about 0.2 deg. Moreover, in the fabrication of our silicon detectors,

the crystals are purposely sliced a few degrees off the ⟨111⟩ plane in order to prevent channeling when particles are incident normal to the face of the detector. In addition, the likelihood of channeling is greatly decreased for incident energies greater than 10 MeV per nucleon. Despite these precautions, there is a small but finite probability that particles "accidentally" become aligned with a preferred direction, and experience a very small energy loss. We judge that channeling does have a relatively small effect in generating the deviation on the low-energy-loss end of the distribution.

Finally, we consider the effect of δ-ray entry and escape from the detector. When a high-energy particle imparts a large energy in a collision with an electron, the resulting knock-on electron, or "δ ray," can have a considerable range of its own, and in certain cases, can escape the detector. Similarly, secondary electrons from collisions in the material in front of the detector can enter the detector. For example, the maximum δ-ray energy for a 730-MeV proton is 2.19 MeV, which corresponds to a range in silicon of 4.5 mm.

Now it should be pointed out that the Vavilov theory predicts the distribution of energy losses by the particles, including energy lost to energetic δ rays, while the experiment measures only the energy absorbed by the detector. As Gooding and Eisberg[59] and others have pointed out, the experimentally measured quantity will be equal to the theoretically predicted energy loss only if there is no net transfer of energy, by energetic δ rays, into or out of the detector.

One might suggest that there is a simple way of eliminating this

problem, by performing the experiment in a magnetic field strong enough to bend the most energetic δ rays into a radius smaller than the thickness of the detector. This is not feasible in our case; we calculate the strength of the field necessary to bend a 2.2-MeV electron (momentum 2.65 MeV/c) into a radius equal to the thickness for our 0.25-mm detector (0.057 g/cm^2 Si) as

$$B = \frac{p}{qr} = k \frac{p \text{ (in MeV/c)}}{r \text{ (in cm)}}, \tag{79}$$

where $k = 0.33 \times 10^4$ gauss, i.e.,

$$B = (0.33 \times 10^4) \text{ gauss} \times (2.65)/(0.025) = 350\,000 \text{ gauss}.$$

Needless to say, a 350-kilogauss magnet is neither practical nor possible for this application, to say nothing of the effect a strong magnetic field might have on charge collection in the detector. Since we cannot eliminate the δ-ray escape, the next step is to try to estimate its effect on the measured "energy-absorption" spectra.

Rosenzweig and Rossi devised an ingenious "track-segment" method of estimating the effect of δ-ray entry and escape for a detector which samples randomly a region that is small compared with a uniform surrounding medium.[64] Since our detectors are not embedded in a larger block of silicon, their method is not directly applicable to our case. We proceed with a qualitative picture of the effects in our case. Clearly if a δ ray escapes the detector, the energy deposited for this particle event is less than the energy lost. The result is to shift an

event from the high-energy-loss tail down to the lower-energy-loss side of the spectrum. In addition, a δ ray entering and stopping in the detector is likely to have already lost some of its initial energy, and thus would add an event to the lower-energy-loss side of the spectrum. A minimum-ionizing secondary passing through the detector will lose slightly less energy than a 730 MeV proton, which is not quite minimum-ionizing, and thus deposit an event which is (most probably) below the most probable energy loss of the proton. For geometric and other reasons, however, the probability of δ-ray entry is smaller than the escape probability. If this picture is correct, the net result of these processes should be to shift events from the high-energy-loss side of the spectrum to the low-energy-loss side. A small perturbation of the spectrum, however, will not be noticed when compared with the spectrum itself, except where the spectrum height is very small, e.g., at the ultrahigh-energy-loss end (which we have not measured) and at the very-low-energy-loss end (which we have measured).

Clearly these effects are attenuated as the detector thickness increases, and become negligible when the thickness is much larger than the maximum δ-ray range. In lieu of an exact calculation (a Monte Carlo calculation would be quite helpful), we estimate the importance of these effects by calculating the fraction of the total energy loss imparted to electrons whose range is comparable to or greater than our detector thicknesses:

$$\frac{\overline{\Delta}\ (\delta\ \text{ray})}{\overline{\Delta}\ (\text{total})} \cong \frac{\xi\ \ell n\ (\epsilon_{max}/\epsilon_{\delta})}{\xi\ \ell n\ (\epsilon_{max}/\epsilon_{min})} = \frac{\ell n\ (\epsilon_{max}/\epsilon_{\delta})}{2\ \ell n\ (\epsilon_{max}/I)} \cong \frac{\ell n\ (\epsilon_{max}/\epsilon_{\delta})}{20} \ . \quad (80)$$

For 730-MeV protons in 0.25-mm Si (range of 250-keV electron), this yields

$$\frac{\ell n\ (2.2\ \text{MeV}/\ 250\ \text{keV})}{20} = \frac{\ell n\ 9}{20} = 11\% \ .$$

For 730-MeV protons in 3-mm Si (range of 1.6-MeV electron) the effect is much less important:

$$\frac{\ell n\ (2.2/1.6)}{20} = \frac{\ell n\ 1.4}{20} = 1.7\% .$$

Since the maximum δ-ray energies of 45-MeV protons and 910-MeV alphas are much smaller, the fraction would be quite negligible. Thus the effect of δ-ray entry and escape is important only for the fastest particles (730-MeV protons, 370-MeV pions) in the thinner detectors, where it is believed to contribute to the deviation found on the low-energy-loss end of the distribution.

(In this work we have tried to minimize channeling and δ-ray effects; we note in passing, however, that this experimental system can profitably be altered for the study of these very interesting effects.)

In summary, there are several small sources of error in our

experiment, including uncertainty in thickness and energy calibration, which might contribute ±2% to the position of the distributions on the energy scale. In addition, the effects of resonance collisions with bound electrons, channeling, and δ-ray entry and escape can contribute to the deviation found on the low-energy-loss end of the distributions.

V. IMPLICATIONS

A. Physical

One of the most effective tools for exploring the structure of matter is the study of the penetration of charged particles in matter. Particle penetration is intimately involved in many experiments in nuclear and high-energy particle physics, atomic physics, radiation chemistry, space physics, and several areas of solid-state physics. Indeed, as B. Rossi has pointed out, charged-particle experiments have provided a basis by which to test the validity of the theory of electromagnetic interactions.[7]

A significant number of these experiments involve measurements of the energy lost by charged particles in passing through matter, and therefore invoke consideration of the fluctuations in energy loss. There are several existing theories of energy-loss fluctuations in "thin" absorbers. Bohr's theory predicts a Gaussian distribution of energy losses when the number of particle-electron collisions in every collision-energy interval is large, and Landau's theory predicts a broad asymmetric distribution with a high-energy-loss "tail" when the number of particle-electron collisions in the higher-collision-energy interval is very small. The validity of both these theories is well established experimentally.

Symon and Vavilov have published theories to cover the broad intermediate range where the number of collisions in the higher interval, as measured by the parameter κ, is neither large nor very small.

The energy-loss distributions predicted by these theories are relatively similar, although there are deviations in distribution shape, and Symon's theory seems to predict a most-probable-energy loss which is 2.5 to 3% lower than Vavilov's.

> For example, Symon predicts the most probable energy loss of 730-MeV protons in 0.66-g/cm^2 Si, $\kappa = 0.0338$, to be 1.12 MeV; the value predicted by Vavilov is 1.09 MeV, and the value we measured is 1.09 MeV.

We believe that Vavilov's expression is more accurate, owing to the interpolations involved in Symon's method. We also find the use of the Vavilov theory to be more convenient, given the FORTRAN computer program devised by Seltzer and Berger for calculating the distribution function.

In order to remedy the sparsity of data in the intermediate region, we have measured energy-loss distributions over a range of κ from 0.0029 to 2.23, and, within the limits of experimental error, find very good agreement with Vavilov's theoretical distributions and with the predicted values of the most-probable-energy loss. In order to make these results more useful to future experimenters, we have prepared graphical tabulations of both measured and calculated quantities, and show them in the Appendix.

B. Biological

Charged-particle energy loss is of vital interest to biology also. In medicine, charged particulate radiation is used for diagnosis and therapy of many diseases. Radiobiological experiments using charged particles yield fundamental information on cell structure and function. Even for nonparticulate or uncharged radiation (e.g., X and γ rays, neutrons) it has been shown that the mechanism of biological damage is ionization or excitation due to charged secondaries (electrons, recoil protons). The question of radiation protection has been given new impetus by the problem of exposure of man in space to fast charged particles in cosmic radiation.

It is clear that the living cell, and indeed the cell nucleus, acts as a "thin" absorber with respect to most forms of charged particulate radiation, and in many cases, the value of the parameter κ is small enough that significant fluctuations of the energy loss occur.

> For example, consider 40-MeV protons traversing cells of 10-micron thickness: with $\rho \approx 1$ g/cm^3, $Z/A \approx 0.5$, the parameter $\kappa = 0.150\, s(Z/A)z^2[(1 - \beta^2)/\beta^4] = 0.15(10 \times 10^{-4})0.5(0.92)/0.0064 = 0.011$. Thus the Landau distribution holds and the most-probable-energy loss in the cells is only about 75% of the average energy loss.

This can be important, because the biological effect of radiation is related to the amount of ionization or excitation energy deposited

in the cell or other sensitive volume. It is commonly stated that the RBE (relative biological effectiveness, compared to equal dose of X or γ radiation) is dependent on the LET (linear energy transfer, comparable to dE/dx, measured in keV/micron or MeV/g/cm^2). Each total-energy-loss spectrum that we have measured can be considered equivalent, for some purposes, to an LET spectrum for a given absorber thickness. In practice, LET distributions for biological irradiation experiments are often measured by methods similar to ours.

This simple picture is complicated by several factors. First, the energy lost in the cell by the particle is equal to the energy deposited in the cell only if there is no net transfer of δ-ray energy out of the cell. Thus the energy deposition pattern for cells irradiated in a uniform medium (i.e., in δ-ray equilibrium with their surroundings) will be different from the energy deposition in isolated cells that are irradiated. Second, cells and other sensitive "targets" are generally not slab-shaped and thus are not of a single thickness. For example, Rossi and Rosenzweig[86] have shown that for a spherical absorber in a uniform radiation field, the distribution of path lengths is triangular; P(x), the probability of path length x in a sphere of radius r is given by

$$P(x) = x/2r^2 . \qquad (81)$$

Thus for a given radiation and given absorber (e.g., cell) shape, the LET distribution must be folded in with the path-length distribution to give the actual distribution of energy depositions in the absorber.

Third, the usefulness of the concept of LET itself has been criticized by several authors. It should be clear from previous arguments that as the size of the examined sensitive volume decreases, so does the value of κ, and the statistical fluctuations in energy deposition increase. Thus the distribution of energy deposition depends on the size of the biological system under consideration. H. H. Rossi and his associates have dealt with this question in a series of papers, in which they have developed the concepts of "event size," Y, defined as the energy deposited in an event divided by the sphere diameter, and "local energy density," Z, defined as the energy deposited by ionizing particles divided by the mass of the sphere; they have also recommended the use of small spherical ionization chambers for microdosimetry so that the shape and mass of cells may be simulated.[86,87] Baily et al. have also studied this problem experimentally.[88]

In the limit of thinness of the absorber, the number of collisions in the lower collision-loss interval is too small for the Vavilov treatment to be valid [i.e., Landau's first condition (45), that $\xi/\epsilon_o \gg 1$, is not satisfied], and Poisson statistics must be used to describe the individual ionization or excitation events.

For example, consider 5-MeV α particles traversing a DNA strand of 20 angstroms thickness (20×10^{-8} cm), $\rho \approx 2$ g/cm^3, $Z/A \approx 0.5$; then

$$\xi = 0.154 \frac{s}{\beta^2} \frac{Z}{A} z^2 = 0.154 \left(\frac{4 \times 10^{-7}}{26 \times 10^{-4}} \right) 0.5(4) = 47 \text{ eV}.$$

Since ϵ_o may be taken to be the mean excitation energy ($I \approx 70$ eV), clearly the number of ionizing events is too small to use the Landau-Vavilov formulation.

Lea first discussed the Poisson type of fluctuation in his treatment of the "target theory" for effects due to ionization in or near a particular molecule or structure,[89] and Oda has recently considered in detail the statistical nature of primary energy transfer in relation to the target theory.[90]

Other criticisms of the LET concept have been offered by Turner and Hollister, who find that the LET dependence of RBE should be replaced by the more precise "velocity" dependence,[91] and Butts and Katz, who find that the RBE for one-hit processes in dry enzymes and viruses is a function of the radial distribution of ionization energy around the particle track.[92]

In any formulation, however, it is clear that fluctuations of energy loss must be taken into account, and either Poisson statistics or the Bohr-Landau-Vavilov theory may be used to predict the energy-loss distribution.

We now consider some of the possible results of energy-loss fluctuations in biological systems.

First, if an energy threshold exists for a given radiation effect, it is possible that even though the mean energy deposition is kept below the threshold, many of the particles (corresponding to the high-energy-loss tail) can deposit greater than threshold energy; conversely, even

if the mean energy deposition is slightly greater than the threshold, many of the particles (corresponding to the most probable energy loss) can deposit less than threshold energy. This example points out that for many purposes, knowledge of the mean energy deposited (or mean LET) is not sufficient; it is necessary to know the distribution of energy deposited (or the LET spectrum). If only a single point on the distribution is to be specified, however, the most probable energy deposited is often more useful than the mean.

In previous sections, we have pointed out a method of accounting for the escape of energetic δ rays from the boundaries of the biological system under consideration. In brief, it consists of using the energy of the δ ray whose range corresponds to the size of the system as the upper limit in the integration over the collision spectrum. One must remember, however, that in a nonisolated system, there will also be δ rays entering and depositing energy. The net result is probably the shifting of events from the high-energy tail to lower energy values.

We present now a simplified calculation of how fluctuations in energy deposition might affect a biological irradiation experiment. Consider a biological system which obeys a simple exponential survival curve, i.e., $S = \exp(-D/D_{37})$, where S is the surviving fraction, D is the dose administered, and D_{37} is the dose that results in 37% survival. If fluctuations of energy deposition cause fluctuations in the dose to different members (e.g. cells) of the system, the nonlinearity of the dose dependence will result in deviation of the net surviving fraction from the fraction that is predicted by use of the mean energy deposition

(or mean LET).

For example, consider a system with D_{37} = 60 rads, and suppose that energy-loss fluctuations can be treated approximately by dividing the system members into two groups, e.g., let 2/3 receive 40 rads and 1/3 receive 100 rads. Thus the net survival is

$$(2/3)e^{-40/60} + (1/3)e^{-100/60} = (0.67)(0.57) + (0.33)(0.19) = 40\% .$$

Note that this value is in conflict with 37%, the value predicted by using the mean dose in this case, 60 rads.

We can propose an experiment that might serve to measure the biological effect of the Landau-Vavilov type of fluctuations: irradiate identical biological systems under two different conditions so that the mean LET is the same but the particle velocities are different, yielding $\kappa \ll 1$ in one case and $\kappa \gtrsim 1$ in the other.

In summary, we emphasize the need to consider the fluctuations of energy deposition in irradiated biological systems, and the desirability of understanding the effects of these fluctuations.

VI. SUMMARY AND CONCLUSIONS

When a charged particle passes through matter, it loses kinetic energy by a series of inelastic collisions with the electrons of the material. Because of the statistical nature of the collision process and the fact that high-energy-loss collisions are much less frequent than low-energy-loss collisions, significant fluctuations may occur in the total energy loss in "thin" absorbers, that is, when the energy loss in the absorber is small compared with the total kinetic energy of the particle. The most significant parameter for characterizing the fluctuations is κ, a measure of the number of particle-electron collisions in the uppermost collision-energy-loss interval,

$$\kappa = 0.150 \frac{sZz^2}{A}\left(\frac{1-\beta^2}{\beta^4}\right),$$

where s is the absorber thickness in g/cm^2, Z is the atomic number of the absorber material, A is the atomic weight of the absorber, z is the charge number of the particle, and β is the particle velocity divided by the speed of light in vacuum.

Several theories predict the fluctuations of energy loss for different values of parameter κ. The Bohr theory, with modifications by Livingston and Bethe, predicts a symmetric Gaussian distribution around the mean energy loss, and is valid when $\kappa \gg 1$. The Landau theory, with modifications by Blunck and Leisegang, is valid for $\kappa \lesssim 0.01$, and predicts a broad asymmetric distribution with a peak around the most probable energy loss (which is significantly less than the

mean) and a long high-energy-loss tail.

For the intermediate region of $0.01 \lesssim \kappa \lesssim 1$, Symon has given an approximate and Vavilov an exact theory to predict the energy-loss distributions, which form a smooth transition between the Landau and Bohr distributions, but experimental data for establishing the validity of theory in this region are scarce.

There are several advantages in the use of semiconductor detectors and accelerator beams of high-energy heavy charged particles in order to verify the Symon-Vavilov theory. Semiconductor detectors offer good energy resolution, linear response, high stopping power, and uniformly thick sensitive layers, while accelerator beams of heavy particles can be precisely controlled and suffer comparatively little scattering in the detectors. We have measured the energy-loss distributions of 45.3-MeV and 730-MeV protons, 910-MeV α particles, and 370-MeV negative pions in lithium-drifted silicon "p-i-n" detectors and silicon "p-n" junction detectors with depletion layers from 0.0085 to 1.094 g/cm^2, covering a range of κ from 0.0029 to 2.23.

Within the limits of experimental error, we find very good agreement with the Vavilov theoretical distributions.

Fluctuations of energy loss can be important in many experiments in radiation physics and biology; for the use of future experimenters, we have prepared graphical tabulations of measured and calculated data on energy-loss distributions.

ACKNOWLEDGMENTS

I want to express my profound appreciation to Dr. Mudundi R. Raju, who has been my teacher and mentor in the period of this work, and to Professor Cornelius A. Tobias, who enabled me to pursue this research.

Thanks are due to my wife, Shirley, for her infinite patience and cooperation in typing the draft of the manuscript, to Dr. Sam Cosper, Dr. Joe Cerny and Dr. Graeme Welch for help with runs at the 88-inch cyclotron, Dr. Fred Goulding, Dr. Don Landis, Dr. Dick Pehl, and Dr. Bob Lothrop for help with detectors and electronics, Dr. John Lyman, Jerry Howard and Dave Love for help at the 184-inch synchrocyclotron, and Dr. Martin J. Berger and Vic Brady for help with computer calculations.

I gratefully acknowledge fellowship support by the Atomic Energy Commission (administered by the Oak Ridge Institute of Nuclear Studies) and by the National Science Foundation. My research was supported by the National Aeronautics and Space Administration and directed by a committee consisting of Professor Cornelius A. Tobias, Chairman, Professor Hans Mark, and Dr. Roger Wallace.

APPENDIX

We tabulate here, in graphical form, some calculated and measured values that may be useful in energy-loss fluctuation problems, for "thin" absorbers.

In general, the first step in the analysis of a fluctuation problem is the determination of the most significant parameter, κ, from the relation

$$\kappa = 0.150 \frac{sZz^2}{A}\left(\frac{1 - \beta^2}{\beta^4}\right),$$

where s is the absorber thickness in g/cm^2, Z is the absorber atomic number, A is the absorber atomic weight, z is the particle charge number, and β is the particle velocity divided by the speed of light in vacuum. Alternatively, the value of $\kappa(A/Zz^2)$ may be obtained from Fig. 27, given the particle energy per atomic-mass-unit and the absorber thickness. Multiplication by(z^2Z/A) yields the value of κ. Interpolation is facilitated by the fact that κ depends linearly on s. If $\kappa \gg 1$, the energy-loss distribution is Gaussian; if $\kappa \lesssim 0.01$ the Landau distribution is valid, and if $0.01 \lesssim \kappa \lesssim 1$, the Vavilov theory is applicable.

The two most useful values for characterizing the energy-loss fluctuations are Δ_{mp}, the most probable energy loss, (i.e., the location of the peak), and the full width of the distribution at half-maximum (FWHM). The ratio of the most probable energy loss to the mean

can be estimated from Fig. 28, given the values of κ and β^2, and the ratio of the FWHM to the mean energy loss $\bar{\Delta}$ can be estimated from Fig. 29. The fact that the variation with β^2 is relatively slow should help interpolation, and the plotted values for silicon should not differ appreciably from the values for other materials. The value of $\bar{\Delta}$ can be obtained for "thin" absorbers by multiplying the absorber thickness by the mean rate of energy loss, dE/dx (see, for example, the Barkas and Berger tables in Ref. 34).

The actual shape of the energy-loss distribution can be estimated from Figs. 30 and 31, given the value of κ. The dimensionless parameter λ is Landau's reduced energy variable, defined by Eq. 42, and $\varphi(\lambda)$ is proportional to the probability of total energy loss. Again, the variation with β^2 is slow. A more complete tabulation of these values has been given by Seltzer and Berger in Ref. 34. (Fig. 31 is on page 79.)

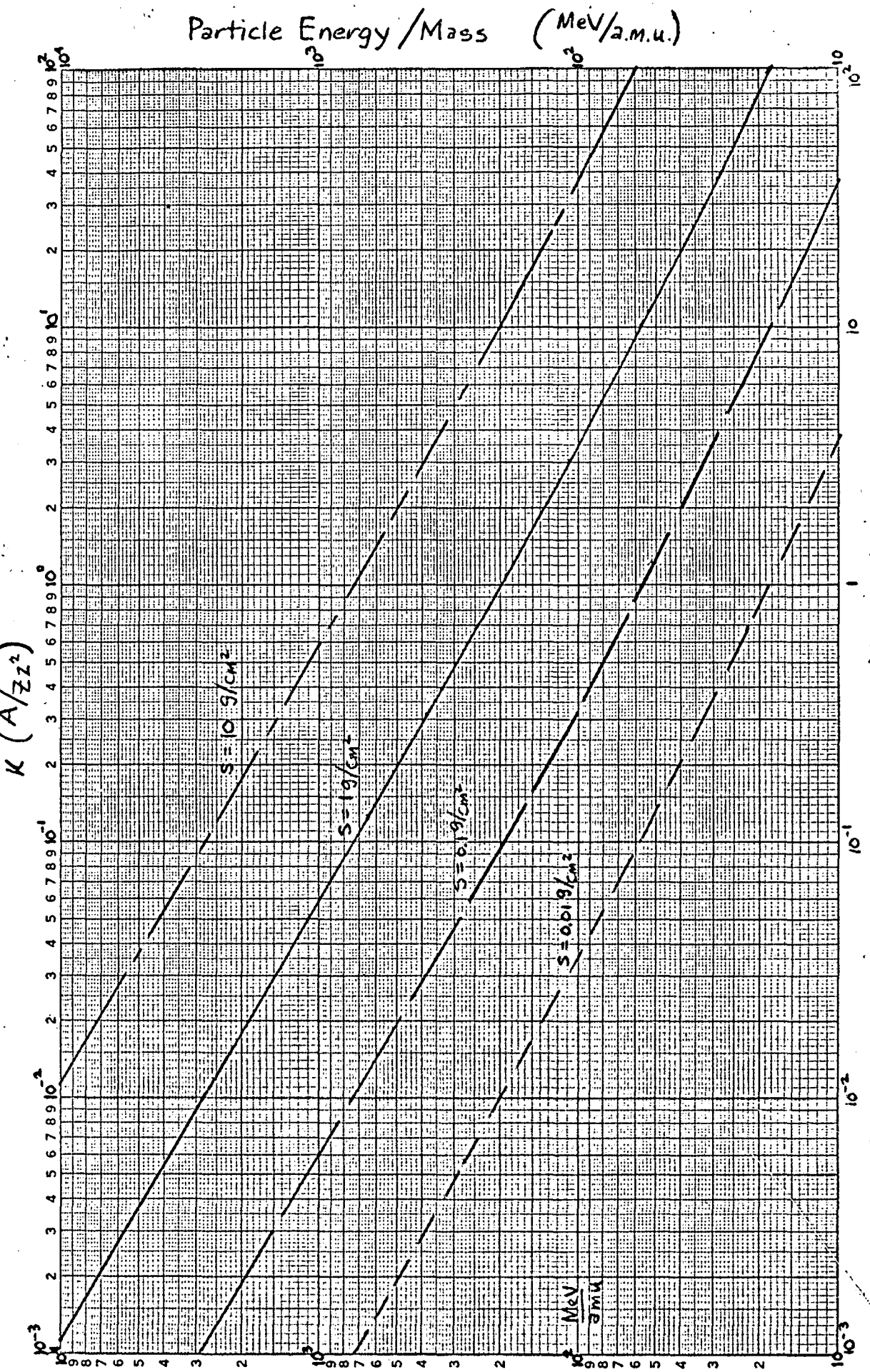
Particle Energy / Mass (MeV/a.m.u.)
K (A/Zz²)
Parameter K (A/Zz²)
S = 10 g/cm²
S = 1 g/cm²
S = 0.1 g/cm²
S = 0.01 g/cm²
MeV/amu

Fig. 27

$\Delta_{MP}/\bar{\Delta}$ versus K for Silicon

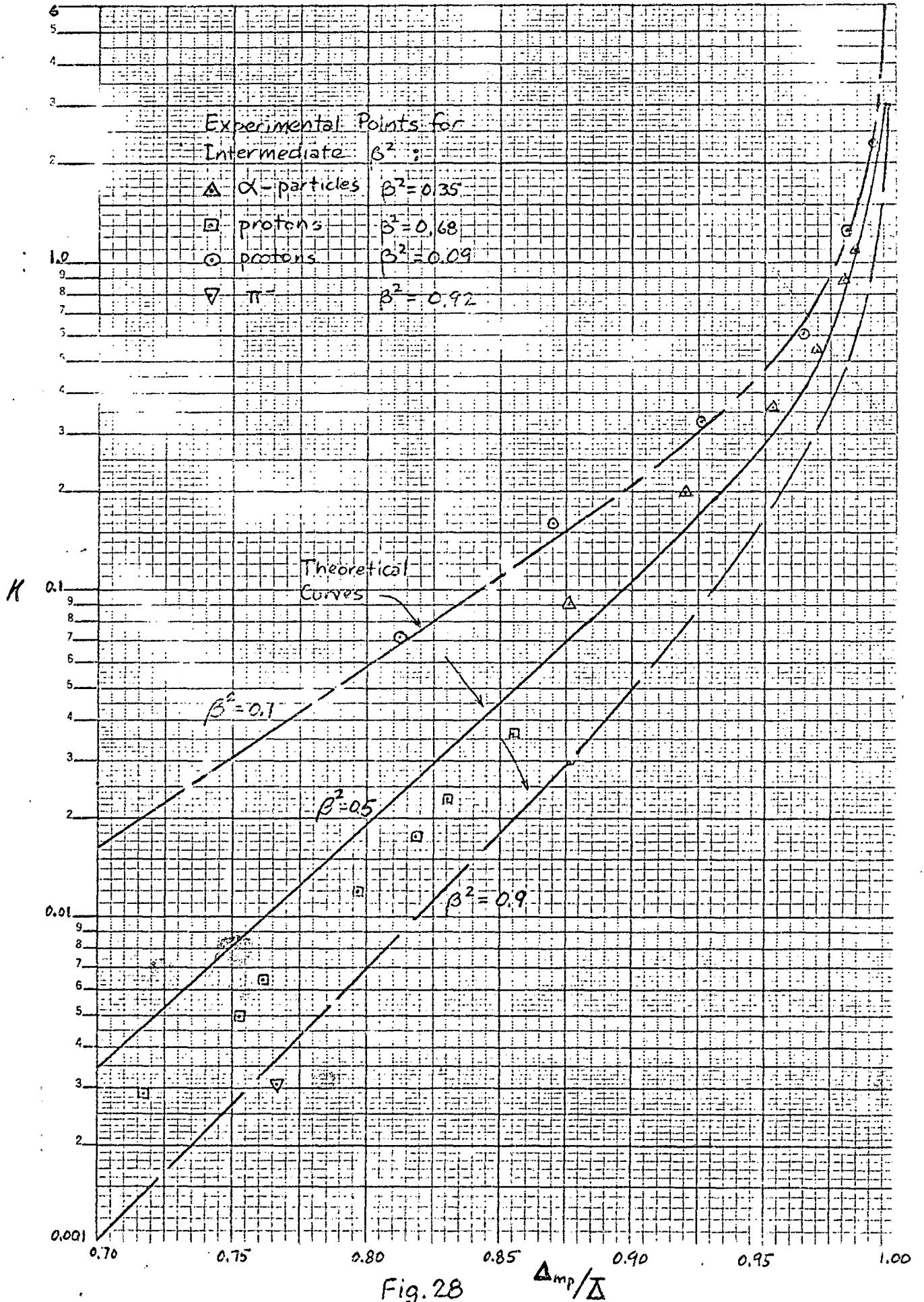

Fig. 28

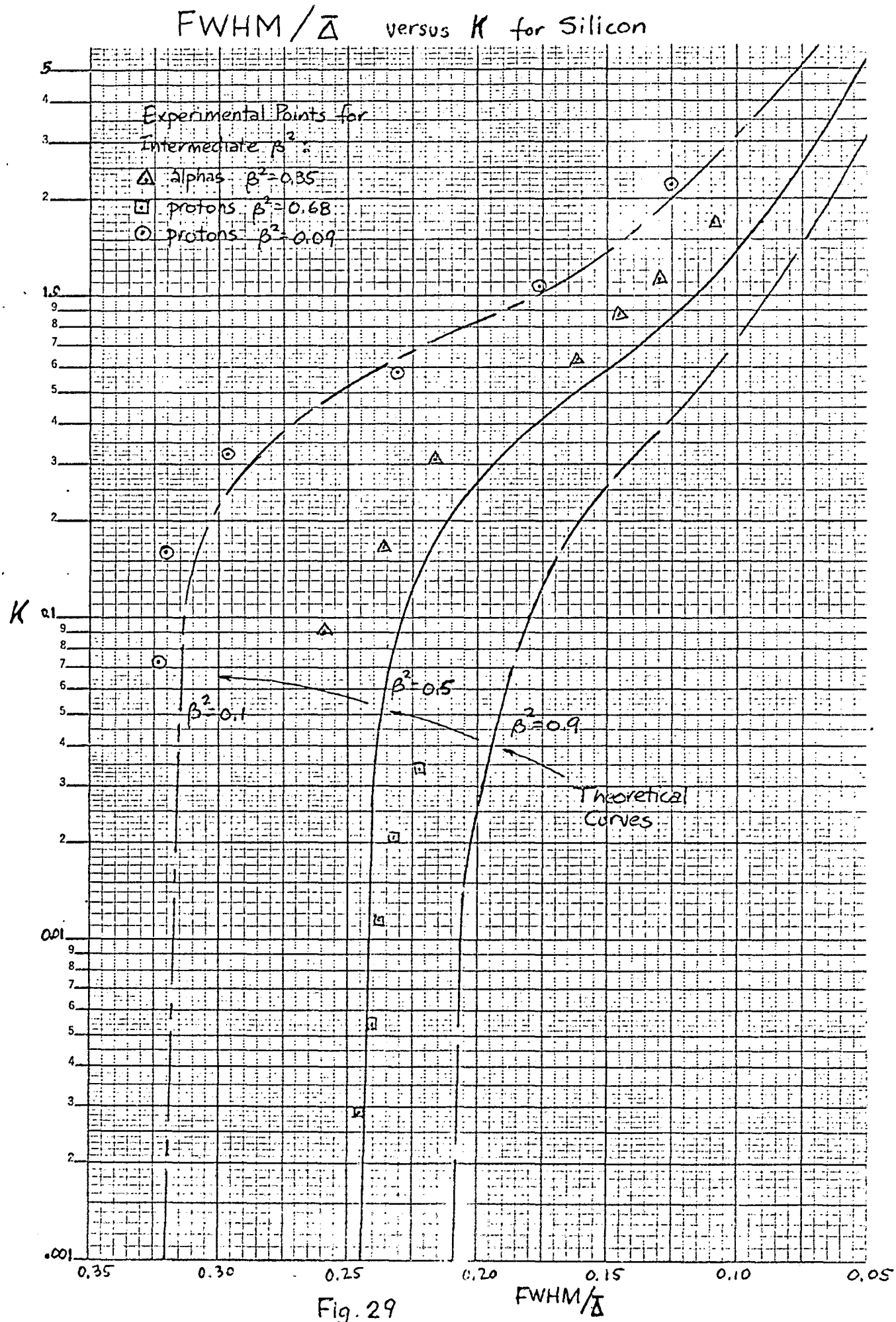
FWHM/Δ versus K for Silicon
Experimental Points for Intermediate β²:
Δ alphas β²=0.35
⊡ protons β²=0.68
⊙ protons β²=0.09
β²=0.1
β²=0.5
β²=0.9
Theoretical Curves
K
FWHM/Δ
0.35
0.30
0.25
0.20
0.15
0.10
0.05

Fig. 29

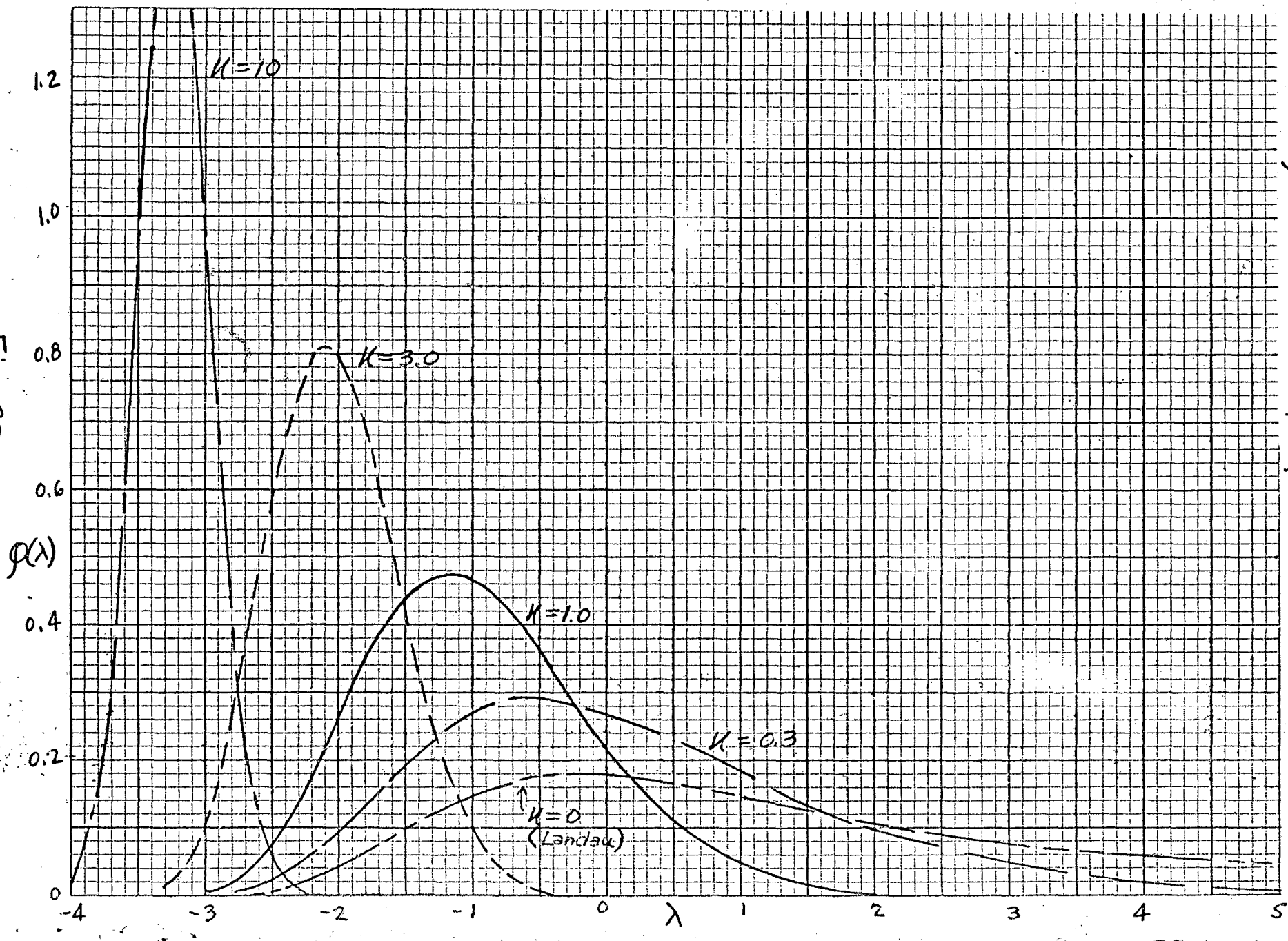
$\varphi(\lambda)$ versus λ for $\beta^2 = 0.5$
$\varphi(\lambda)$
λ
$\kappa = 10$
$\kappa = 3.0$
$\kappa = 1.0$
$\kappa = 0.3$
$\kappa = 0$
(Landau)
0
0.2
0.4
0.6
0.8
1.0
1.2
-4
-3
-2
-1
0
1
2
3
4
5

Fig. 30

REFERENCES

1. U. Fano, Ann. Rev. Nucl. Sci. 13, 1 (1963).
2. S. V. Starodubtsev and A. M. Romanov, The Passage of Charged Particles Through Matter, AEC-tr-6468, 1962 (transl. from Russian).
3. H. Bichsel, Am. Inst. of Phys. Hdbk., 8-20, 1963.
4. E. A. Uehling, Ann. Rev. Nucl. Sci. 4, 315 (1954).
5. H. A. Bethe and J. Ashkin, Experimental Nuclear Physics, Vol. 1 (Wiley, New York, 1953), p. 166.
6. R. Evans, The Atomic Nucleus (McGraw Hill, New York, 1955), p. 632.
7. B. Rossi, High Energy Particles (Prentice-Hall, New York, 1952), p. 10.
8. S. K. Allison and S. D. Warshaw, Rev. Mod. Phys. 25, 779 (1953).
9. N. Bohr, Phil. Mag. 25, 10 (1913).
10. N. Bohr, Phil. Mag. 30, 581 (1915).
11. H. A. Bethe, Ann. Physik 5, 325 (1930).
12. L. Flamm, Akad. Wiss. Wien, Math.-Naturw. Kl. 123, 1393 (1914) and 124, 597 (1915).
13. E. J. Williams, Proc. Roy. Soc. (London) A125, 420 (1929).
14. M. S. Livingston and H. A. Bethe, Rev. Mod. Phys. 9, 245 (1937).
15. N. Bohr, Kgl. Danske Videnskab. Selskab. Mat.-Fys. Medd. 18 [8] (1948).
16. L. Landau, J. Phys. U.S.S.R. 8 201 (1944).
17. K. R. Symon, Ph.D. Thesis, Harvard University, 1948; summary in Ref. 7, p. 32.

18. O. Blunck and S. Leisegang, Z. Physik 128, 500 (1950).

19. O. Blunck and K. Westphal, Z. Physik 130, 641 (1951).

20. H. W. Lewis, Phys. Rev. 85, 20 (1952).

21. U. Fano, Phys. Rev. 92, 328 (1953).

22. J. E. Moyal, Phil. Mag. 46, 263 (1955).

23. K. C. Hines, Phys. Rev. 97, 1725 (1955).

24. J. R. Herring and E. Merzbacher, J. Elisha Mitchell Sci. Soc. 73, 267 (1957).

25. P. V. Vavilov, Zh. Experim. i Teor. Fiz. 32, 920 (1957); English transl.: Soviet Phys. JETP 5, 749 (1957).

26. W. Rosenzweig, Phys. Rev. 115, 1683 (1959).

27. W. Borsch-Supan, J. Res. Natl. Bur. Std. 658, 245 (1961).

28. D. M. Ritson, Techniques of High Energy Physics (Interscience, New York, 1961), p. 18.

29. J. Lindhard and V. Nielsen, Phys. Letters 2, 209 (1962).

30. M. J. Berger, Methods in Computational Physics, Vol. 1 (Academic Press, New York, 1963), p. 135.

31. A. L. Morsell, Phys. Rev. 135, A1436 (1964).

32. J. G. Skofronick et al., Phys. Rev. 135, A1429 (1964).

33. H. Breuer, Nucl. Instr. Methods 33, 226 (1965).

34. S. Seltzer and M. Berger, in Studies in Penetration of Charged Particles in Matter, NAS-NRC Publ. no. 1133, 1964, p. 187. Note: this publication, a "state of the art" survey, is extremely useful to workers in the field of charged-particle penetration.

35. B. M. Golovin, L. A. Kulyukina, S. V. Medved, P. Pavlovitch, and P. Shulek, On Fluctuations of Ionization Losses, Preprint--2615, Joint Institute for Nuclear Research, Dubna U.S.S.R., 1966 (submitted to Yadern, Fiz.).

36. P. White and G. Millington, Proc. Roy. Soc. (London) 120, 701 (1928).

37. G. H. Briggs, Proc. Roy. Soc. (London) A114, 313 (1927); W. B. Lewis and C. E. Wynn-Williams, Proc. Roy. Soc. (London) A136, 349 (1932); W. E. Bennett, Proc. Roy. Soc. (London) A155, 419 (1936); W. H. Furry, Phys. Rev. 52, 569 (1937); W. Paul and H. Reich, Z. Physik 127, 429 (1950).

38. J. J. L. Chen and S. D. Warshaw, Phys. Rev. 84, 355 (1951).

39. R. D. Birkhoff, Phys. Rev. 82, 448 (1951).

40. P. Rothwell, Proc. Phys. Soc. (London) B64, 911 (1951).

41. E. L. Goldwasser, F. E. Mills, and A. O. Hanson, Phys. Rev. 88, 1137 (1952).

42. F. Kalil and R. D. Birkhoff, Phys. Rev. 91, 505 (1953).

43. E. T. Hungerford and R. D. Brikhoff, Phys. Rev. 95, 6 (1954).

44. S. Kageyama, J. Phys. Soc. Japan 11, 348 (1956).

45. A. M. Rauth and F. Hutchinson, in Biological Effects of Ionizing Radiation at the Molecular Level (IAEA, Vienna, 1962), p. 25.

46. F. Bowen and F. X. Roser, Phys. Rev. 85, 992 (1952).

47. A. Hudson and R. Hofstadter, Phys. Rev. 88, 589 (1952).

48. T. E. Cranshaw, Progr. Nucl. Phys. 2, 271 (1952).

49. J. K. Parry, H. D. Rathgeber, and J. L. Rouse, Proc. Phys. Soc. (London) A66, 541 (1953).

50. T. Bowen, Phys. Rev. 96, 754 (1954).

51. E. D. Palmatier, J. T. Meers, and C. M. Askey, Phys. Rev. 97, 486 (1955).

52. J. D. Van Putten and J. C. Vander Velde, IRE Trans. Nucl. Sci. NS-8 [1], 124 (1961).

53. C. B. Madsen and P. Venkateswarlu, Phys. Rev. 74, 1782 (1948).

54. C. B. Madsen, Kgl. Danske Videnskab. Selskab Mat.-Fys. Medd. 27 [13] (1953).

55. L. P. Nielsen, Kgl. Danske Videnskab. Selskab Mat.-Fys. Medd. 33 [6] (1961); J. Lindhard and M. Scharff, ibid. 27 [15] (1953).

56. P. T. Porter and J. I. Hopkins, Phys. Rev. 91, 209 (1953).

57. G. J. Igo, D. D. Clark and R. M. Eisberg, Phys. Rev. 89, 879 (1953); G. J. Igo and R. M. Eisberg, Rev. Sci. Instr. 25, 450 (1954).

58. A. B. Chilton, J. N. Cooper, and J. C. Harris, Phys. Rev. 93, 413 (1954).

59. T. J. Gooding and R. M. Eisberg, Phys. Rev. 105, 357 (1957).

60. F. Demichelis, Nuovo cimento 13, 562 (1959).

61. L. Koch, J. Messier, and J. Valin, Nucl. Electronics, Vol. 1 (IAEA, Vienna, 1962) p. 465.

62. G. L. Miller, B. M. Foreman, L. C. L. Yuan, P. F. Donovan, and W. M. Gibson, IRE Trans. Nucl. Sci. NS-8 [1], 73 (1961); G. L. Miller, S. Wagner, and L. C. L. Yuan, Nucl. Instr. Methods 20, 303 (1963).

63. L. Labeyrie, in Proceedings of the International School of Physics Enrico Fermi, Course XIX (Academic Press, New York, 1963), p. 187.

64. W. Rosenzweig and H. H. Rossi, Statistical Fluctuations in the Energy Loss of 5.8 MeV Alpha Particles Passing Through an Absorber of Variable Thickness. Columbia Radiological Research Laboratory Report NYO-10716, Nov. 1963 (unpublished).

65. Y. V. Galaktionov, F. A. Yech, and V. A. Lyubimov, Nucl. Instr. Methods 33, 353 (1961).

66. R. L. Lander, W. A. W. Mehlhop, H. J. Lubatti, and G. L. Schnurmacher, Solid State Devices as Detectors of Coherent High Energy Interactions, UCRL-16603, Dec. 1965 (unpublished).

67. G. Grew, IEEE Trans. Nucl. Sci. NS-12 [1], 308 (1965).

68. E. Rotondi and K. W. Geiger, Nucl. Instr. Methods 40, 192 (1966).

69. "The 184-Inch Synchrocyclotron," LRL Publication No. 2d, June, 1964.

70. See, for example: G. Crawford, Bull. Am. Phys. Soc. II, 10, 723 (1965) or Ref. 71.

71. F. S. Goulding, Semiconductor Detectors for Nuclear Spectrometry, UCRL-16231, July, 1965 (unpublished).

72. E. M. Pell, J. Appl. Phys. 31, 291 (1960); J. L. Blankenship and C. J. Borkowski, IRE Trans. Nucl. Sci. NS-9 [3], 181 (1962).

73. G. Dearnaley and D. C. Northrop, Semiconductor Counters for Nuclear Radiations (Wiley, New York, 1963).

74. R. P. Lothrop and H. E. Smith, Lithium-Drifted Silicon Radiation Detector Production Process, UCRL-16190, June, 1965 (unpublished); F. S. Goulding and W. L. Hansen, IEEE Trans. Nucl. Sci. NS-11 [3] 286 (1964).

75. W. Van Roosbroeck, Phys. Rev. 139, A1702 (1965).

76. H. M. Mann and J. L. Yntema, IRE Trans. Nucl. Sci. NS-11 [3], 201 (1964).

77. F. S. Goulding and D. Landis, in Instrumentation Techniques in Nuclear Pulse Analysis, NAS-NRC Publ. No. 1184, p. 61, 124.

78. M. R. Raju, H. Aceto, and C. Richman, Nucl. Instr. Methods 37, 152 (1965); H. D. Maccabee and M. R. Raju, Nucl. Instr. Methods 37, 176 (1965).

79. M. J. Berger (Natl. Bur. Std, Washington, D.C.) private communication, May, 1965; Victor Brady (Lawrence Radiation Laboratory, Berkeley), private communication, June, 1965.

80. J. E. Turner, in Ref. 34, p. 99.

81. H. Bichsel and C. Tschalär, Bull. Am. Phys. Soc. II, 10, 723 (1965).

82. F. P. Denisov, R. A. Latipova, V. P. Milovanov, and P. A. Cerenkov, J. Nucl. Phys. U.S.S.R. 1, 329 (1965), translation in Soviet J. Nucl. Phys. 1, 234 (1965).

83. F. S. Goulding (Lawrence Radiation Laboratory, Berkeley), private communication, June, 1966.

84. G. Dearnaley, IEEE Trans. Nucl. Sci. NS-11 [3], 249 (1964).

85. C. Erginsoy, Passage of Charged Particles Through Crystal Lattices, BNL-944, 1965 (unpublished); H. E. Wegner, C. Erginsoy, and W. M. Gibson, IEEE Trans. Nucl. Sci. NS-12 [1], 240 (1965).

86. H. H. Rossi and W. Rosenzweig, Radiology 64, 404 (1955).

87. H. H. Rossi and W. Rosenzweig, Radiology 66, 105 (1956); H. H. Rossi, Radiation Res. 10, 522 (1959); H. H. Rossi, Radiation Res. Suppl. 2, 290 (1960); H. H. Rossi, M. H. Biavati, and W. Gross, Radiation Res. 15, 431 (1961); H. H. Rossi, in Proceedings of the International

School of Physics Enrico Fermi, Course XXX (Academic Press, New York, 1964), p. 42 ff.

88. Hughes Research Laboratories Summary Technical Report NAS-2-2366, 1965 (unpublished).

89. D. E. Lea, Actions of Radiations on Living Cells (Cambridge University Press, London, 1962).

90. N. Oda, Relationship Between Primary Energy Transfer and Target Theory (Tokyo Institute of Technology) (preprint), 1965 (unpublished).

91. J. E. Turner and H. Hollister, Nature 208, 36 (1965).

92. J. J. Butts and R. Katz, Theory of RBE for Heavy Ion Bombardment of Dry Enzymes and Viruses, Kansas State University, preprint, 1965.